MOLECULAR MECHANISMS OF METABOLIC CONTROL IN THE ARCTIC GROUND SQUIRREL

A

DISSERTATION

Presented to the Faculty

of the University of Alaska Fairbanks

in Partial Fulfillment of the Requirements

for the Degree of

DOCTOR OF PHILOSOPHY

By

Jamie Louis Barger, B.S.

Fairbanks, Alaska

August 2002

UMI Number: 3059718

ProQuest Information and Learning Company
300 North Zeeb Road
P.O. Box 1346
Ann Arbor, MI 48106-1346

MOLECULAR MECHANISMS OF METABOLIC CONTROL IN

THE ARCTIC GROUND SQUIRREL

By

Jamie Louis Barger

RECCOMMENDED:

Advisory Committee Co-Chair

Advisory Committee Co-Chair

Department Chair

APPROVED:

Dean, College of Science, Engineering, and Mathematics

Dean of the Graduate School

8-1-02

Date

ABSTRACT

The annual cycle of the arctic ground squirrel (*Spermophilus parryii*) is characterized by periods of intense energy deposition and utilization, and therefore this species an attractive model for investigating the molecular mechanisms of metabolic control in mammals. In late summer, animals become hyperphagic and undergo intense fattening prior to hibernation. Leptin, a hormone produced by white adipose tissue, reverses obesity in rodent genetic models, but the effects of leptin on outbred rodent strains and wild species is modest. Similarly, administration of mouse recombinant leptin did not affect food intake or adiposity during prehibernation fattening in arctic ground squirrels. These results suggest that either prehibernation fattening is insensitive to negative feedback from leptin or that animals in general lack a negative feedback system controlling adiposity.

At the terminus of prehibernation fattening, arctic ground squirrels commence hibernation, during which time nonshivering thermogenesis is invoked to maintain a high body temperature relative to sub-freezing ambient conditions. Thermogenesis occurs primarily by uncoupling oxidative phosphorylation and is catalyzed by mitochondrial membrane transport proteins. I compared the expression patterns of an established and a putative uncoupling protein gene (*Ucp1* and *Ucp3*, respectively) in arctic ground squirrels as a function of temperature, hibernation, or fasting. As expected, levels of brown adipose tissue *Ucp1* mRNA and protein were increased by cold exposure and hibernation and decreased by fasting. In contrast, levels of *Ucp3* mRNA in skeletal muscle were not increased by cold or hibernation, but were paradoxically increased by fasting.

Furthermore, I describe two independent studies that show that increases in the amount of UCP3 do not uncouple oxidative phosphorylation in vitro, suggesting that UCP3 does not mediate thermogenesis in skeletal muscle.

Finally, I measured several parameters of mitochondrial bioenergetics in active and hibernating arctic ground squirrels to investigate if the reduced metabolic rate during hibernation is attributable to active suppression of metabolic rate or is instead a secondary consequence of the effects of low body temperature on enzyme kinetics. I show that mitochondrial substrate oxidation is depressed during hibernation, supporting the hypothesis that the reduced metabolic rate during hibernation is a partial consequence of active metabolic depression.

TABLE OF CONTENTS

LIST OF FIGURES

LIST OF TABLES

ACKNOWLEDGEMENTS

An iceberg is much like graduate study, for just as only a fraction of the whole remains above water, a dissertation is the visible, yet scant, component of the entire experience that is buoyed by the extensive contributions from numerous individuals. Thus, it is fitting that those individuals and organizations that have made this work possible be duly recognized at the outset, lest they remain submerged in the icy waters of anonymity.

Thanks are extended to the co-chairs of my advisory committee, Drs. Bert Boyer and Brian Barnes, for their constant encouragement in matters scientific and otherwise. I am especially grateful for their patience in giving me the latitude to investigate those questions which piqued my curiosity, even if it seemed like I was occasionally out in left field. Thanks are also extended to the other individuals who served as members of my advisory committee, including Drs. Abel Bult-Ito, Kelly Drew, and Tom Kuhn. They have been invaluable references for proposal writing, experimental design, and intellectual stimulation. I have also had the great fortune of interacting with a number of individuals outside the University of Alaska Fairbanks, namely Drs. Sean Adams and Martin Brand. They have been generous with their time, encouragement, and technical expertise. The successful completion of numerous experiments would not have been possible without their input and collaboration.

Much of this research has relied heavily on the excellent technical assistance of Ruth Stafford. Her mastery of skills, her ability to keep the lab in good order despite the less than fastidiousness of lab members (myself included), and her fine selection of music (what is good gel-loading music, anyway?) kept the Boyer lab a much more productive

environment than it would have been in her absence. Animal care was expertly provided by the Institute of Arctic Biology's Veterinary Services Facility, occasionally under conditions of extreme cold and darkness. Having an animal care staff that is proficient at maintaining wild animals in captivity has been a great asset to this research, and I would like to especially thank Rob Aikman and Chris Terzi for sharing their knowledge with me. Additionally, I would like to thank the staff members of the Department of Biology and Wildlife and the Institute of Arctic Biology, both past and present, including: Judy Romans, Beth Laursen, Carol Piser, Laura Morisky, Carol Button, Alma Davis, Genelle Tilton, and Marta Conner. They have made the daily grind more enjoyable and have shown great patience in steering me through the occasionally rough waters of policies and procedures.

Financial support for these studies was provided by numerous agencies, including the American Heart Association, the Alaska NSF-EPSCoR program, and United States' Department of Defense EPSCoR program. In addition, financial support for travel to scientific meetings was provided by the Graduate School of the University of Alaska Fairbanks, the Department of Biology and Wildlife, the Institute of Arctic Biology, and the Alaska NSF-EPSCoR program.

I have had the fortune of interacting with many other graduate students over the years, and their friendship has been a tremendous benefit to my well-being. They are too numerous to mention here, but I would like to specifically mention Steve LePage for encouraging me to enjoy life outside the lab, sometimes to Bert's displeasure; Mark Herzog for teaching me the finer aspects of ice hockey; Chris Swingley for lengthy

discussions of lofty matters, such as how to calculate the area of a trapezoid; and Jason Knight for his daily humor, assistance in the lab, and help with trapping arctic ground squirrels (ask him for his "tuber delight" recipe).

I owe a great deal of gratitude to my family, including my parents, grandparents, aunts and uncles. They instilled a sense of curiosity about the natural world from an early age, fostered a spirit of skepticism, and taught me the importance of balancing hard work with levity, humility, and humor, all of which have sustained me throughout graduate school. Thanks also for your patience during my lengthy tour in graduate school—rest assured that I will have a real job soon.

Finally, but most importantly, I wish to thank my wife Laurie, my son Peter, and my daughter Madeleine. I have often been asked if having children makes graduate study more difficult, and admittedly being a parent necessitates an additional suite of adaptations to the graduate student morph. However, I dare say it has made my tenure more enjoyable; their unflagging encouragement during the lows and their unquestioning celebration of the obscure highs have made the completion of the degree all the more rewarding. My thanks to them vastly exceeds my ability to describe in words.

Although this is a singly-authored dissertation, each chapter has been written as a manuscript for publication and is co-authored. Thus, the "we" in each chapter refers to the authors who have assisted in collecting and analyzing data.

INTRODUCTION

Advances in the field of molecular biology have resulted in a proliferation of studies relating changes in gene expression to various disease states (Brown 1998; Celis et al. 2000). In the post-genomic era, however, an understanding of the function of these genes has lagged far behind their discovery, and an active area of investigation seeks to link changes in gene expression with functional responses at the cellular and organismal levels (Strausberg and Austin 1999). Currently, this integrative approach is being used extensively in the field of obesity research to identify the genes and biochemical pathways that exert control over energy metabolism. While many genes have been implicated in the pathogenesis of obesity (Elbein 2002), a small number of candidate regulatory genes have recently received considerable attention. The focus of this dissertation is to evaluate the role of several of these genes and their biochemical pathways in the control of metabolism using a unique animal model.

The identification of the leptin (*lep*) gene in 1994 sparked an explosion of studies investigating the control of food intake and energy expenditure via negative feedback from adipose tissue. The *lep* gene is expressed predominantly in white adipose tissue and encodes a 16 kDa protein that circulates in the blood to affect local and systemic metabolism. Mice with a defect in the *lep* gene (*lep/lep*) lack the functional protein and are severely hyperphagic, hypometabolic, and consequently extremely obese (Zhang et al. 1994). The observation that administration of recombinant leptin potently reverses obesity in *lep/lep* mice (Pelleymounter et al. 1995) sparked an array of studies centered on the premise that leptin was an anti-obesity hormone that may have promise in

reversing human obesity. Indeed, humans with a genetic defect in the leptin gene are obese and are responsive to recombinant leptin therapy (Farooqi et al. 1999). The discovery of leptin was a major advance in metabolic physiology because it provided a potential mechanism for the long-hypothesized system for adipostatic control of body mass (Weigle 1994).

One mechanism by which leptin may control metabolism is by increasing the abundance of proteins found in the mitochondrial inner membrane that catalyze an inducible proton leak and lead to futile cycling. Uncoupling protein 1 (UCP1) is expressed almost exclusively in brown adipose tissue and plays a vital role in the development of homeothermy in neonatal mammals and in mediating cold-induced thermogenesis in small mammals (Nicholls and Rial 1999). UCP1 was first identified in 1976 (Ricquier and Kader 1976), and it its mechanism of action has been studied extensively. UCP1 short-circuits the proton gradient across the mitochondrial inner membrane, bypassing the ATP synthase, and catalyzes a futile cycle of proton pumping and leak. Because energy released from substrate oxidation is not conserved as ATP, UCP1 elicits a both potent thermogenic response and leads to the depletion of energy reserves such as adipose tissue (Nicholls and Locke 1984). Between 1997 and 1999, four novel genes were identified (*Ucp2-4* and brain mitochondrial carrier protein, *Bmcp1*) that encode proteins with significant structural homology to UCP1 (Boss et al. 1997; Fleury et al. 1997; Mao et al. 1999; Sanchis et al. 1998; Vidal-Puig et al. 1997). Numerous reports demonstrated that regulation of these genes was similar to that of UCP1, namely increased expression during cold-exposure, high-fat feeding, and thyroid hormone (Gong

et al. 1997; Lanni et al. 1997; Larkin et al. 1997; Yu et al. 2000). Additionally, mitochondrial membrane potential was decreased in yeast transfected with the *Ucp* homologues, further suggesting that these proteins may function similar to UCP1 (Hagen et al. 1999; Hinz et al. 1999). Indeed, *Ucp3* knockout mice have an increased mitochondrial membrane potential (Vidal-Puig et al. 2000), and the temperature of skeletal muscle is increased in mice overexpressing *Ucp3* (Clapham et al. 2000). Because the expression of the *Ucp* homologues shows a wide tissue distribution, it was proposed that that these proteins may exert significant control over metabolism and provide a means for pharmacological manipulation for the treatment of obesity. Accordingly, *lep/lep* mice treated with recombinant leptin had increased mRNA levels of the *Ucp* homologues in multiple tissues (Liu et al. 1998; Zhou et al. 1997).

While many studies in rodent genetic models of obesity support a role for leptin and UCP homologues in the control of metabolism, later studies using outbred rodent strains, obese humans, and wild species cast serious doubt on the proposed role of these proteins to prevent obesity. For example, the anti-obesity effects of recombinant leptin are less substantial, and sometimes absent, in wild-type mice (Harris et al. 1998) and several wild species (Baker et al. 2000; Boyer et al. 1997; Klingenspor et al. 1996; Ormseth et al. 1996). Additionally, leptin levels in the blood are elevated and are proportional to adiposity in obese humans (Considine et al. 1996), but the magnitude of negative feedback on adiposity does not increase when leptin levels are elevated above the physiological range. More careful studies of the UCP homologues suggested that although levels of *Ucp* homologue mRNA are increased under various circumstances, the

abundance of the protein in mitochondria is 2-3 orders of magnitude lower than the levels of UCP1 in brown adipose tissue. Furthermore, the increased uncoupling observed in yeast transfected with *Ucp* homologues was shown to be an artifact of supraphysiological expression, and that when yeast express the homologues at levels found in mice, they did not appear to mediate a significant mitochondrial uncoupling in vitro (Harper et al. 2002; Stuart et al. 2001). Despite significant experimentation, the role of leptin and the UCP homologues in metabolic control (if any) remains uncertain.

The selection of a particular model system appears to explain the divergence between the studies supporting and rejecting a role for leptin and the UCP homologues in metabolic control: experiments using inbred strains and transgenic models show support, whereas studies using non-genetic models of obesity reject the hypothesis. To understand if these mechanisms exert control over metabolic processes in vivo, an experimental model system must be chosen that reflects the pathogenesis of the obesity in natural populations. Clearly, the use of genetic models is not adequate in this regard; species which show natural and/or spontaneous changes in adiposity may be more suitable.

The arctic ground squirrel (*Spermophilus parryii*) displays seasonal shifts between periods of extreme energy deposition and utilization, and therefore this species provides a potentially useful model system to investigate some of the molecular and cellular mechanisms of metabolic control. In late summer, arctic ground squirrels are hyperphagic and rapidly increase body fat reserves to as much as 50% of total body mass (Galster and Morrison 1976). Administration of recombinant leptin modestly decreases adiposity after prehibernation fattening in the arctic ground squirrel (Ormseth et al.

1996), but its effects during the period of prehibernation fattening are unknown. It is possible that as in obese humans, arctic ground squirrels are resistant to the effects of elevated leptin that accompany prehibernation fattening, and this possibility is addressed in Chapter 1. At the terminus of seasonal fatting, arctic ground squirrels begin a 7-8 month hibernation season during which time animals must activate thermogenic mechanisms to defend a high body temperature against sub-freezing ambient conditions. The Appendix and Chapter 2 of this dissertation investigate the relationships between UCP homologues, cellular thermogenesis, and whole-animal metabolism. If the UCP homologues catalyze a thermogenic proton leak, then levels of *Ucp* homologue mRNA and protein should be increased under thermogenic conditions but decreased under conditions where fuel metabolism should be spared. Furthermore, if *Ucp* homologues mediate thermogenesis, then the temperatures of tissues expressing these genes should be elevated. Additionally, changes in the abundance of UCPs should correlate with changes in proton leak measured in isolated mitochondria.

While UCPs may catalyze a regulated proton leak, all mitochondria exhibit a basal proton leak that constitutes approximately 30% of resting metabolism (Brand 1990; Brand et al. 1994). Although this inefficiency is an inherent property of mitochondria, the magnitude of the leak can be influenced physiologically by thyroid hormones (Harper and Brand 1993) and the fatty acid composition of mitochondrial membranes (Brookes et al. 1998). Using the techniques outlined in Chapter 2 and Appendix 1 (measurement of mitochondrial proton leak), Chapter 3 of this dissertation investigates if the reduced

metabolic rate during hibernation is achieved in part by a reduction in proton cycling in multiple tissues of the arctic ground squirrel.

CHAPTER 1 - EFFECTS OF LEPTIN ON HIBERNATION, BODY MASS, AND UNCOUPLING PROTEINS DURING PREHIBERNATION FATTENING IN ARCTIC GROUND SQUIRRELS

Barger, J.L., Barnes, B.M., Fried, S.K., Nicolson, M.A., Boyer, B.B. Effects of leptin on hibernation, body mass, and uncoupling proteins in arctic ground squirrels. Prepared for submission to Comparative Biochemistry and Physiology - Part A: Molecular & Integrative Physiology.

ABSTRACT

We investigated the role of leptin in the regulation of body mass, body composition, timing of hibernation, and uncoupling protein (*Ucp*) homologue gene mRNA levels in arctic ground squirrels (*Spermophilus parryii*), a species that exhibits high amplitude seasonal changes in food intake and adiposity. We continuously infused mouse recombinant leptin to ground squirrels during prehibernation fattening at low (LL, 0.04 $mg \cdot kg^{-1} \cdot day^{-1}$) and high (HL, 0.20 $mg \cdot kg^{-1} \cdot day^{-1}$) doses. Total body and fat-free masses were greater in LL (vs. HL) squirrels; however, leptin administration did not prevent fattening, adipocyte hypertrophy, affect food intake, or induce hibernation at either dose. Levels of leptin (*lep*) and *Ucp2* mRNA in subcutaneous white adipose tissue were significantly decreased at both doses. Levels of brown adipose tissue *Ucp1* mRNA were decreased in the LL group but not the HL group, while skeletal muscle *Ucp3* mRNA levels did not differ among groups. These results suggest that prehibernation fattening is not inhibited by administration of leptin. Rather, modest increases in serum leptin appear to promote mass gain, possibly via regulation of insulin and the UCP homologues.

INTRODUCTION

Many hibernating mammals undergo a period of rapid fattening prior to hibernation that is hypothesized to be regulated by an adipostat with a sliding set-point (Mrosovsky, 1976). This theory predicts that lipid stores are regulated at a level that is appropriate for the particular time in the seasonal cycle of fattening, and has received experimental support: golden-mantled ground squirrels (*Spermophilus lateralis*) subjected to lipectomy rapidly restore fat reserves compared to sham-operated controls (Dark et al., 1984). Interestingly, maintenance of seasonally-appropriate lipid stores occurs without compensatory changes in food intake (Dark et al., 1985), suggesting that multiple mechanisms are involved in seasonal regulation of adiposity. While there is an empirical basis for the sliding set-point hypothesis, the means by which the quantity of adipose reserves is conveyed to the central mechanisms controlling food intake and energy expenditure is unresolved.

The discovery of the peptide hormone leptin provided a novel link between fat stores and mechanisms regulating energy balance (Zhang et al., 1994). Leptin is secreted by, and in proportion to the amount of, white adipose tissue (WAT) and reduces food intake and adipose tissue mass when given to leptin deficient (*lep/lep*) mice, but to a lesser extent in lean mice (Halaas et al., 1995; Harris et al., 1998; Pelleymounter et al., 1995). Leptin also participates in the regulation of energy balance by reversing the hypometabolic and hypothermic state of *lep/lep* mice via increased thermogenesis through the activity of uncoupling protein 1 (UCP1) in brown adipose tissue (BAT) (Commins et al., 1999; Porter and Andrews, 1998; Scarpace et al., 1997). Metabolic heat

is produced in BAT because UCP1 dissipates the H^+ gradient across the mitochondrial inner membrane and prevents the conservation of energy as ATP (Nicholls and Locke, 1984). Leptin may also help to counteract excess lipid accumulation in peripheral tissues by activating the expression of two genes (*Ucp2* and *Ucp3*) whose proteins show homology to UCP1 and are expressed in a wide array of tissues (Boss et al., 1997; Fleury et al., 1997; Vidal-Puig et al., 1997). Leptin-induced increases in the abundance of *Ucp2* mRNA are correlated with increased oxidation of fatty acids in WAT and pancreatic islets (Ceddia et al., 2000; Zhou et al., 1997). Skeletal muscle (SKM) may be an additional target for leptin, as levels of *Ucp3* mRNA are increased in *lep/lep* mice after leptin administration (Liu et al., 1998).

Arctic ground squirrels (*Spermophilus parryii*) prepare for the thermogenic demands of a 6-9 month hibernation season by increasing lipid reserves to as much as 50% of body mass (Buck and Barnes, 1999) and by increasing BAT mass and UCP1 synthesis (Boyer et al., 1993). Administration of pharmacological doses of leptin (approximately 40 times greater than basal levels) slightly decreased food intake and body mass of arctic ground squirrels in late fall following the prehibernation hyperphagic period of fattening (Ormseth et al., 1996), but little else is known about the effects of leptin on prehibernation physiology. Woodchucks (*Marmota monax*) undergo an increase in body mass which is paralleled by a four- to eightfold increase in serum leptin (Concannon et al., 2001); if such an increase occurs in the arctic ground squirrel, this would paradoxically increase energy expenditure and lipid oxidation via UCP homologues. Alternatively, mechanisms regulating energy balance during seasonal

fattening may be resistant to the effects of leptin, as evidenced by the lack of a decrease in BAT UCP1 and energy expenditure with leptin treatment during the increase in body mass following hibernation (Boyer et al., 1997).

In one study, a low dose of leptin (0.1 mg · kg^{-1} · day^{-1}) increased body mass relative to saline-injected controls and mice receiving higher doses of leptin (1.0 and 10 mg · kg^{-1} · day^{-1}) (Pelleymounter et al., 1995), but the effects of leptin closer to the physiological range in the arctic ground squirrel are unknown. Therefore, we designed the current study to determine the effect of administering leptin during prehibernation fattening at doses that were slightly elevated above the physiological range found in this species in addition to pharmacological doses used previously (Ormseth et al., 1996). We also measured changes in *Ucp1-3* mRNA levels and adipocyte size as a function of leptin administration to determine if leptin activates *Ucp* homologues in multiple tissues and reduces triglyceride content in adipocytes. Finally, we tested the hypothesis that leptin serves as a peripheral signal of adiposity regulating onset of hibernation (Mrosovsky, 1971b) by assessing if the timing of entry into hibernation was advanced in leptin-infused ground squirrels. Our results suggest that leptin does not influence prehibernation fattening or the onset of hibernation, but has dose-dependent effects on total body and fat-free masses, serum insulin, and *Ucp1* mRNA levels.

METHODS

Leptin administration

Arctic ground squirrels were lab-born juveniles of females captured 14-16 May or juvenile arctic ground squirrels live trapped 28-30 July in the Alaska Range (64°N

146°W, elevation 850m). Ground squirrels were brought to the University of Alaska Fairbanks and cared for as previously described (Ormseth et al., 1996). Body masses were measured every 4-6 days starting 1 August. To standardize leptin delivery on a mass-specific basis, food availability was restricted in some animals beginning 18 August such that animals ≤ 450g were given food ad libitum, and animals weighing > 450g were given 70-95% of ad libitum intake. The degree of food restriction did not vary among subsequently assigned treatment groups. At the start of leptin administration (25 August), the average body mass of all ground squirrels was 550g (range: 472 to 608g). Animals were randomly assigned to one of three treatment groups: a control group that received saline (CTRL, n = 10 with five males and five females), a group that received a low dose of leptin (LL, n = 9 with five males and four females), and a group that received a high dose of leptin (HL, n = 9 with four males and five females) for 28 days (until 21 September). Mouse recombinant leptin (Amgen; Thousand Oaks, CA) or saline were continuously administered via a single osmotic minipump (Model 2ML4, AlzA; Palo Alto, CA) surgically implanted through a 1.5 cm incision into the mid-dorsal subcutaneous space in squirrels under anesthesia (Halothane U.S.P., Halocarbon Labs). By manipulating the concentration of leptin in the pumps (flow rate = 2.5 $\mu L \cdot h^{-1}$), animals received approximately (depending on body mass) 0.04 mg leptin $\cdot$ $kg^{-1} \cdot day^{-1}$ (LL) or 0.20 mg leptin $\cdot$ $kg^{-1} \cdot day^{-1}$ (HL).

Body mass, food intake, and body composition

After surgery, squirrels were allowed to recover for two days at 18°C before being placed in an environmental chamber at 5 ± 1°C with a photoperiod adjusted two times per week

to match the prevailing photoperiod near the capture site (range of photoperiod in experiment was 16L:8D to 12L:12D). Body mass was measured at the beginning and end of the experiment and food intake (Mazuri Rodent Chow) was measured weekly. Food intake was estimated as the difference between mass of food provided and food remaining. Body composition was estimated at the beginning and end of the experiment by total body electrical conductance (TOBEC) using an Emscan Model SA-3000. Body composition was measured using an equation previously validated for this species during the period of prehibernation fattening (Ormseth et al., 1996). Fat-free mass was estimated as $\left(4.77\sqrt{TOBEC \times BL} - 241.5\right)$, where *TOBEC* is the average of three values from the instrument and *BL* is the body length (cm) from the tip of the nose to the base of the tail. Fat mass was estimated as the difference between total and fat-free masses.

Tissue collection

Before surgery to implant pumps, animals were anesthetized with Metofane (Methoxyfluorane, Mallinckrodt Veterinary) and a 3 mL blood sample was collected by cardiac puncture from each animal; serum was stored at -70°C until assayed for concentrations of leptin, insulin, triglycerides, and nonesterified fatty acids (NEFA) (Ormseth et al., 1996). Serum leptin levels were quantified using the multispecies leptin radioimmunoassay kit from Linco Inc. (St. Louis, MO); the intra- of interassay assay coefficients of variation were 8.3% and 8.1%, respectively. Immediately prior to implanting osmotic mini-pumps, three samples of subcutaneous WAT (~50 mg each) were removed from the dorsal region for determination of adipocyte size as described previously (Hirsch and Gallian, 1968) with the following modifications: the fixed tissue

was washed using a 400 μm mesh and a 25 μm mesh was used to collect the cells. Cells were counted in a Coulter counter using a 560 μm aperture.

At the end of the 28 day leptin administration period, a second blood sample was obtained, and animals were euthanized by an intracardiac injection of pentobarbital. Samples of subcutaneous WAT, interaxillary BAT, and gastrocnemius muscle (hereafter referred to as SKM) were collected, frozen in liquid nitrogen, and stored at -70°C for northern analysis. In addition, another three samples (~50 mg each) of subcutaneous WAT were obtained for adipocyte size determination.

Northern analysis

Total RNA was isolated (TriReagent, Sigma) and fractionated on 1.25% denaturing agarose gels. RNA was then blotted and UV crosslinked to nylon membranes (Hybond N+, Amersham Biosciences). *Ucp1* mRNA was detected using a highly conserved 27 bp *Ucp1* cDNA probe (Brander et al., 1993), *Ucp2* mRNA was detected using a full-length mouse cDNA probe (Vidal-Puig et al., 1997), *Ucp3* mRNA was detected using a 29 bp *Ucp3* cDNA probe (5'-CCTTCCTCCCTGGCGATGGTTCTGTAGGC-3') derived from the mouse cDNA (Vidal-Puig et al., 1997), and *lep* mRNA was detected using a full-length arctic ground squirrel cDNA probe (Boyer, unpublished). Probes for *Ucp2* mRNA, *lep* mRNA, and 18S rRNA were random prime radiolabeled (Boehringer Mannheim) with α-[^{32}P] dCTP (Amersham); *Ucp1* and *Ucp3* mRNA probes were polynucleotide kinase end-labeled (New England Biolabs) with γ-[^{32}P] ATP (Amersham).

Prior to hybridization, all blots were hydrated in 5× SSC (1× SSC is 150 mM sodium chloride and 15 mM sodium citrate, pH 7.0) for at least 1h, and then

prehybridized for 4-6 h at 45°C in 50% (v/v) deionized formamide, 5× SSPE (1× SSPE is 180 mM sodium chloride, 10 mM NaH_2PO_4, 1 mM EDTA), 5× Denhardt's solution, 0.5% SDS (w/v), and 50 $\mu g \cdot mL^{-1}$ denatured salmon sperm DNA. Blots were hybridized at 45°C for 14-16 h in a hybridization oven (Robbins Scientific, Model 1000). Washing stringencies and exposure times were as follows: *Ucp1* mRNA and 18S rRNA blots were washed in a solution of 2× SSC / 0.2% SDS for 15 min at 22°C, 0.1× SSC / 0.2% SDS for 20 min at 45°C, 0.1× SSC / 0.2% SDS for 20 min at 55°C, and 0.1× SSC / 1% SDS for 20 min at 65°C and exposed for 20 min (18S rRNA) or 9 h (*Ucp1* mRNA). Blots probed for *Ucp2*, *Ucp3*, and *lep* mRNA were washed in 2× SSC / 0.2% SDS for 15 min at 22°C and for an additional 15-20 min at 45°C; exposure times (at -70°C) ranged from 3-7 days. All autoradiograph exposures were maintained within the linear range of the film (Amersham Hyperfilm). Densitometric analysis was performed using an IS 100 Digital Imaging System (Alpha Inotech).

Statistical analysis

Data were analyzed using SAS for Windows (SAS Institute, Cary, North Carolina). For parameters with pre- and posttest observations, a repeated measures analysis of variance (ANOVA) was performed with treatment as the main effect. Posttest *Ucp1-3* mRNA levels were analyzed by ANOVA (no repeated measures). Least-squares means were used for post-hoc comparisons of means when ANOVA revealed a main effect. Because the effects of leptin administration were similar in males and females for every parameter measured, data for both sexes have been pooled for all analyses.

RESULTS

Serum parameters

Serum leptin levels were similar among all treatments at the beginning of the experiment (Figure 1.1A); however, after 28 days of continuous infusion, serum leptin concentrations were significantly different among all groups (CTRL = 8.3 ± 1.0, LL = 16.0 ± 3.1, HL = 114 ± 24). Serum insulin was similar among all treatments at the beginning of the experiment (Figure 1.1B); however, after 28 days of leptin infusion, insulin levels in the LL group were greater than both the CTRL and HL groups, but levels did not differ between the CTRL and HL groups. Serum levels of triglycerides increased during the experiment for all groups but were not significantly different among treatments at either time period (Figure 1.1C). Serum NEFA levels did not differ between pretest and posttest measurements and were not different among treatment groups at either time period (Figure 1.1D).

Food intake, body mass dynamics, and hibernation

Food intake decreased during the experiment for all treatment groups but did not differ among treatments at any interval during the experiment (Table 1.1). The mean pretest body masses were similar among all treatments (Figure 1.2A). After leptin administration, total body masses differed among groups such that the mean body mass of LL squirrels was significantly greater than HL squirrels, although neither treatment group differed from controls. The amount of fat-free body mass paralleled total body mass: pretest masses were similar among treatments, but the fat-free mass of LL squirrels was significantly higher than HL squirrels after leptin administration (Figure 1.2B). The

mass of body fat increased during the experiment for all treatment groups but was not significantly different among treatment groups during pretest or posttest conditions (Figure 1.2C). Similarly, prehibernation fattening was associated with an increase in adipocyte size (Table 1.2), although adipocyte size did not differ among treatment groups at either time period. Only one ground squirrel entered hibernation: after 25 days of leptin administration, a female in the HL group began hibernating and remained torpid until the end of the experiment.

Relationships between adiposity, leptin expression, and serum leptin

In saline-infused (CTRL) animals, the change in serum leptin levels was significantly related to the change in fat mass over the experimental period (Figure 1.3A); because of limited sample volume, two pretest leptin values are missing from the analysis. The change in serum leptin levels was also significantly related to the change in WAT *lep* mRNA levels over the experimental period in CTRL squirrels (Figure 1.3B); in addition to the missing pretest serum leptin samples, one posttest *lep* mRNA sample was not included in this analysis due to sample degradation.

Leptin and Ucp homologue gene expression as a function of leptin administration

Abundance of *lep* mRNA in WAT did not differ among treatments at the beginning of the experiment, but was significantly reduced in LL and HL groups compared to the CTRL group (Figure 1.4). Posttest *Ucp1* mRNA abundance in BAT was significantly lower in LL squirrels compared to both CTRL and HL squirrels (Figure 1.5A). Leptin administration reduced levels of *Ucp2* mRNA in both LL and HL groups compared to the

CTRL group (Figure 1.5B). *Ucp3* mRNA abundance in SKM showed a trend similar to BAT *Ucp1*, but levels were not significantly different among treatments (Figure 1.5C).

DISCUSSION

Previous studies investigating the role of leptin in arctic ground squirrels administered leptin at pharmacological levels, which resulted in serum leptin concentrations up to 40 times greater than those measured in wild and lab-maintained individuals of this species [(Boyer et al., 1997; Ormseth et al., 1996), and unpublished observations]. However, it is unknown if responses to pharmacological doses of leptin are indicative of how arctic ground squirrels respond to physiological increases in circulating leptin that may accompany prehibernation fattening. To evaluate the response to leptin administration closer to the physiological range, and to determine if the response to pharmacological doses is different, we administered mouse recombinant leptin to arctic ground squirrels in doses that modestly (twofold, LL group) and substantially (14-fold, HL group) elevated serum leptin levels compared to posttest values of saline-infused controls. Our results indicate that serum leptin correlates with its own expression and whole-animal adiposity, although arctic ground squirrels did not respond to exogenous murine recombinant leptin with an advanced onset of hibernation or decreases in fat mass and food intake during the period of prehibernation fattening measured during this study. A low dose of leptin increased total and fat-free body masses relative to the HL group, possibly as a secondary consequence of increased serum insulin levels and decreased energy expenditure via the UCP homologues.

Lack of "classical" leptin effects

Leptin is widely regarded as an anti-obesity hormone because it has potent effects on body mass and food intake in rodent models of obesity (Chen et al., 1996; Harris et al., 1998; Pelleymounter et al., 1995). Similarly, humans with a defect in the *lep* gene lack serum leptin, are obese (Strobel et al., 1998), and lose body mass in response to administration of recombinant leptin (Farooqi et al., 1999). However, the effects of recombinant leptin on wild-type rodent strains (Harris et al., 1998; Pelleymounter et al., 1995), obese humans (Heymsfield et al., 1999), and wild species (Baker et al., 2000; Boyer et al., 1997; Klingenspor et al., 2000; Ormseth et al., 1996; Reddy et al., 1999) have been less robust or not detectable. During prehibernation fattening, serum leptin levels parallel body mass in woodchucks (Concannon et al., 2001) and adiposity in arctic ground squirrels (Figure 1.3A). However, continuous infusion of murine recombinant leptin did not decrease food intake (Table 1.1), fat mass (Figure 1.2C), or the amount of lipid stored in adipocytes sampled from subcutaneous WAT (Table 1.2).

The term "leptin resistance" has been used to explain why high serum leptin levels fail to prevent obesity and hyperphagia (Frederich et al., 1995), and such a phenomenon may occur in arctic ground squirrels—sensitivity to the anorectic effects of leptin during the early stages of prehibernation fattening would be undesirable as this would prevent acquisition of energy reserves needed for hibernation. Alternatively, the physiological role of leptin may not be to decrease food intake, but rather to maintain energy balance during times of limited food availability (Flier, 1998). This hypothesis is supported by experimental evidence showing that fasting decreases serum leptin and increases neuropeptide Y (NPY) mRNA (Ahima et al., 1996), which would stimulate

food intake and decrease energy expenditure in BAT (Billington et al., 1994). Furthermore, it is unlikely that there would be selection against mechanisms promoting fat deposition during times of energy availability, as wild organisms rarely encounter unlimited resources. Therefore, leptin resistance may not be due to impaired signaling but rather result from the lack of a potent negative feedback regulatory mechanism that inhibits food intake via leptin (Flier, 1998).

The amount of body fat coordinates reproductive activity (Bray, 1997) and seasonal behaviors such as dispersal (Nunes et al., 1998) and the onset of hibernation (Mrosovsky, 1971b). The relationship between adiposity and levels of leptin in the serum suggests a straightforward mechanism for relaying the status of fat reserves to neural mechanisms controlling such behaviors. For example, mice injected with leptin reproduced earlier than controls, presumably because exogenous leptin signaled that nutrient reserves were sufficient for pregnancy (Chehab et al., 1997). However, we were unable to advance the onset of hibernation by administering leptin to arctic ground squirrels during prehibernation fattening, suggesting that leptin may not play a role in triggering the onset of hibernation. The specific mechanisms regulating the entrance into hibernation are unknown, and may be further complicated by the unpredictable nature of hibernation under laboratory conditions (Mrosovsky, 1971a). Although increasing concentrations of recombinant leptin in the blood do not elicit hibernation, leptin could influence the onset of hibernation if the sensitivity to endogenous leptin is increased. Possible mechanisms that might increase sensitivity include enhanced transport of leptin across the blood-brain barrier (Banks et al., 1999), altered leptin signaling due to binding

of circulating leptin to a soluble receptor (Lahlou et al., 2000) and activation of the post-receptor signaling pathway via inhibition of the family of suppressors of cytokine signaling (SOCS) proteins (Bjorbaek et al., 1999; Wang et al., 2000). Seasonal leptin sensitivity has been demonstrated in the Djungarian hamster, *Phodopus sungorus* (Klingenspor et al., 2000), thus warranting further studies to identify putative mechanisms of leptin resistance (and its reversal) in the timing of seasonal behaviors such as hibernation.

Effects of leptin on gene expression

In contrast to the lack of an effect of leptin on adiposity and food intake, infusion of murine recombinant leptin did alter levels of *lep* mRNA in WAT of arctic ground squirrels. Posttest levels of *lep* mRNA were reduced to one-third of the posttest level in saline-infused squirrels (Figure 1.4), and this agrees with published studies demonstrating that leptin gene expression is inhibited by an autocrine negative feedback mechanism (Zhang et al., 2001; Zhang et al., 1997). However, the endogenous increase in serum leptin (CTRL group) did not decrease leptin secretion (Figure 1.3B). Rather, levels of leptin mRNA nearly doubled over the course of the experiment (Figure 1.4), suggesting that a higher level of serum leptin, which may occur with continued fattening, is required to inhibit its expression.

The regulation of *Ucp* homologue gene expression by leptin is unclear and appears to differ depending on the species and tissue studied. Moreover, the effects on levels of *Ucp1-3* mRNA are difficult to interpret because the dose of leptin varies among studies, the resulting serum leptin levels are often not reported, and the physiological

function of the *Ucp* homologues is as yet uncertain. Many studies report that leptin increases levels of *Ucp1-3* mRNA, presumably as part of a negative feedback loop controlling adiposity (Liu et al., 1998; Scarpace et al., 1997; Zhou et al., 1997), while other studies show no effect (Sivitz et al., 1999) or a reduction in *Ucp2-3* mRNA levels (Combatsiaris and Charron, 1999). It is tempting to speculate that the decreased levels of BAT *Ucp1* mRNA seen in the LL group (Figure 1.5A) and decreased levels of WAT *Ucp2* mRNA in both leptin-treated groups (Figure 1.5B) result in decreased energy expenditure and therefore enhance energy deposition during prehibernation fattening. However, this should be interpreted with caution as levels of BAT *Ucp1* mRNA do not necessarily reflect the activity of the protein which is regulated *in vivo* by purine nucleotides (Klingenberg and Huang, 1999) and the sympathetic nervous system (Thomas and Palmiter, 1997). Moreover, recent studies suggest that UCP2 and UCP3 do not catalyze thermoregulatory uncoupling when present at physiological concentrations (Harper et al., 2002; Stuart et al., 2001), and therefore precautions should be applied to functional interpretations based solely upon levels of *Ucp2-3* mRNA.

Bidirectional effects of leptin

While unexpected, the relative increase in total body and fat-free mass of LL squirrels (21% and 23% increase compared to HL, respectively) agrees with an early study showing that a low dose of leptin (0.1 mg · kg^{-1}) increased body mass relative to saline-injected controls and mice receiving higher doses of leptin (1.0 and 10 mg · kg^{-1}) (Pelleymounter et al., 1995). The bidirectional effects of leptin on body mass observed in this study (Figure 1.2A) are in close agreement with a recent study of woodchucks held

under a natural photoperiod: body mass increased during seasonal fattening despite concomitant increases in serum leptin levels. However, body mass began to decline when levels of leptin increased approximately fivefold compared to basal leptin levels measured before seasonal fattening (Concannon et al., 2001). The dose-dependent differences in body mass dynamics may be explained by leptin's control of insulin secretion. At a physiological concentration (1 nM, approximately 16 ng · mL^{-1}), leptin increased insulin secretion from pancreatic beta cells (Tanizawa et al., 1997) and a physiological dose of leptin (that raised serum levels to 16.0 ng · mL^{-1}) increased serum insulin levels by 92% in this study (LL group). Higher concentrations of leptin (10, 80, 100 nM) decreased insulin secretion in pancreatic beta cells (Ishida et al., 1997; Tanizawa et al., 1997) and in this study a pharmacological dose of leptin decreased serum insulin levels by 47%, although this was not significantly different from controls. Modest increases in endogenous serum leptin (Concannon et al., 2001) may be responsible for the increase in serum insulin during prehibernation fattening in arctic (Feist et al., 1986) and golden-mantled (Boswell et al., 1994) ground squirrels, thereby increasing fat deposition, whereas decreased serum insulin may have resulted in decreased lipogenesis (as evidenced by the slightly lower fat mass of HL squirrels). It is tempting to speculate that decreased fat-free mass of the HL group (relative to the LL group) was the result a compensatory mechanism to increase fat mass at the expense of protein (mediated by decreased insulin), although this was not tested explicitly.

In summary, leptin is a reliable index of adiposity, but neither endogenous fluctuations in serum levels of leptin nor peripheral leptin administration affected

prehibernation fattening, food intake, or timing of hibernation in arctic ground squirrels. Emerging evidence suggests that the predominant role of leptin is to stimulate food intake during energy restriction, rather than to decrease food intake in obesity. If leptin plays a physiological role during prehibernation fattening, its function may be to indirectly enhance fat deposition through regulation of insulin and the UCP homologues. Furthermore, seasonal modulation of leptin sensitivity may be a mechanism used by hibernating species to initiate hibernation.

ACKNOWLEDGEMENTS

The authors would like to thank Melinda Lyons and Ruth Stafford for technical assistance, Dr. Brad Lowell for providing the mouse *Ucp2* cDNA, and Drs. Abel Bult-Ito, Kelly Drew, and Dana Thomas for reviewing the manuscript. This work was done during the tenure of graduate student research fellowships from the American Heart Association Alaska Affiliate and from NSF-EPSCoR (J.L.B.). Additional funding was provided by NSF OPP9819540 (B.M.B.) and grants from the National Institute of Health (DK45711), NSF CAREER Award (IBN9514675), and Amgen, Inc. (B.B.B.).

REFERENCES

Ahima, R.S., Prabakaran, D., Mantzoros, C., Qu, D., Lowell, B., Maratos-Flier, E., Flier, J.S., 1996. Role of leptin in the neuroendocrine response to fasting. Nature 382, 250-252.

Baker, D.M., Larsen, D.A., Swanson, P., Dickhoff, W.W., 2000. Long-term peripheral treatment of immature coho salmon (*Oncorhynchus kisutch*) with human leptin has no clear physiologic effect. Gen. Comp. Endocrinol. 118, 134-138.

Banks, W.A., DiPalma, C.R., Farrell, C.L., 1999. Impaired transport of leptin across the blood-brain barrier in obesity. Peptides 20, 1341-1345.

Billington, C.J., Briggs, J.E., Harker, S., Grace, M., Levine, A.S., 1994. Neuropeptide y in hypothalamic paraventricular nucleus: A center coordinating energy metabolism. Am. J. Physiol. 266, R1765-1770.

Bjorbaek, C., El-Haschimi, K., Frantz, J.D., Flier, J.S., 1999. The role of socs-3 in leptin signaling and leptin resistance. J. Biol. Chem. 274, 30059-30065.

Boss, O., Samec, S., Paoloni-Giacobino, A., Rossier, C., Dulloo, A., Seydoux, J., Muzzin, P., Giacobino, J.P., 1997. Uncoupling protein-3: A new member of the mitochondrial carrier family with tissue-specific expression. FEBS Lett. 408, 39-42.

Boswell, T., Woods, S.C., Kenagy, G.J., 1994. Seasonal changes in body mass, insulin, and glucocorticoids of free-living golden-mantled ground squirrels. Gen. Comp. Endocrinol. 96, 339-346.

Boyer, B.B., Barnes, B.M., Kopecky, J., Jacobsson, A., Hermanska, J., 1993. Molecular control of prehibernation brown fat growth in arctic ground squirrels. In: Carey, C., Florant, G. L., Wunder, B. A. & Horwitz, B. (Ed.), Life in the cold: Ecological, physiological, and molecular mechanisms. Westview Press, Boulder, pp. 483-492.

Boyer, B.B., Ormseth, O.A., Buck, L., Nicolson, M., Pelleymounter, M.A., Barnes, B.M., 1997. Leptin prevents posthibernation weight gain but does not reduce energy expenditure in arctic ground squirrels. Comp. Biochem. Physiol. 118C, 405-412.

Brander, F., Keith, J.S., Trayhurn, P.A., 1993. A 27-mer oligonucleotide probe for the detection and measurement of the mrna for uncoupling protein in brown adipose tissue of different species. Comp. Biochem. Physiol. 104B, 125-131.

Bray, G.A., 1997. Obesity and reproduction. Hum. Reprod. 12 Suppl 1, 26-32.

Buck, C.L., Barnes, B.M., 1999. Annual cycle of body composition and hibernation in free-living arctic ground squirrels. J. Mamm. 80, 430-442.

Ceddia, R.B., William, W.N., Lima, F.B., Flandin, P., Curi, R., Giacobino, J.P., 2000. Leptin stimulates uncoupling protein-2 mrna expression and krebs cycle activity and inhibits lipid synthesis in isolated rat white adipocytes. Eur. J. Biochem. 267, 5952-5958.

Chehab, F.F., Mounzih, K., Lu, R., Lim, M.E., 1997. Early onset of reproductive function in normal female mice treated with leptin. Science 275, 88-90.

Chen, G., Koyama, K., Yuan, X., Lee, Y., Zhou, Y.T., O'Doherty, R., Newgard, C.B., Unger, R.H., 1996. Disappearance of body fat in normal rats induced by adenovirus-mediated leptin gene therapy. Proc. Natl. Acad. Sci. 93, 14795-14799.

Combatsiaris, T.P., Charron, M.J., 1999. Downregulation of uncoupling protein 2 mRNA in white adipose tissue and uncoupling protein 3 mrna in skeletal muscle during the early stages of leptin treatment. Diabetes 48, 128-133.

Commins, S.P., Watson, P.M., Padgett, M.A., Dudley, A., Argyropoulos, G., Gettys, T.W., 1999. Induction of uncoupling protein expression in brown and white adipose tissue by leptin. Endocrinology 140, 292-300.

Concannon, P., Levac, K., Rawson, R., Tennant, B., Bensadoun, A., 2001. Seasonal changes in serum leptin, food intake, and body weight in photoentrained woodchucks. Am. J. Physiol. 281, R951-959.

Dark, J., Forger, N.G., Stem, J.S., Zucker, I., 1985. Recovery of lipid mass after removal of adipose tissue in ground squirrels. Am. J. Physiol. 249, R73-78.

Dark, J., Forger, N.G., Zucker, I., 1984. Rapid recovery of body mass after surgical removal of adipose tissue in ground squirrels. Proc. Natl. Acad. Sci. 81, 2270-2272.

Farooqi, I.S., Jebb, S.A., Langmack, G., Lawrence, E., Cheetham, C.H., Prentice, A.M., Hughes, I.A., McCamish, M.A., O'Rahilly, S., 1999. Effects of recombinant leptin therapy in a child with congenital leptin deficiency. N. Engl. J. Med. 341, 879-884.

Feist, D.D., Florant, G., Greenwood, M.R.C., Feist, C., 1986. Regulation of energy stores in arctic ground squirrels: Brown fat thermogenic capacity, lipoprotein lipase, and pancreatic hormones during fat deposition. In: Heller, H. C. (Ed.), Living in the cold:Physiological and biochemical adaptations. Elsevier Press, New York, pp. 281-285.

Fleury, C., Neverova, M., Collins, S., Raimbault, S., Champigny, O., Levi-Meyrueis, C., Bouillaud, F., Seldin, M.F., Surwit, R.S., Ricquier, D., Warden, C.H., 1997. Uncoupling protein-2: A novel gene linked to obesity and hyperinsulinemia. Nat. Genet. 15, 269-272.

Flier, J.S., 1998. What's in a name? In search of leptin's physiologic role. J. Clin. Endocrinol. Metab. 83, 1407-1413.

Frederich, R.C., Hamann, A., Anderson, S., Lollmann, B., Lowell, B.B., Flier, J.S., 1995. Leptin levels reflect body lipid content in mice: Evidence for diet- induced resistance to leptin action. Nat. Med. 1, 1311-1314.

Halaas, J.L., Gajiwala, K.S., Maffei, M., Cohen, S.L., Chait, B.T., Rabinowitz, D., Lallone, R.L., Burley, S.K., Friedman, J.M., 1995. Weight-reducing effects of the plasma protein encoded by the obese gene. Science 269, 543-546.

Harper, J.A., Stuart, J.A., Jekabsons, M.B., Roussel, D., Brindle, K.M., Dickinson, K., Jones, R.B., Brand, M.D., 2002. Artifactual uncoupling by uncoupling protein 3 in yeast mitochondria at the concentrations found in mouse and rat skeletal-muscle mitochondria. Biochem. J. 361, 49-56.

Harris, R.B.S., Zhou, J., Redmann, S.M., Smagin, G.N., Smith, S.R., Rodgers, E., Zachwieja, J.J., 1998. A leptin dose-response study in obese *(ob/ob)* and lean *(+/?)* mice. Endocrinology 139, 8-19.

Heymsfield, S.B., Greenberg, A.S., Fujioka, K., Dixon, R.M., Kushner, R., Hunt, T., Lubina, J.A., Patane, J., Self, B., Hunt, P., McCamish, M., 1999. Recombinant leptin for weight loss in obese and lean adults - a randomized, controlled, dose-escalation trial. J. Am. Med. Assn. 282, 1568-1575.

Hirsch, J., Gallian, E., 1968. Methods for the determination of adipose cell size in man and animals. J. Lipid Res. 9, 110-119.

Ishida, K., Murakami, T., Mizuno, A., Iida, M., Kuwajima, M., Shima, K., 1997. Leptin suppresses basal insulin secretion from rat pancreatic islets. Regul. Pept. 70, 179-182.

Klingenberg, M., Huang, S.G., 1999. Structure and function of the uncoupling protein from brown adipose tissue. BBA Biomembranes 1415, 271-296.

Klingenspor, M., Niggemann, H., Heldmaier, G., 2000. Modulation of leptin sensitivity by short photoperiod acclimation in the Djungarian hamster, *Phodopus sungorus*. J. Comp. Physiol. B 170, 37-43.

Lahlou, N., Clement, K., Carel, J.C., Vaisse, C., Lotton, C., Le Bihan, Y., Basdevant, A., Lebouc, Y., Froguel, P., Roger, M., Guy-Grand, B., 2000. Soluble leptin receptor in serum of subjects with complete resistance to leptin: Relation to fat mass. Diabetes 49, 1347-1352.

Liu, Q.Y., Bai, C., Chen, F., Wang, R.P., MacDonald, T., Gu, M.C., Zhang, Q., Morsy, M.A., Caskey, C.T., 1998. Uncoupling protein-3: A muscle-specific gene upregulated by leptin in *ob/ob* mice. Gene 207, 1-7.

Mrosovsky, N., 1971a. The conditions for torpor. (Ed.), Hibernation and the hypothalamus. Appleton-Century-Crofts, New York, pp. 168-207.

Mrosovsky, N., 1971b. Control systems for annual cycles. (Ed.), Hibernation and the hypothalamus. Appleton-Century-Crofts, New York, pp. 103-146.

Mrosovsky, N., 1976. Lipid programmes and life history strategies. Amer. Zool. 16, 685-697.

Nicholls, D.G., Locke, R.M., 1984. Thermogenic mechanisms in brown fat. Physiol. Rev. 64, 1-64.

Nunes, S., Ha Cd, T., Garrett, P.J., Mueke, E., Smale, L., Holekamp, K.E., 1998. Body fat and time of year interact to mediate dispersal behaviour in ground squirrels. Anim. Behav. 55, 605-614.

Ormseth, O.A., Nicolson, M., Pelleymounter, M.A., Boyer, B.B., 1996. Leptin inhibits prehibernation hyperphagia and reduces body weight in arctic ground squirrels. Amer. J. Physiol. 271, R1775-1779.

Pelleymounter, M.A., Cullen, M.J., Baker, M.B., Hecht, R., Winters, D., Boone, T., Collins, F., 1995. Effects of the obese gene product on body weight regulation in *ob/ob* mice. Science 269, 540-543.

Porter, R.K., Andrews, J.F., 1998. Effects of leptin on mitochondrial 'proton leak' and uncoupling proteins: Implications for mammalian energy metabolism. Proc. Nutr. Soc. 57, 455-460.

Reddy, A.B., Cronin, A.S., Ford, H., Ebling, F.J.P., 1999. Seasonal regulation of food intake and body weight in the male siberian hamster: Studies of hypothalamic orexin (hypocretin), neuropeptide y (NPY) and pro-opiomelanocortin (POMC). Eur. J. Neurosci. 11, 3255-3264.

Scarpace, P.J., Matheny, M., Pollock, B.H., Tumer, N., 1997. Leptin increases uncoupling protein expression and energy expenditure. Amer. J. Physiol. 273, E226-230.

Sivitz, W.I., Fink, B.D., Donohoue, P.A., 1999. Fasting and leptin modulate adipose and muscle uncoupling protein: Divergent effects between messenger ribonucleic acid and protein expression. Endocrinology 140, 1511-1519.

Strobel, A., Issad, T., Camoin, L., Ozata, M., Strosberg, A.D., 1998. A leptin missense mutation associated with hypogonadism and morbid obesity. Nat. Genet. 18, 213-215.

Stuart, J.A., Harper, J.A., Brindle, K.M., Jekabsons, M.B., Brand, M.D., 2001. Physiological levels of mammalian uncoupling protein 2 do not uncouple yeast mitochondria. J. Biol. Chem. 276, 18633-18639.

Tanizawa, Y., Okuya, S., Ishihara, H., Asano, T., Yada, T., Oka, Y., 1997. Direct stimulation of basal insulin secretion by physiological concentrations of leptin in pancreatic beta cells. Endocrinology 138, 4513-4516.

Thomas, S.A., Palmiter, R.D., 1997. Thermoregulatory and metabolic phenotypes of mice lacking noradrenaline and adrenaline. Nature 387, 94-97.

Vidal-Puig, A., Solanes, G., Grujic, D., Flier, J.S., Lowell, B.B., 1997. Ucp3: An uncoupling protein homologue expressed preferentially and abundantly in skeletal muscle and brown adipose tissue. Biochem. Biophys. Res. Commun. 235, 79-82.

Wang, Z., Zhou, Y.T., Kakuma, T., Lee, Y., Kalra, S.P., Kalra, P.S., Pan, W., Unger, R.H., 2000. Leptin resistance of adipocytes in obesity: Role of suppressors of cytokine signaling. Biochem. Biophys. Res. Commun. 277, 20-26.

Zhang, Y., Hufnagel, C., Eiden, S., Guo, K., Diaz, P., Leibel, R.L., Schmidt, I., 2001. Mechanisms for lepr-mediated regulation of leptin expression in brown and white adipocytes in rat pups. Physiol. Genomics 4, 189-199.

Zhang, Y., Olbort, M., Schwarzer, K., Nuesslein-Hildesheim, B., Nicolson, M., Murphy, E., Kowalski, T.J., Schmidt, I., Leibel, R.L., 1997. The leptin receptor mediates apparent autocrine regulation of leptin gene expression. Biochem. Biophys. Res. Commun. 240, 492-495.

Zhang, Y., Proenca, R., Maffei, M., Barone, M., Leopold, L., Friedman, J.M., 1994. Positional cloning of the mouse obese gene and its human homologue. Nature 372, 425-432.

Zhou, Y.T., Shimabukuro, M., Koyama, K., Lee, Y., Wang, M.Y., Trieu, F., Newgard, C.B., Unger, R.H., 1997. Induction by leptin of uncoupling protein-2 and enzymes of fatty acid oxidation. Proc. Natl. Acad. Sci. 94, 6386-6390.

Table 1.1. Daily food intake of during prehibernation fattening.

	Week 1	Week 2	Week 3	Week 4
CTRL	27.3 ± 5.1	27.5 ± 4.3	28.1 ± 4.5	23.4 ± 2.9
LL	33.4 ± 2.5	30.6 ± 2.8	30.9 ± 4.9	27.2 ± 3.5
HL	27.8 ± 4.4	22.5 ± 4.3	18.6 ± 3.7	17.2 ± 4.0

Food intake decreased for all groups over the duration of the experiment ($P < 0.01$), but did not differ among treatments at any timepoint. Values are means ± SE expressed as grams food consumed per squirrel per day.

Table 1.2. Adipocyte size as a function of leptin administration during prehibernation fattening.

	CTRL	LL	HL
Pretest	0.80 ± 0.07	0.85 ± 0.08	1.06 ± 0.14
Posttest	1.41 ± 0.12	1.62 ± 0.13	1.56 ± 0.20

Adipocyte size increased over the duration of the experiment for all groups ($P < 0.001$) but did not differ among groups for either pretest or posttest measurements. Values are means ± SE expressed as μg lipid · $cell^{-1}$.

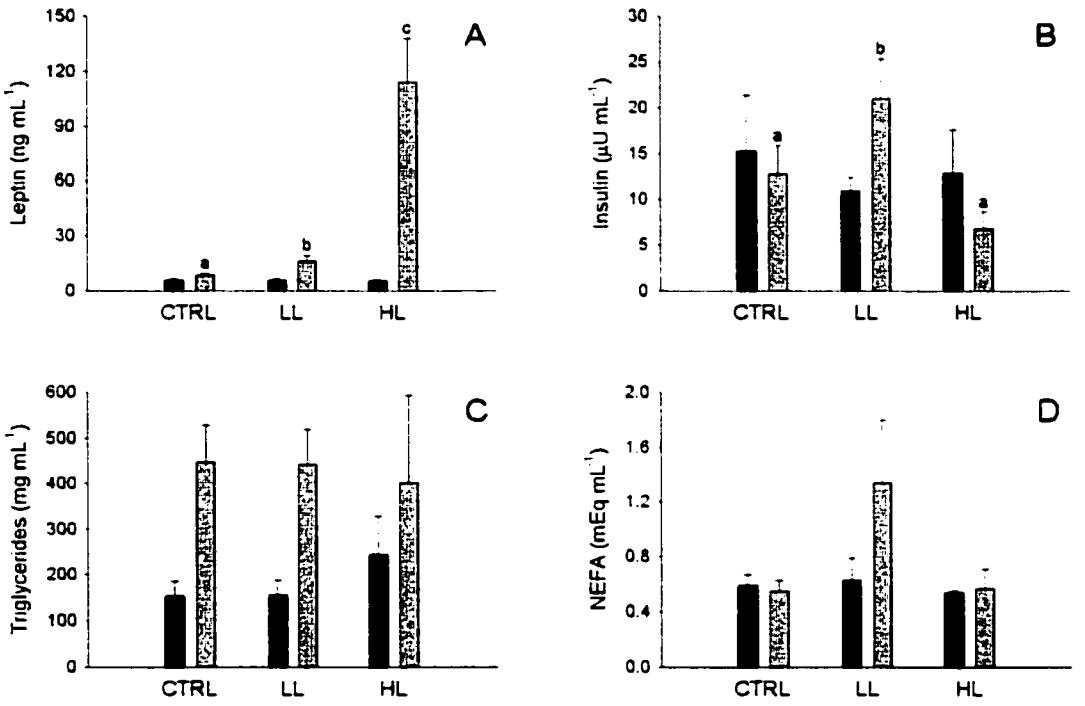

Figure 1.1. Serum parameters as a function of saline and leptin administration. Serum leptin (A), insulin (B), triglyceride (C), and nonesterified fatty acid (NEFA) (D) levels as a function of leptin administration in arctic ground squirrels during prehibernation fattening. CTRL = saline-infused, LL = low dose of mouse recombinant leptin (0.04 mg · kg^{-1} · day^{-1}), HL = high dose of mouse recombinant leptin (0.20 mg · kg^{-1} · day^{-1}). Black and gray bars represent pretest and posttest measurements, respectively. Values are means ± SE. Means within a given time period having different letters are significantly different ($P < 0.05$). Not indicated are significant increases in serum triglyceride levels ($P < 0.01$).

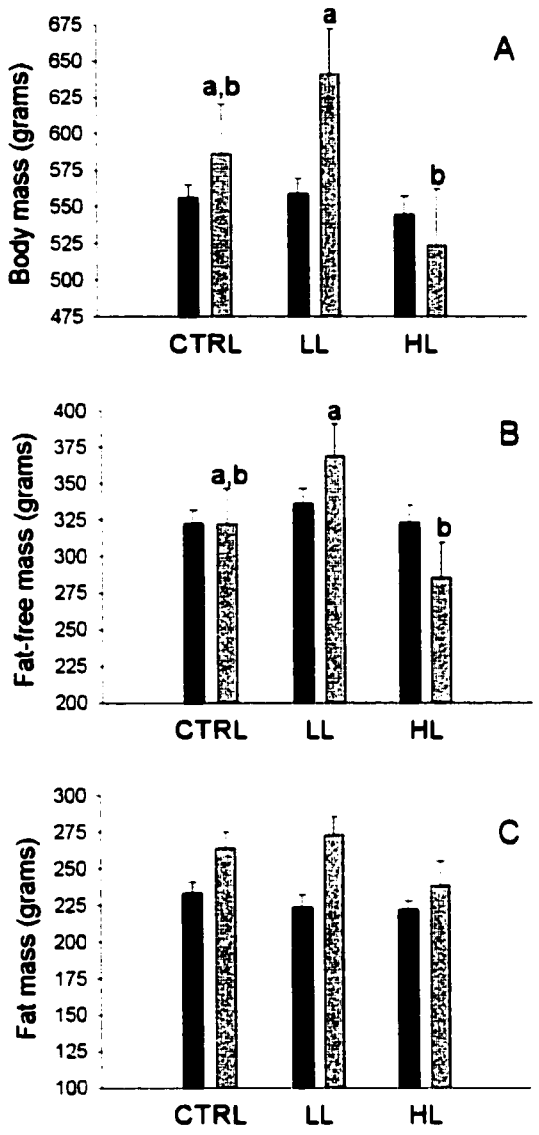

Figure 1.2. Body composition as a function of saline and leptin administration. Effect of continuous infusion of mouse recombinant leptin on body mass and composition (black and gray bars represent pretest and posttest measurements, respectively): total body mass (A), fat-free mass (B), and fat mass (C). Values are means + SE. Means for a given time period with different letters are significantly different ($P < 0.05$). Not indicated is a significant increase in fat mass over the duration of the experiment for all groups ($P < 0.001$).

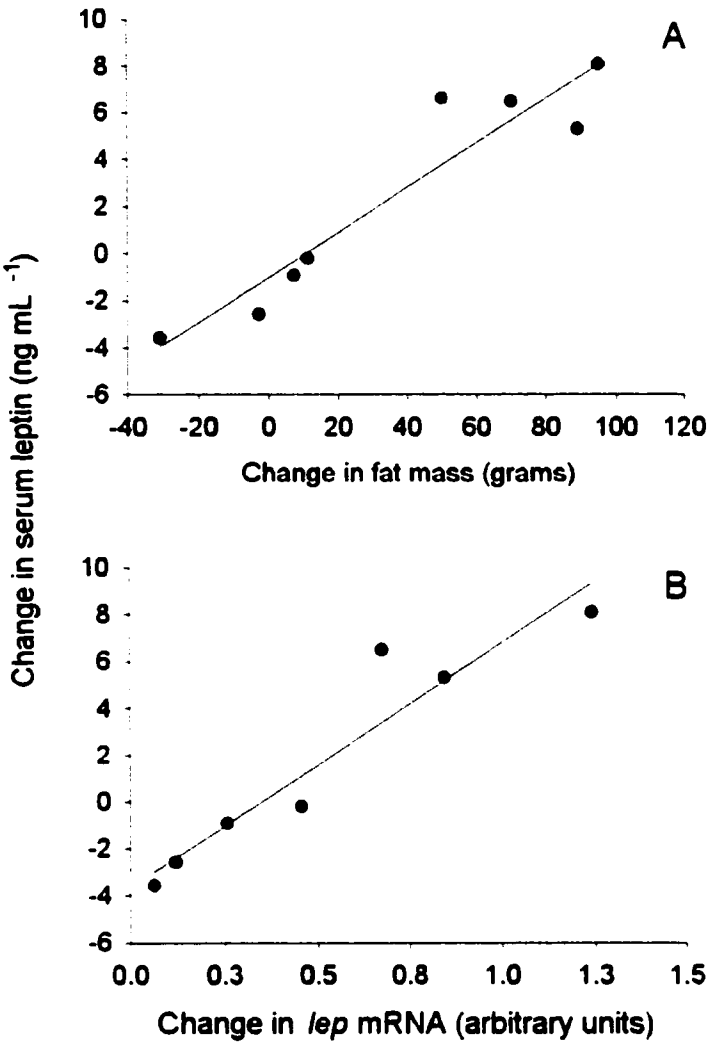

Figure 1.3. Relationships between fat mass, leptin expression, and serum leptin. Relationships between fat mass, leptin expression, and serum leptin in non-infused (CTRL) arctic ground squirrels over the period of prehibernation fattening. The change in fat mass was significantly related to the change in serum leptin ($P < 0.01$; $r^2 = 0.75$) (A); the change in *lep* mRNA levels was significantly related to serum leptin levels for CTRL squirrels over the period of prehibernation fattening ($P < 0.001$; $r^2 = 0.90$) (B). Not all animals could be included in these analyses due to missing samples (see RESULTS).

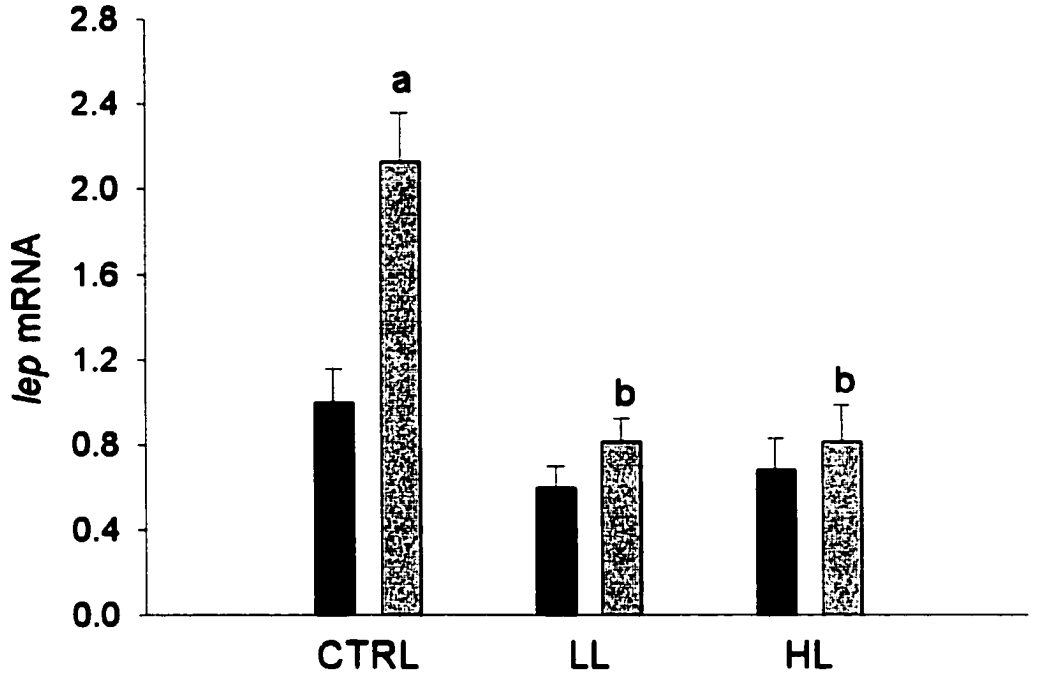

Figure 1.4. Effect of leptin infusion on *lep* mRNA levels.
Effect of continuous infusion of mouse recombinant leptin on *lep* mRNA levels (standardized to 18S rRNA) in subcutaneous white adipose tissue. Black and gray bars represent pretest and posttest measurements, respectively. Values are means + SE. Means for a given time period with different letters are significantly different ($P < 0.001$).

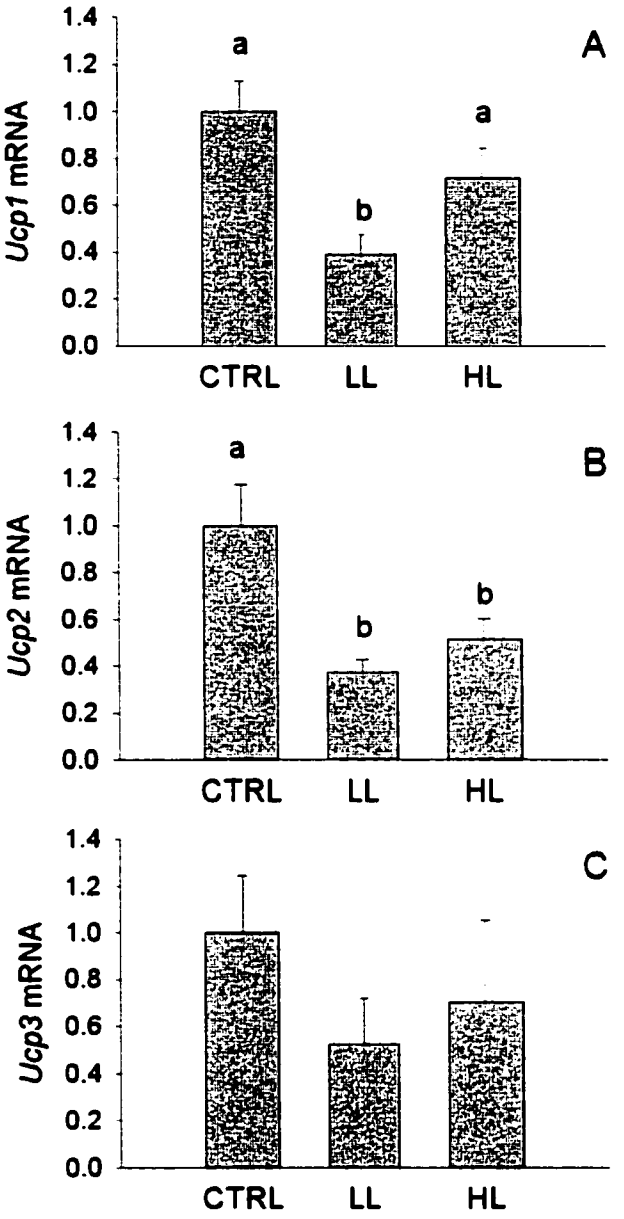

Figure 1.5. Uncoupling protein homologue mRNA levels as a function of saline and leptin administration.
Effect of continuous infusion of mouse recombinant leptin on posttest abundance of uncoupling protein (*Ucp*) homologue mRNAs (standardized to levels of 18S rRNA): *Ucp1* mRNA levels in brown adipose tissue (A); *Ucp2* mRNA levels in subcutaneous white adipose tissue (B); *Ucp3* mRNA levels in skeletal (gastrocnemius) muscle (C). Values are means + SE. Means with different letters are significantly different ($P < 0.01$).

CHAPTER 2 - REGULATION OF UCP1 AND UCP3 IN ARCTIC GROUND SQUIRRELS AND CORRELATION WITH MITOCHONDRIAL PROTON LEAK

Barger, J.L., Brand, M.D., Barnes, B.M., Boyer, B.B. Regulation of UCP1 and UCP3 in arctic ground squirrels and correlation with mitochondrial proton leak. Prepared for submission to Physiological Genomics.

ABSTRACT

Uncoupling protein 1 (UCP1) catalyzes a proton leak in brown adipose tissue (BAT) mitochondria that results in nonshivering thermogenesis (NST). UCP homologues have been identified in other tissues, but their contribution to NST is controversial. To clarify the role of *Ucp3* in thermoregulation during hibernation, we measured levels of *Ucp3* mRNA in skeletal muscle of arctic ground squirrels housed at 5°C or -10°C that were not hibernating, not hibernating and fasted for 48 h, or hibernating, and compared these to levels of *Ucp1* mRNA and UCP1 in BAT in the same animals. *Ucp3* mRNA levels were not affected by temperature but increased 10-fold with fasting and more than threefold during hibernation compared to non-hibernators. In a separate study, proton leak kinetics were unchanged in mitochondria isolated from skeletal muscle of fasted squirrels despite a nearly fivefold increase in UCP3 compared to fed controls. In contrast to *Ucp3*, *Ucp1* mRNA and UCP1 levels were increased upon cold exposure, decreased with fasting, and UCP1 levels were greatest in thermogenic hibernators. Mitochondrial proton leak did not differ between fed and fasted animals, but did show classical inhibition by purine nucleotides. Because levels of nonesterified fatty acids were highest during hibernation, we propose that the associated increase in *Ucp3* expression does not serve a thermogenic function, but instead protects against the accumulation of fatty acids in the mitochondrial matrix.

INTRODUCTION

Non-shivering thermogenesis (NST) is classically associated with the presence of uncoupling protein 1 (UCP1) in brown adipose tissue (BAT). UCP1 is a transmembrane protein located in the mitochondrial inner membrane, which upon activation by the sympathetic nervous system, allows for protons to re-enter the mitochondrial matrix without passing through ATP synthase. Heat is generated because the energy released in substrate oxidation is not conserved as ATP [reviewed in (55)]. Because UCP1 is found almost exclusively in BAT (54), the molecular mechanisms underlying NST in animals lacking BAT have remained elusive (2; 23; 33; 60).

Four genes have recently been identified that encode proteins homologous to UCP1 and may provide a possible explanation for NST in tissues other than BAT: UCP2 is expressed in a wide array of tissues and 55% similar to UCP1 (28); UCP3 is expressed in skeletal muscle and BAT and is 57% similar to UCP1 (5; 77); UCP4 and BMCP1 are expressed predominantly in neural tissues (48; 62) and are 29% and 34% similar to UCP1, respectively. In addition to sequence homology, the expression pattern of the new *Ucp* homologues is consistent with a role in NST: thyroid hormone, cold exposure, and high-fat diet were associated with increased levels of *Ucp* homologue mRNA levels (31; 44; 45; 81). Moreover, yeast transfected with human *Ucp3* have decreased membrane potential, suggesting that UCP3 may catalyze mitochondrial uncoupling (34; 38). Finally, *Ucp3* knockout mice have increased ATP synthesis in muscle (21) and mice overexpressing human *Ucp3* have elevated muscle temperatures (20), consistent with a role in energy metabolism.

However, other studies suggest that the UCP homologues other than UCP1 may not catalyze a mitochondrial proton leak that would contribute to NST *in vivo*. Decreased membrane potential in yeast expressing human *Ucp3* and increased uncoupled respiration in mice overexpressing human *Ucp3* may be an artifact of supraphysiological UCP3 levels, as mitochondrial proton leak in these model systems is not activated by superoxide or inhibited by nucleotides (16; 35). Furthermore, mitochondria isolated from the *Ucp3* (-/-) mice appear to be more coupled than wild-type mice, but *Ucp3* (-/-) mice are not obese, cold-sensitive, or hypothermic, suggesting that UCP3 does not exert a significant effect on whole-animal metabolism (32; 78). Finally, fasting, a physiological state characterized by energy sparing, decreases BAT *Ucp1* mRNA and UCP1 (19; 53) yet paradoxically increases *Ucp3* expression in skeletal muscle (31; 61) and heart muscle (75).

While the vast majority of studies investigating the function of the newly identified UCP homologues have utilized mice and rats, species which possess a greater capacity for metabolic heat production may be ideally suited for testing the hypothesis that UCP homologues mediate NST. The arctic ground squirrel (*Spermophilus parryii*) is able to its lower body temperature to -2.9°C during hibernation and then rewarm to 37°C during periodic arousal episodes (1). Consistent with a thermoregulatory role, levels of white adipose tissue *Ucp2* mRNA and skeletal muscle *Ucp3* mRNA are increased during hibernation in this species (6). In that study, however, squirrels classified as hibernators were housed at a range of ambient temperatures which itself influences levels of BAT UCP1 (41) and hibernating metabolic rate (12), and therefore the effects of temperature

and hibernation could not be separated. Because hibernation is essentially a prolonged period of fasting, it is possible that UCP2 and UCP3 do not serve a thermogenic purpose during hibernation, but are instead involved in the shift towards fatty acid metabolism (37).

To distinguish between these possibilities, we measured levels of *Ucp1* mRNA and UCP1 in BAT and levels of skeletal muscle *Ucp3* mRNA in arctic ground squirrels housed at 5°C or -10°C that were not hibernating, not hibernating and fasted for 48 h, or hibernating. If a gene (or its protein) is associated with NST, its abundance should increase when the animal is thermogenic but decrease during fasting. Similarly, the temperatures of tissues where the gene is expressed should be significantly elevated above ambient conditions during NST. Although *Ucp2* mRNA levels are elevated in WAT during hibernation in this species, the low mitochondrial density and oxidative capacity of this tissue (18) would have made it unsuitable for bioenergetic studies (below). Because fatty acids are the primary metabolic fuel during hibernation (69), and because a fasting-induced increase in *Ucp3* mRNA may be associated with the utilization of lipids as a metabolic substrate (80), serum nonesterified fatty acid (NEFA) levels are expected to be associated with hibernation and fasting. Finally, we determined whether fasting-induced changes in UCP1 and UCP3 were associated with changes in the kinetics of proton leak in mitochondria isolated from BAT and skeletal muscle.

MATERIALS AND METHODS

Experimental design

The first set of experiments were designed to determine if the increased levels of *Ucp3* mRNA during hibernation (6) are associated with thermoregulation or the fasted state by comparing the patterns of *Ucp3* mRNA abundance to that of *Ucp1* which encodes a protein (UCP1) known to mediate NST in BAT (55). Arctic ground squirrels were captured in the Alaska Range (64°N, elevation 1,200m) during late July and were transported to the University of Alaska Fairbanks. Animals were housed for one month at 15°C with a photoperiod tracking natural conditions at the site of capture and then were transferred to environmental chambers with a 4L:20D photoperiod and kept at either 5 or -10°C; these temperatures correspond to the lower end of the thermoneutral zone (63) and a typical burrow temperature (11) for this species, respectively. Mazuri Rodent Chow (St. Louis, MO), sunflower seeds, carrots and apple slices were available ad libitum for all animals; water was provided to animals housed at 5°C.

Animals were observed twice daily and on the first day of a hibernation bout (determined by posture and reduced respiration) wood shavings were applied to the dorsal surface of a squirrel. The persistence of wood shavings on the animal was used as the criterion for maintenance of torpor. Ground squirrels were included in the hibernating treatment group (HIB: $n_{5°C} = 8$, $n_{-10°C} = 11$) when they had remained torpid for at least five days after at least their third torpor bout. Active squirrels (ACT: $n_{5°C} = 5$, $n_{-10°C} = 9$) consisted of individuals who had not shown any incidence of torpor according to the above criterion. An additional group of non-hibernating squirrels at each temperature was subjected to a 48 h fast (FAST: $n_{5°C} = 4$, $n_{-10°C} = 4$). All animals were sampled between 12 November and 2 February. In order to control for possible seasonal variation (56),

ACT and HIB squirrels were pair-sampled; FAST squirrels were collected at three time points with ACT and HIB squirrels. Tissues from these animals were used for determination of levels of *Ucp1* mRNA, UCP1, *Ucp3* mRNA, and nonesterified fatty acids (NEFA). In seven squirrels hibernating at -10°C, a thermocouple was used to measure the temperature of several tissues immediately after they were exposed, but before the tissue was excised from the animal.

The second set of experiments in this study sought to determine if changes in *Ucp1,3* mRNA and UCP1,3 levels are accompanied by changes in mitochondrial proton leak. An additional set of arctic ground squirrels housed at 5°C was randomly assigned to a fed (n = 5) or fasted (n = 4) treatment group; feeding regimens were exactly as described above. To verify that the regulation of *Ucp1,3* during fasting was similar to that in the first study, tissues were collected from these animals for analysis of *Ucp1,3* mRNA. In addition, tissues were collected to isolate mitochondria for measurement of UCP1,3 and proton leak. All animals in this second set of experiments were sampled between 22 February and 28 March.

Tissue collection

Active (ACT and FAST) animals were lightly anesthetized with Halothane (Halocarbon Products; North Augusta, SC) and rectal temperature (T_{rect}) was measured by inserting a thermocouple approximately 2-3 cm into the rectum and allowing one minute for the reading to stabilize. Active animals with a T_{rect} less than 35°C were not used in this study. Blood was collected by cardiac puncture and serum was stored at -70°C for analysis of nonesterified fatty acids (NEFA) using a commercially available kit (Wako NEFA-C;

Richmond, VA). Following blood collection, active animals were deeply anesthetized with Halothane and decapitated. Hibernating animals were removed from their cage, T_{rect} was measured as described above, and blood was collected by cardiac puncture within five minutes; hibernators were then euthanized by decapitation. Axillary BAT and gastrocnemius muscle (hereafter referred to as skeletal muscle) were collected within five minutes, flash frozen in liquid nitrogen and stored at -70°C. When needed, additional quantities of BAT and skeletal muscle were excised and transferred to ice-cold buffers for isolation of mitochondria.

Uncoupling protein mRNA levels

Messenger RNA levels were quantified by northern analysis as described previously (6). Briefly, total RNA was isolated (TriReagent®) and fractionated on 1.25% denaturing agarose gels. RNA was then blotted and UV-crosslinked to nylon membranes (Hybond N+, Amersham Biosciences; Piscataway, NJ). *Ucp1* mRNA was detected using a highly conserved 27-bp oligonucleotide probe (10) and *Ucp3* mRNA was detected using a 29-bp oligonucleotide probe (5'-CCTTCCTCCCTGGCGATGGTTCTGTAGGC-3') specific to arctic ground squirrel *Ucp3* (Boyer, unpublished). Blots were later reprobed for 18S rRNA to adjust for variations in RNA loading. All autoradiograph exposures were maintained within the linear range of the film (Amersham Hyperfilm). Quantification of *Ucp* homologue mRNA levels was determined by densitometric analysis of autoradiographs (6).

Uncoupling protein abundance

UCP1 protein was detected from BAT homogenates (UCP1 expression pattern experiments) and from mitochondria isolated from BAT (UCP1 and proton leak experiments) by chemiluminesence (ECL Western Blotting System; Amersham Biosciences). BAT homogenates were prepared in ice-cold buffer (50 mM PIPES, 25 mM KCl, 1 mM EGTA, 1 mM $MgCl_2$, and 1 mM PMSF) with a protease inhibitor cocktail (1 mM benzamidine, 0.1 mM phenanthroline, 1 mg aprotonin $\cdot$ mL^{-1}, 1 mg leupeptin $\cdot$ mL^{-1}, and 1 mg pepstatin A $\cdot$ mL^{-1}) added immediately before homogenization at a concentration of 0.1 mL per 10 mL of buffer. Dithiothreitol was added to the final homogenate at a concentration of 0.1 mM. Total protein concentration was determined using the bicinchoninic acid assay (Pierce Chemical BCA Protein Assay Kit) and homogenates were then stored at -70°C.

BAT homogenates and previously frozen mitochondria were fractionated (5 μg protein) in 12.5% SDS-polyacrylamide gels and transferred to nitrocellulose membranes (Hybond ECL; Amerhsam Biosciences). UCP1 was detected with a rabbit anti-rat UCP1 serum as described (7). To estimate the absolute concentration of UCP1, at least four known concentrations of murine UCP1 purified from *E. coli* inclusion bodies (70) were included in each blot. The abundance of arctic ground squirrel UCP1 was estimated by interpolation of the linear regression between the known UCP1 concentration and subsequent densitometric units.

We attempted to quantify UCP3 using both mitochondrial protein isolated from the frozen tissue and from previously frozen mitochondria; however, UCP3 was consistently degraded and consequently unsuitable for quantitation. Therefore, skeletal

muscle mitochondria were isolated (see below) from an additional set of fed (n = 4) and fasted (n = 5) arctic ground squirrels and immediately used for western blotting. UCP3 was detected using 25 μg of mitochondrial protein essentially as described for UCP1 except that blots were hybridized for 12 h at 5°C with an antibody specific to amino acids 295-308 of mouse and rat UCP3 (Affinity Bioreagents; Golden, CO) at a concentration of 1:1000. Under these conditions, arctic ground squirrel UCP3 was observed at the same molecular weight as a positive control (approximately 34kDa in mouse heart mitochondrial protein) and no hybridization was observed with a negative control (mitochondrial protein from *Ucp3* (-/-) mice). UCP3 levels were quantified by interpolation from known concentrations of human UCP3 obtained from *E. coli* inclusion bodies (35).

Isolation of mitochondria

All procedures were performed on ice and all centrifuge spins were conducted at 2 ± 2°C. Unless otherwise noted, all reagents were obtained from Sigma-Aldrich (St. Louis, MO). Mitochondria were isolated from BAT essentially as described (17). Briefly, axillary BAT was excised from the animal and rapidly transferred to an excess of ice-cold homogenization buffer (250 mM sucrose, 5 mM K-TES (*N*-tris[hydroxymethyl]-2-aminoethanesulfonic acid) pH 7.2). The tissue was then minced with a razor blade on a glass plate over ice and transferred to a Dounce tissue homogenizer. Using a loose-fitting pestle, the tissue was homogenized using 5-6 strokes, filtered through two layers of gauze, and centrifuged at 8,500 *g* for 10 min. The lipid layer was removed by aspiration, the supernatant was discarded, and the lipid remaining

on the inside walls of the tube were removed using a paper tissue. The pellet was resuspended in homogenization buffer, centrifuged at 800 *g* for 10 min, and the resulting supernatant was transferred to a new tube and centrifuged at 8,500 *g* for 10 min. The crude mitochondrial pellet was then resuspended in homogenization buffer containing 0.5% fatty acid-free bovine serum albumin (BSA; Intergen, Purchase, NY) to chelate endogenous fatty acids. This suspension was centrifuged at 8,500 *g* for 10 min, and the final mitochondrial pellet was resuspended in a buffer to expand the mitochondria matrix (100 mM KCl and 5 mM K-TES pH 7.2). Integrity of isolated mitochondria was estimated by duplicate measurements of the respiratory control ratio, defined as state 3 respiration (in the presence of 250 μM ADP) divided by state 4 respiration (see below). BAT mitochondria isolated by this procedure always had respiratory control ratios > 2 in the presence of 2 mM guanosine diphosphate (GDP) which blocks the proton leak pathway in UCP1.

Skeletal muscle was trimmed of fat and connective tissue, finely minced with a razor blade on a glass plate over ice, and transferred to a beaker containing ice-cold wash buffer (100 mM KCl, 50 mM Tris-HCl, and 2 mM EGTA). The excess buffer was poured off and replaced with additional buffer; this process was repeated an additional five times to remove any hair, fat, and connective tissue from the preparation. After the final wash, excess buffer was poured off and replaced with a digestion buffer (10 mL · g^{-1} tissue) containing 100 mM KCl, 50 mM Tris-HCl, 2 mM EGTA, 0.5% fatty acid-free BSA, 5 mM $MgCl_2$, 1 mM ATP, and nagarse (18.7 units · g^{-1} tissue). This mixture was kept on ice for 10 min with occasional stirring and was then briefly (20 s) homogenized with a

Polytron. This homogenate was kept on ice for an additional 10 min with occasional stirring and then spun at 490 *g* for 10 min. The supernatant was filtered through three layers of gauze and spun at 10,500 *g* for 10 min. The crude mitochondrial pellet was resuspended in excess wash buffer and subjected to an additional high-speed spin cycle. The final pellet was resuspended in a minimal volume of wash buffer and kept on ice. Skeletal muscle mitochondria isolated by this procedure always had respiratory control ratios > 3.5.

Protein concentration of all mitochondria preparations was determined in duplicate by the bicinchoninic acid assay (Pierce Chemical BCA Protein Assay Kit; Rockford, IL) with BSA as the standard. Mitochondria not used for the proton leak assay were stored at -70°C for determination of UCP content by western blotting.

Proton leak assay

A convenient method to assess mitochondrial uncoupling involves parallel measurements of state 4 oxygen consumption and mitochondrial membrane potential ($\Delta\psi_m$); under these conditions, the only avenue for protons to return to the mitochondrial matrix is via a specific transport protein (such as UCP1) or by the idiopathic proton leak pathway endogenous to all mitochondria (8). A dual-channel chart recorder (Kipp and Zonen; The Netherlands) was interfaced with both a Rank Brothers Model 10 oxygen electrode (Cambridge, UK) to record oxygen consumption and an ion-specific electrode to measure mitochondrial membrane potential ($\Delta\psi_m$), determined by uptake of the lipophilic cation triphenylmethylphosphonium (TPMP) using the following equation:

$$\Delta\psi m = 61.5 \log \left\{ \frac{([\text{TPMP}]\ \text{added} - [\text{TPMP}]\ \text{external}) \times \text{TPMP binding correction}}{0.001 \times [\text{protein}] \times [\text{TPMP}]\ \text{external}} \right\}$$

To estimate the concentration of TPMP in the assay buffer ([TPMP] external), a standard curve of TPMP concentration and chart recorder distance was generated with incremental additions of TPMP (1, 2, 3, 4, 5 μM) for each assay (9). Mitochondrial TPMP binding corrections were 0.2 for BAT (52) and 0.35 for skeletal muscle (59). Electrode drift was corrected after each run by addition of 2 μM carbonyl cyanide *p*-(trifluoromethoxy)phenylhydrazone (FCCP). All assays were performed at least in duplicate and frequently in triplicate.

Mitochondria (BAT = 1 mg protein · mL^{-1}, skeletal muscle = 0.5 mg · mL^{-1}) were assayed at 37°C in buffer containing 120 mM KCl, 5mM KH_2PO_4, 3 mM HEPES, 1 mM EGTA, 0.3% fatty-acid free BSA, pH 7.2; it was assumed that this buffer contained 406 nmol O · mL^{-1} buffer (58). All proton leak assays contained 5 μM rotenone (to inhibit oxidation of endogenous NADH), 1 μg oligomycin · mL^{-1} assay buffer (to inhibit the F_oF_1 ATP synthase and therefore establish state 4 conditions), and 80 ng nigericin · mL^{-1} assay buffer (to clamp ΔpH at zero); these additions were allowed to equilibrate with mitochondria for at least one minute prior to analysis. Succinate (5 mM) was used as a substrate in all experiments and malonate was added in 0.3 mM increments to titrate the $\Delta\psi_m$; BAT mitochondria were assayed in the absence or presence of 2 mM GDP; this was the minimum concentration of GDP required to completely inhibit proton leak (data not shown). Skeletal muscle mitochondria were assayed in the presence of 2 mM $MgCl_2$

to minimize pathways for nonphysiological proton leak (14). Representative traces for the proton leak assay in BAT mitochondria are shown in Figure 2.1.

Statistical analysis

Data were analyzed using SAS for Windows (SAS Institute, Cary, NC). All means are presented with standard errors. Levels of serum NEFA and expression patterns of uncoupling proteins were analyzed using a two-way analysis of variance (ANOVA) with housing temperature (5 or -10°C) and activity (ACT, FAST, and HIB) as main effects; post-hoc comparisons among means were made using least-squares means. Tissue temperatures of hibernating arctic ground squirrels were compared by ANOVA with tissue as the main effect; Duncan's multiple comparisons procedure was used to identify significant differences among tissues. Comparisons between fed and fasted animals (UCP/proton leak experiments) were made using Student's *t*-tests.

RESULTS

Body and tissue temperatures

The mean T_{rect} of all hibernators housed at 5°C was significantly greater than that of all hibernators housed at -10°C (5.6 ± 0.2 vs. 0.4 ± 0.3°C; $P < 0.0001$), with three animals in the latter group having a T_{rect} less than 0°C. The mean temperatures of several tissues from seven animals housed at -10°C were significantly different among regions (Table 1). Average temperatures in brain, axillary BAT and neck were higher than all other regions. Average temperatures in the rectum, liver, and abdominal white adipose tissue were similar to each other but lower than the previous tissues. Average gastrocnemius

temperature was similar to abdominal white adipose tissue, but was significantly lower than all other regions measured.

Patterns of Ucp1 expression and abundance of UCP1

Levels of *Ucp1* mRNA and UCP1 were significantly greater in cold- versus warm-exposed animals. Activity status significantly affected both *Ucp1* mRNA and UCP1 levels, but the effect of activity on *Ucp1* mRNA levels was statistically similar for each housing temperature (Figure 2A). At the protein level, however, there was a significant interaction between the effects of housing temperature and activity class (Figure 2B): UCP1 levels were highest in hibernators housed at -10°C, followed by active animals housed at -10°C and 5°C. Levels of BAT UCP1 were lowest in hibernators housed at 5°C and both fasted groups. *Ucp1* mRNA was not detected in skeletal muscle (data not shown), and therefore all references to *Ucp1* mRNA and UCP1 will hereafter pertain specifically to results obtained in BAT.

Relationship between Ucp1 and proton leak

To assess the relationship between fasting-induced changes in UCP1 and mitochondrial proton leak, we quantified the levels of *Ucp1* mRNA and UCP1 in the same tissues from which mitochondria were isolated. Similar to the study of *Ucp1* expression patterns (above), a 48 h fast significantly decreased levels of *Ucp1* mRNA but only marginally ($P = 0.05$) decreased levels of UCP1 (Figure 2.3).

The maximal rate of proton leak occurs under state 4 conditions, and in the absence of GDP the maximal leak rate and membrane potential were not significantly different between fed and fasted groups. Similarly, maximal proton leak rate and

membrane potential were not significantly different between treatments in the presence of 2 mM GDP. However, addition of 2 mM GDP significantly decreased state 4 oxygen consumption and increased state 4 membrane potential, although the magnitude of these changes did not differ between fed and fasted groups. At both concentrations of GDP, the overall kinetics of the proton leak in BAT mitochondria were unaffected by fasting-induced decreases in UCP1 as oxygen consumption did not differ between fed and fasted groups at common values of $\Delta\psi_m$ (Figure 2.4).

Patterns of Ucp3 expression

Levels of *Ucp3* mRNA were unaffected by cold exposure. However, *Ucp3* mRNA abundance was significantly different among activity classes with levels being greatest in fasted animals, followed by hibernating animals, with active animals having the lowest levels of *Ucp3* mRNA. This trend among activity states was statistically similar for each housing temperature (no significant interaction between housing temperature and activity status; Figure 2.5). *Ucp3* mRNA was not detected in BAT (data not shown), and therefore, all references to *Ucp3* mRNA and UCP3 will hereafter pertain specifically to results obtained in skeletal muscle.

Relationship between Ucp3 and proton leak

To assess the relationship between fasting-induced changes in UCP3 and mitochondrial proton leak, we quantified the levels of *Ucp3* mRNA in the same tissues from which mitochondria were isolated and quantified levels of UCP3 in mitochondria isolated from animals that were treated identically to those used in the proton leak experiments. Similar to the study of *Ucp3* expression patterns (above), a 48 h fast significantly increased levels

of *Ucp3* mRNA (Fig 6*A*); levels of UCP3 were also significantly increased after fasting (Figure 2.6B).

Maximal rates of proton leak and membrane potential (state 4 conditions) were not significantly different between fed and fasted groups. Similarly, the overall kinetics of the mitochondrial proton leak were similar between groups, as the oxygen consumption was not significantly different between groups at common values of $\Delta\psi_m$ (Figure 2.7).

Serum nonesterified fatty acids

Serum NEFA levels were not significantly different between housing temperatures. NEFA levels were significantly affected by the activity class, with hibernating animals having the greatest concentration, followed by active and fasted groups which were not significantly different. The trend among activity states was statistically similar for each housing temperature (Figure 2.8).

DISCUSSION

The overall goal of this study was to determine if the increase in *Ucp3* mRNA levels reported previously in this species (6) reflects a novel mechanism for NST during hibernation by integrating measurements at the molecular, sub-cellular, and tissue levels. Consistent with its established role in mediating NST, levels of *Ucp1* mRNA and UCP1 in BAT were increased during cold exposure and decreased after fasting. In contrast, levels of *Ucp3* mRNA did not change as a function of cold exposure and levels of both *Ucp3* mRNA and UCP3 increased after a 48 h fast. Despite a nearly fivefold increase in UCP3, mitochondrial proton leak was unchanged. Furthermore, the temperature of the

gastrocnemius muscle was significantly colder than that of BAT in squirrels housed at -10°C. Together, these data do not support the hypothesis that UCP3 is a mediator of NST in skeletal muscle; rather, the increased levels of *Ucp3* mRNA and during fasting and hibernation are more readily explained by the hypothesized role of UCP3 as a mediator of fatty acid metabolism.

Regulation of Ucp1 by temperature, fasting, and hibernation

Cold exposure increases thermogenic capacity of BAT via mitochondrial biogenesis and increases in UCP1 content (41; 71); conversely, the amount and activity of UCP1 are decreased during fasting to promote metabolic efficiency (36; 53; 74). We explored this paradigm in the arctic ground squirrel by housing groups of animals (non-hibernators and non-hibernators subjected to a 48 h fast, and hibernators) under one of two ambient temperatures (5 and -10°C). Results from the expression pattern experiments clearly support the hypothesis that UCP1 is a mediator of futile proton cycling. In agreement with a thermoregulatory role, cold-exposed animals had significantly greater levels of *Ucp1* mRNA and UCP1 (-10°C versus 5°C). Consistent with studies in mice (53; 74) and rats (19), a 48 h fast decreased levels of both *Ucp1* mRNA and UCP1 in arctic ground squirrels (Figure 2.2). However, the magnitude of the fasting-induced decrease in *Ucp1* mRNA levels was not different between housing temperatures.

During steady-state hibernation at temperatures > 0°C, thermogenesis is minimal, body temperature parallels ambient temperature, and the role of UCP1 in hibernating species is instead associated with rewarming to a high body temperature during periodic arousal bouts (68). In general, levels of *Ucp1* mRNA and UCP1 for a given species are

similar among non-hibernators housed at cold temperatures (> 0°C), hibernators in deep torpor, and during arousal from hibernation—heat is generated during arousal by activating the preexisting UCP1 (46; 49; 51). In this study, we observed a similar absence of NST during hibernation: the rectal temperature of hibernators housed at 5°C averaged 5.6 ± 0.2°C and levels of *Ucp1* mRNA and UCP1 were not elevated in hibernators housed at 5°C compared to non-hibernators (Figure 2.2). In contrast to the pattern at 5°C, BAT UCP1 appears to play a vital role in maintaining a relatively high body temperature in hibernators housed at -10°C (average rectal temperature of these animals was 0.2 ± 0.4°C, Table 1): levels of UCP1 were greatest in hibernators housed at -10°C compared to all other treatment groups, and were more than twofold greater than hibernators housed at 5°C (Figure 2.2B). This agrees with a previous study in this species that reported increased levels of *Ucp1* mRNA in hibernators housed under similar conditions (6), although the data from this study suggest that the increase at the mRNA level is due to cold exposure and not hibernation. In addition to the abundance of UCP1, measurements of the BAT temperature support the importance of UCP1-mediated NST during thermogenic hibernation. The average temperature of the axillary BAT pad of cold-exposed hibernators was 3.5 ± 0.7°C, significantly greater than peripheral tissues such as liver, abdominal white adipose tissue, and gastrocnemius muscle (Table 1), and approximately 13.5°C warmer than the ambient temperature. The metabolic rate of hibernating arctic ground squirrels is also elevated at low ambient temperatures < 0°C (12), and our data suggest that the increased metabolic rate is accounted for in part by increased activity of UCP1-mediated NST. It is interesting to note that while hibernation

is essentially a prolonged fast, the abundance of UCP1 depends on the thermogenic context: UCP1 is maintained at low levels at 5°C but increased in squirrels housed at -10°C, possibly as a result of increased adrenergic stimulation of BAT leading to a increased half-life of UCP1 (57). Thus, hibernation at temperatures < 0°C is qualitatively and quantitatively different at both the molecular and whole-animal levels.

UCP1-mediated proton leak

In the proton leak experiments, fasting decreased levels of *Ucp1* mRNA and UCP1 in animals housed at 5°C (Figure 2.3), although the magnitude of the decrease in UCP1 was smaller than in the experiments comparing the expression patterns of UCP1 (Figure 2.2B). Despite a 27% reduction in the mitochondrial content of UCP1, the kinetics of the proton leak assayed in BAT mitochondria were identical between fed and fasted groups: mitochondrial membrane potential was not increased and respiration was not decreased (Figure 2.4). Although the reduction in UCP1 was modest, the technique used to estimate proton leak should have been able to resolve a difference in proton leak: we observed an absolute decrease of 4.7 μg UCP1 · mg^{-1} BAT mitochondrial protein without a change in kinetics, whereas Stuart et al. (70) detected increased proton leak kinetics of UCP1-transformed yeast mitochondria (1 μg UCP1 · mg^{-1} mitochondrial protein) compared to empty vector controls using similar methods. An inability to detect changes in proton leak may be due to contamination of cytosolic nucleotides liberated during the isolation of mitochondria (39). These nucleotides (probably ATP) mask UCP1-mediated proton leak by binding to regions of the proton that inhibit proton translocation. It is therefore possible that small concentrations of cytosolic nucleotides caused mitochondria

from the fed groups to appear more coupled, despite a greater concentration of UCP1 (compared to the fed groups). Alternatively, if UCP1 is activated by fatty acids (47), a difference in UCP1-mediated leak would not be observed when mitochondria were assayed in the presence of BSA. Unfortunately, this cannot be directly tested because BSA is required to prevent the non-specific uncoupling effect of fatty acids in all mitochondria (67). In any case, we did observe the classical inhibition of proton leak by purine nucleotides in isolated BAT mitochondria: in the presence of 2 mM GDP maximal state 4 respiration was significantly decreased and membrane potential was increased, although values did not differ between fed and fasted groups (Figure 2.4). Moreover, proton leak at a membrane potential of approximately 130 mV was nearly 10-fold lower in the presence of 2 mM GDP.

Interestingly, absolute levels of BAT UCP1 measured in this study appear to be lower than those reported in the literature for other species: the average UCP1 concentration for all of the non-fasted animals in the UCP1 expression experiments was 8 μg UCP1 $\cdot$ mg^{-1} BAT protein, approximately one-sixth of that reported for mice, rats, and hamsters (70), and one-tenth of that reported for Richardson's ground squirrels, *Spermophilus richardsonii* (51). The low levels observed in Figure 2.2B are due in part to procedural differences: UCP1 was quantified in homogenates of brown adipose tissue, whereas published studies typically measure the quantity of UCP1 from the mitochondrial fraction of BAT. Accordingly, when UCP1 levels were estimated from mitochondria isolated from BAT (Figure 2.3B), levels of UCP1 were closer to (but still lower than) values reported in the literature for other species. Our estimate of UCP1

protein is probably underestimated due to the differential hybridization affinity between the antigens (arctic ground squirrel UCP1 and mouse UCP1 standards) and the antibody (rabbit anti-rat UCP1 serum); other studies have isolated a species-specific UCP1 for protein standards in conjunction with either anti-rat (51) or species-specific antiserum (56), which undoubtedly increases the accuracy of the estimate of the true UCP1 abundance.

Regulation of Ucp3 by temperature, fasting, and hibernation

Although UCP3 possesses sequence homology to UCP1, it is not regulated in a similar manner by temperature, and is regulated in the opposite direction during fasting (Figure 2.5). In skeletal muscle, we found no cold-induced increase in the levels of *Ucp3* mRNA: for a given activity class, *Ucp3* mRNA levels were nearly identical between the two housing temperatures. Additionally, a 48 h fast induced an approximately 10-fold increase in *Ucp3* mRNA compared to active squirrels. These results are not surprising, as cold exposure does not increase skeletal muscle *Ucp3* mRNA levels in other species (4; 45; 65; 79, but see 66) and fasting elicited an increase in *Ucp3* mRNA in numerous studies (50; 61; 75; 80).

Levels of *Ucp3* mRNA were significantly increased more than threefold in hibernators compared to fed non-hibernators, but were lower than fasted squirrels. Boyer et al. (6) reported a similar finding in this species, but it was previously unknown if the increase in *Ucp3* mRNA levels during hibernation could be attributed to the effects of fasting. The data from this study cannot eliminate this possibility, but fasting elicited a much larger increase than that observed in hibernators which suggests an effect of

hibernation *per se*. The increase in *Ucp3* mRNA levels during hibernation is intriguing, but our data do not suggest that it serves a thermogenic role in this context: levels of *Ucp3* mRNA were unaffected by cold exposure even though animals housed at -10°C have a greater demand for NST. Additionally, the average temperature of the gastrocnemius muscle (the same tissue from which levels of *Ucp3* mRNA were measured) of hibernators housed at -10°C was -1.5 ± 0.4 °C, significantly lower than all other tissues measured except for abdominal adipose tissue (Table 1). Even though skeletal muscle temperatures were 8.5°C warmer than ambient conditions, this is significantly lower than an actively thermogenic organ such as BAT. The increased temperature of skeletal muscle relative to ambient temperature is more likely achieved by perfusion of blood warmed by BAT rather than a local increase in metabolic activity (29). Taken together, these data cast doubt on the hypothesis that UCP3 mediates NST in skeletal muscle.

UCP3-mediated proton leak

In the proton leak experiments, levels of *Ucp3* mRNA were elevated about fourfold and levels of UCP3 protein were elevated nearly fivefold after a 48 h fast (Figure 2.6). Despite the pronounced increase in *Ucp3* mRNA and UCP3, the kinetics of the proton leak in mitochondria isolated from skeletal muscle were unchanged: an increase in proton leak would be seen as both an increase in the rate of oxygen consumption at high membrane potentials and as a decrease in maximal membrane potential, but no such change was observed (Figure 2.7). These data agree with other studies wherein changes in proton leak in skeletal muscle mitochondria did not correlate with fasting-induced

changes in UCP3 (3; 15; 40), but are at odds with other studies that suggest that mitochondrial proton leak is increased in yeast expressing human *Ucp3* (38; 82) and transgenic mice overexpressing human *Ucp3* (20).

Recent studies suggest that genetic manipulation of *Ucp3* expression increases proton leak due to supraphysiological expression of *Ucp3* leading to artifactual mitochondrial uncoupling. When transfected yeast express *Ucp3* at levels similar to that found in mouse and rat skeletal muscle mitochondria (~0.15 μg UCP3 · mg^{-1} mitochondrial protein), proton leak is identical to empty-vector controls (35), suggesting that physiological levels of UCP3 do not uncouple yeast mitochondria. When yeast express *Ucp3* at high levels (~0.90 μg UCP3 · mg^{-1} mitochondrial protein), mitochondrial proton leak is increased; however, this increased proton cycling is not physiological as the proton leak is not sensitive to GDP which has been shown to inhibit UCP3-mediated proton leak in proteoliposomes (26). Similarly, proton leak in skeletal muscle mitochondria isolated from transgenic mice overexpressing human *Ucp3* is increased fourfold, but this was due to a 20-fold increase in UCP3 (> 3,000 μg UCP3 · mg^{-1} mitochondrial protein) compared to wild type (16). Moreover, the stimulation of proton leak by superoxide (25) and fatty acids was similar between wild type and *Ucp3* overexpressing mice (16), suggesting that decreased membrane potential and increased respiration are an artifact of a high abundance of non-native UCP3. It is worth noting that the absolute levels of UCP3 in mouse skeletal muscle are 200-700 times lower than that of UCP1 in BAT mitochondria (35); similarly, skeletal muscle UCP3 is found at a concentration approximately 400 times lower than that of UCP1 in BAT of arctic ground

squirrels housed at 5°C (Figs. 3B and 6B). Although *Ucp3* expression is increased during hibernation, the comparatively low abundance of UCP3 underscores the notion that UCP3 is not a likely candidate for thermoregulatory uncoupling in skeletal muscle.

Regulation of Ucp3 by fatty acids

Expression of *Ucp3* is stimulated by fasting-induced increases in fatty acids (76) and by lipid infusion (27; 43; 80). In arctic ground squirrels, fasting induced a 10-fold increase in skeletal muscle *Ucp3* mRNA (pooled across temperature groups), although the resulting twofold increase in NEFA levels was not significantly different compared to active squirrels (Figure 2.8). Regulation of *Ucp3* expression by fatty acids is mediated by the family of peroxisome proliferator-activated receptors (PPARs) (42), and activation of a particular PPAR subtype may explain the induction of *Ucp3* with only modest increases in NEFAs: administration of PPARα agonists increased expression of *Ucp3* in BAT (72) and PPARγ agonists increased expression of *Ucp3* in skeletal muscle (72) and in C_2C_{12} myotubes cultured in the presence of oleic acid (13). Interestingly, the highest levels of NEFAs were seen in hibernating squirrels (increased by more than fivefold compared to fasted animals), yet skeletal muscle *Ucp3* mRNA levels were one-third of the levels seen in fasted squirrels. It is unclear why further increases in NEFA do not result in further increases in *Ucp3* mRNA levels, although levels of UCP3 may have increased to sufficient levels by the time tissues were sampled from hibernators. Because NEFA levels are significantly elevated during hibernation, and because UCP3 does not appear to function in a thermoregulatory context, we propose that the increase in *Ucp3* mRNA during hibernation likely serves to protect against mitochondrial lipotoxicity as proposed

by Himms-Hagen and Harper (37). Confirmation of this hypothesis requires further experimentation.

In summary, the bulk of the experimental evidence suggests that UCP3 is not involved in mediating NST in skeletal muscle during hibernation. While it is possible that we may have observed an increase in UCP3-mediated proton leak using alternative assay conditions (25; 66), this uncoupling is not likely to be thermogenic for at least two reasons: (1) expression of *Ucp3* mRNA is regulated in a dissimilar manner compared to that of a known thermogenic mediator, *Ucp1*, and (2) the levels of UCP3 in skeletal muscle are several hundred-fold less than that of UCP1 in BAT. Furthermore, the temperature of BAT strongly suggests it is a site of potent thermogenesis during hibernation, whereas the temperature of skeletal muscle remains extremely low despite the increase in *Ucp3* mRNA during hibernation.

PERSPECTIVES

The data from this study demonstrate that the increase in *Ucp3* mRNA during hibernation is unlikely to reflect an alternative source of NST. These results are in agreement with a growing body of evidence that suggests that the primary function of UCP3 is to export fatty acid anions from the mitochondrial matrix when they circulate in an excessive concentration and protect against mitochondrial lipotoxicity (37; 64). This model is supported by the observation that fasting involves a shift towards lipid metabolism (reflected by increased circulating NEFA levels) and that the transport of fatty acid anions is an established attribute of UCP1 (30). Because NEFA levels are significantly elevated during hibernation, it seems more likely that the increase in *Ucp3* mRNA during

hibernation is related to protection against mitochondrial lipotoxicity. Alternatively, the finding that proton leak via UCP2 and UCP3 is stimulated by superoxide (24; 25) suggests that elevated levels of uncoupling proteins may serve to decrease production of reactive oxygen species that may be formed during reperfusion of peripheral tissues during arousal from hibernation. Activation of UCP3 by superoxide requires the presence of fatty acids, and the high levels of serum NEFA in this species during hibernation may provide a suitable milieu for activation of this proton leak pathway in multiple tissues. Previous studies have implicated antioxidants (e.g. ascorbate) as a mechanism to protect against oxidative damage during arousal from hibernation (22; 73), but prevention of the formation of reactive oxygen species via UCP homologues may provide a frontline of defense against oxidative damage.

ACKNOWLEDGEMENTS

The authors wish to thank Ruth Stafford for excellent technical assistance, Drs. Barbara Cannon and Jan Nedergaard for anti-rat UCP1 serum, Dr. Brad Lowell for mitochondrial protein from *Ucp3* knockout mice, Dr. James Harper for assistance with UCP3 westerns, and Drs. Abel Bult-Ito, Kelly Drew, and Dana Thomas for evaluation of the manuscript. This work was done during the tenure of graduate student research fellowships from the American Heart Association Alaska Affiliate and from the NSF Alaska-EPSCoR program (J.L.B.) and was supported by DEPSCoR grant #N00014-01-1-0907 (B.B.B).

REFERENCES

1. **Barnes BM**. Freeze avoidance in a mammal: body temperatures below 0°C in an Arctic hibernator. *Science* 244: 1593-1595, 1989.

2. **Barre H, Cohen-Adad F and Rouanet JL**. Two daily glucagon injections induce nonshivering thermogenesis in Muscovy ducklings. *Am J Physiol Endocrinol Metab* 252: E616-E620, 1987.

3. **Bezaire V, Hofmann W, Kramer JK, Kozak LP and Harper ME**. Effects of fasting on muscle mitochondrial energetics and fatty acid metabolism in *Ucp3(-/-)* and wild-type mice. *Am J Physiol Endocrinol Metab* 281: E975-E982, 2001.

4. **Boss O, Samec S, Kuhne F, Bijlenga P, AssimacopoulosJeannet F, Seydoux J, Giacobino JP and Muzzin P**. Uncoupling protein-3 expression in rodent skeletal muscle is modulated by food intake but not by changes in environmental temperature. *J Biol Chem* 273: 5-8, 1998.

5. **Boss O, Samec S, Paoloni-Giacobino A, Rossier C, Dulloo A, Seydoux J, Muzzin P and Giacobino JP**. Uncoupling protein-3: a new member of the mitochondrial carrier family with tissue-specific expression. *FEBS Lett* 408: 39-42, 1997.

6. **Boyer BB, Barnes BM, Lowell BB and Grujic D**. Differential regulation of uncoupling protein gene homologues in multiple tissues of hibernating ground squirrels. *Amer J Physiol Regulatory Integrative Comp Physiol* 44: R1232-R1238, 1998.

7. **Boyer BB, Ormseth OA, Buck L, Nicolson M, Pelleymounter MA and Barnes BM**. Leptin prevents posthibernation weight gain but does not reduce energy expenditure in arctic ground squirrels. *Comp Biochem Physiol* 118C: 405-412, 1997.

8. **Brand MD**. The proton leak across the mitochondrial inner membrane. *Biochim Biophys Acta* 1018: 128-133, 1990.

9. **Brand MD**. Measurement of mitochondrial protonmotive force. In: *Bioenergetics: a practical approach*. Oxford: Oxford University Press, 1995, p. 39-62.

10. **Brander F, Keith JS and Trayhurn PA**. A 27-mer oligonucleotide probe for the detection and measurement of the mRNA for uncoupling protein in brown adipose tissue of different species. *Comp Biochem Physiol* 104B: 125-131, 1993.

11. **Buck CL and Barnes BM**. Temperatures of hibernacula and change in body composition of Arctic ground squirrels over winter. *J Mamm* 80: 1264-1276, 1999.

12. **Buck CL and Barnes BM**. Effects of ambient temperature on metabolic rate, respiratory quotient, and torpor in an arctic hibernator. *Am J Physiol Regulatory Integrative Comp Physiol* 279: R255-R262, 2000.

13. **Cabrero A, Alegret M, Sanchez RM, Adzet T, Laguna JC and Vazquez M**. Down-regulation of uncoupling protein-3 and -2 by thiazolidinediones in C_2C_{12} myotubes. *FEBS Lett* 484: 37-42, 2000.

14. **Cadenas S and Brand MD**. Effects of magnesium and nucleotides on the proton conductance of rat skeletal-muscle mitochondria. *Biochem J* 348: 209-213, 2000.

15. **Cadenas S, Buckingham JA, Samec S, Seydoux J, Din N, Dulloo AG and Brand MD**. UCP2 and UCP3 rise in starved rat skeletal muscle but mitochondrial proton conductance is unchanged. *FEBS Lett* 462: 257-260, 1999.

16. **Cadenas S, Echtay KS, Harper JA, Jekabsons MB, Buckingham JA, Grau E, Abuin A, Chapman H, Clapham JC and Brand MD**. The basal proton conductance of

skeletal muscle mitochondria from transgenic mice overexpressing or lacking uncoupling protein-3. *J Biol Chem* 277: 2773-2778, 2002.

17. **Cannon B, Matthias A, Golozoubova V, Ohlson KBE, Andersson U, Jacobsson A and Nedergaard J**. Unifying and distinguishing features of brown and white adipose tissues: UCP1 versus other UCPs. In: *Progress in obesity research*, edited by Guy-Grand B and Ailhaud G. John Libbey & Company, Ltd./8th International Congress on Obesity, 1999, p. 13-26.

18. **Cannon B and Nedergaard J**. Respiratory and thermogenic capacities of cells and mitochondria from brown and white adipose tissue. *Methods Mol Biol* 155: 295-303, 2001.

19. **Champigny O and Ricquier D**. Effects of fasting and refeeding on the level of uncoupling protein mRNA in rat brown adipose tissue: evidence for diet-induced and cold- induced responses. *J Nutr* 120: 1730-1736, 1990.

20. **Clapham JC, Arch JR, Chapman H, Haynes A, Lister C, Moore GB, Piercy V, Carter SA, Lehner I, Smith SA, Beeley LJ, Godden RJ, Herrity N, Skehel M, Changani KK, Hockings PD, Reid DG, Squires SM, Hatcher J, Trail B, Latcham J, Rastan S, Harper AJ, Cadenas S, Buckingham JA, Brand MD and Abuin A**. Mice overexpressing human uncoupling protein-3 in skeletal muscle are hyperphagic and lean. *Nature* 406: 415-418, 2000.

21. **Cline GW, Vidal-Puig AJ, Dufour S, Cadman KS, Lowell BB and Shulman GI**. In vivo effects of uncoupling protein-3 gene disruption on mitochondrial energy metabolism. *J Biol Chem* 276: 20240-20244, 2001.

22. **Drew KL, Osborne PG, Frerichs KU, Hu Y, Koren RE, Hallenbeck JM and Rice ME**. Ascorbate and glutathione regulation in hibernating ground squirrels. *Brain Res* 851: 1-8., 1999.

23. **Duchamp C, Barre H, Rouanet JL, Lanni A, Cohen-Adad F, Berne G and Brebion P**. Nonshivering thermogenesis in king penguin chicks. I. Role of skeletal muscle. *Am J Physiol Regulatory Integrative Comp Physiol* 261: R1438-R1445, 1991.

24. **Echtay KS and Brand MD**. Coenzyme Q induces GDP-sensitive proton conductance in kidney mitochondria. *Biochem Soc Trans* 29: 763-768, 2001.

25. **Echtay KS, Roussel D, St-Pierre J, Jekabsons MB, Cadenas S, Stuart JA, Harper JA, Roebuck SJ, Morrison A, Pickering S, Clapham JC and Brand MD**. Superoxide activates mitochondrial uncoupling proteins. *Nature* 415: 96-99, 2002.

26. **Echtay KS, Winkler E, Frischmuth K and Klingenberg M**. Uncoupling proteins 2 and 3 are highly active H+ transporters and highly nucleotide sensitive when activated by coenzyme Q (ubiquinone). *Proc Natl Acad Sci USA* 98: 1416-1421, 2001.

27. **Fabris R, Nisoli E, Lombardi AM, Tonello C, Serra R, Granzotto M, Cusin I, Rohner-Jeanrenaud F, Federspil G, Carruba MO and Vettor R**. Preferential channeling of energy fuels toward fat rather than muscle during high free fatty acid availability in rats. *Diabetes* 50: 601-608, 2001.

28. **Fleury C, Neverova M, Collins S, Raimbault S, Champigny O, Levi-Meyrueis C, Bouillaud F, Seldin MF, Surwit RS, Ricquier D and Warden CH**. Uncoupling protein-2: a novel gene linked to obesity and hyperinsulinemia. *Nat Genet* 15: 269-272, 1997.

29. **Foster DO and Frydman ML**. Nonshivering thermogenesis in the rat. II. Measurements of blood flow with microspheres point to brown adipose tissue as the dominant site of the calorigenesis induced by noradrenaline. *Can J Physiol Pharmacol* 56: 110-122, 1978.

30. **Garlid KD, Jaburek M, Jezek P and Varecha M**. How do uncoupling proteins uncouple? *Biochim Biophys Acta* 1459: 383-389, 2000.

31. **Gong DW, He YF, Karas M and Reitman M**. Uncoupling protein-3 is a mediator of thermogenesis regulated by thyroid hormone, beta 3-adrenergic agonists, and leptin. *J Biol Chem* 272: 24129-24132, 1997.

32. **Gong DW, Monemdjou S, Gavrilova O, Leon LR, Marcus-Samuels B, Chou CJ, Everett C, Kozak LP, Li CL, Deng CX, Harper ME and Reitman ML**. Lack of obesity and normal response to fasting and thyroid hormone in mice lacking uncoupling protein-3. *J Biol Chem* 275: 16251-16257, 2000.

33. **Grav HI and Blix AS**. A source of nonshivering thermogenesis in fur seal skeletal muscle. *Science* 204: 87-89, 1979.

34. **Hagen T, Zhang CY, Slieker LJ, Chung WK, Leibel RL and Lowell BB**. Assessment of uncoupling activity of the human uncoupling protein 3 short form and three mutants of the uncoupling protein gene using a yeast heterologous expression system. *FEBS Lett* 454: 201-206, 1999.

35. **Harper JA, Stuart JA, Jekabsons MB, Roussel D, Brindle KM, Dickinson K, Jones RB and Brand MD**. Artifactual uncoupling by uncoupling protein 3 in yeast

mitochondria at the concentrations found in mouse and rat skeletal-muscle mitochondria. *Biochem J* 361: 49-56, 2002.

36. **Hayashi M and Nagasaka T**. Suppression of norepinephrine-induced thermogenesis in brown adipose tissue by fasting. *Am J Physiol Endocrinol Metab* 245: E582-586., 1983.

37. **Himms-Hagen J and Harper ME**. Physiological role of UCP3 may be export of fatty acids from mitochondria when fatty acid oxidation predominates: An hypothesis. *Exp Biol Med* 226: 78-84, 2001.

38. **Hinz W, Faller B, Gruninger S, Gazzotti P and Chiesi M**. Recombinant human uncoupling protein-3 increases thermogenesis in yeast cells. *FEBS Lett* 448: 57-61, 1999.

39. **Huang SG and Klingenberg M**. Nature of the masking of nucleotide-binding sites in brown adipose tissue mitochondria. Involvement of endogenous adenosine triphosphate. *Eur J Biochem* 229: 718-725, 1995.

40. **Iossa S, Lionetti L, Mollica MP, Crescenzo R, Botta M, Samec S, Dulloo AG and Liverini G**. Differences in proton leak kinetics, but not in UCP3 protein content, in subsarcolemmal and intermyofibrillar skeletal muscle mitochondria from fed and fasted rats. *FEBS Lett* 505: 53-56, 2001.

41. **Jacobsson A, Muhleisen M, Cannon B and Nedergaard J**. The uncoupling protein thermogenin during acclimation: indications for pretranslational control. *Am J Physiol Regulatory Integrative Comp Physiol* 267: R999-R1007, 1994.

42. **Kelly LJ, Vicario PP, Thompson GM, Candelore MR, Doebber TW, Ventre J, Wu MS, Meurer R, Forrest MJ, Conner MW, Cascieri MA and Moller DE**.

Peroxisome proliferator-activated receptors γ and α mediate in vivo regulation of uncoupling protein (UCP-1, UCP-2, UCP-3) gene expression. *Endocrinology* 139: 4920-4927, 1998.

43. **Khalfallah Y, Fages S, Laville M, Langin D and Vidal H**. Regulation of uncoupling protein-2 and uncoupling protein-3 mRNA expression during lipid infusion in human skeletal muscle and subcutaneous adipose tissue. *Diabetes* 49: 25-31, 2000.

44. **Lanni A, DeFelice M, Lombardi A, Moreno M, Fleury C, Ricquier D and Goglia F**. Induction of UCP2 mRNA by thyroid hormones in rat heart. *FEBS Lett* 418: 171-174, 1997.

45. **Larkin S, Mull E, Miao W, Pittner R, Albrandt K, Moore C, Young A, Denaro M and Beaumont K**. Regulation of the third member of the uncoupling protein family, UCP3, by cold and thyroid hormone. *Biochem Biophys Res Commun* 240: 222-227, 1997.

46. **Liu XT, Lin QS, Li QF, Huang CX and Sun RY**. Uncoupling protein mRNA, mitochondrial GTP-binding, and T-4 5'-deiodinase activity of brown adipose tissue in Daurian ground squirrel during hibernation and arousal. *Comp Biochem Physiol* 120A: 745-752, 1998.

47. **Locke RM, Rial E and Nicholls DG**. The acute regulation of mitochondrial proton conductance in cells and mitochondria from the brown fat of cold-adapted and warm-adapted guinea pigs. *Eur J Biochem* 129: 381-387, 1982.

48. **Mao WG, Yu XX, Zhong A, Li WL, Brush J, Sherwood SW, Adams SH and Pan GH**. UCP4, a novel brain-specific mitochondrial protein that reduces membrane potential in mammalian cells. *FEBS Lett* 443: 326-330, 1999.

49. **Martins R, Atgie C, Gineste L, Nibbelink M, Ambid L and Ricquier D.** Increased GDP binding and thermogenic activity in brown adipose tissue mitochondria during arousal of the hibernating garden dormouse (Eliomys quercinus L.). *Comp Biochem Physiol* 98A: 311-316, 1991.

50. **Millet L, Vidal H, Andreelli F, Larrouy D, Riou JP, Ricquier D, Laville M and Langin D.** Increased uncoupling protein-2 and -3 mRNA expression during fasting in obese and lean humans. *J Clin Invest* 100: 2665-2670, 1997.

51. **Milner RE, Wang LC and Trayhurn P.** Brown fat thermogenesis during hibernation and arousal in Richardson's ground squirrel. *Amer J Physiol Regulatory Integrative Comp Physiol* 256: R42-R48, 1989.

52. **Monemdjou S, Kozak LP and Harper ME.** Mitochondrial proton leak in brown adipose tissue mitochondria of Ucp1-deficient mice is GDP insensitive. *Amer J Physiol Endocrinol Metab* 39: E1073-E1082, 1999.

53. **Muralidhara DV and Desautels M.** Changes in brown adipose tissue composition during fasting and refeeding of diet-induced obese mice. *Am J Physiol Regulatory Integrative Comp Physiol* 266: R1907-R1915, 1994.

54. **Nibbelink M, Moulin K, Arnaud E, Duval C, Penicaud L and Casteilla L.** Brown fat UCP1 is specifically expressed in uterine longitudinal smooth muscle cells. *J Biol Chem* 276: 47291-47295, 2001.

55. **Nicholls DG and Locke RM.** Thermogenic mechanisms in brown fat. *Physiol Rev* 64: 1-64, 1984.

56. **Nizielski SE, Billington CJ and Levine AS**. Cold-induced alterations in uncoupling protein and its mRNA are seasonally dependent in ground squirrels. *Am J Physiol Regulatory Integrative Comp Physiol* 269: R357-R364, 1995.

57. **Puigserver P, Herron D, Gianotti M, Palou A, Cannon B and Nedergaard J**. Induction and degradation of the uncoupling protein thermogenin in brown adipocytes in vitro and in vivo. Evidence for a rapidly degradable pool. *Biochem J* 284: 393-398, 1992.

58. **Reynafarje B, Costa LE and Lehninger AL**. O_2 solubility in aqueous media determined by a kinetic method. *Anal Biochem* 145: 406-418, 1985.

59. **Rolfe DFS, Hulbert AJ and Brand MD**. Characteristics of mitochondrial proton leak and control of oxidative phosphorylation in the major oxygen-consuming tissues of the rat. *Biochim Biophys Acta* 1188: 405-416, 1994.

60. **Rose RW, West AK, Ye JM, McCormack GH and Colquhoun EQ**. Nonshivering thermogenesis in a marsupial (The Tasmanian bettong *Bettongia gaimardi*) is not attributable to brown adipose tissue. *Physiol Biochem Zool* 72: 699-704, 1999.

61. **Samec S, Seydoux J and Dulloo AG**. Role of UCP homologues in skeletal muscles and brown adipose tissue: mediators of thermogenesis or regulators of lipids as fuel substrate? *FASEB J* 12: 715-724, 1998.

62. **Sanchis D, Fleury C, Chomiki N, Goubern M, Huang Q, Neverova M, Gregoire F, Easlick J, Raimbault S, Levi-Meyrueis C, Miroux B, Collins S, Seldin M, Richard D, Warden C, Bouillaud F and Ricquier D**. BMCP1, a novel mitochondrial carrier with high expression in the central nervous system of humans and rodents, and respiration uncoupling activity in recombinant yeast. *J Biol Chem* 273: 34611-34615, 1998.

63. **Scholander PF, Hock RJ, Walters V, Johnson F and Irving L**. Heat regulation in some arctic and tropical mammals and birds. *Biol Bull* 99: 237-258, 1950.

64. **Schrauwen P, Saris WHM and Hesselink MKC**. An alternative function for human uncoupling protein 3: protection of mitochondria against accumulation of nonesterified fatty acids inside the mitochondrial matrix. *FASEB Journal* 15: 2497-2502, 2001.

65. **Schrauwen P, Westerterp-Plantenga MS, Kornips E, Schaart G and van Marken Lichtenbelt WD**. The effect of mild cold exposure on UCP3 mRNA expression and UCP3 protein content in humans. *Int J Obes* 26: 450-457, 2002.

66. **Simonyan RA, Jimenez M, Ceddia RB, Giacobino JP, Muzzin P and Skulachev VP**. Cold-induced changes in the energy coupling and the UCP3 level in rodent skeletal muscles. *Biochim Biophys Acta* 1505: 271-279, 2001.

67. **Skulachev VP**. Uncoupling: new approaches to an old problem of bioenergetics. *Biochim Biophys Acta* 1363: 100-124, 1998.

68. **Smith RE and Horwitz BA**. Brown fat and thermogenesis. *Physiol Rev* 49: 330-425, 1969.

69. **South FE and House WA**. Energy metabolism in hibernation. In: *Mammalian Hibernation III*, edited by Fisher KC, Dawe AP, Lyman CP, Schonbaum E and South FE. New York: Elsevier, 1967, p. 305-324.

70. **Stuart JA, Harper JA, Brindle KM, Jekabsons MB and Brand MD**. A mitochondrial uncoupling artifact can be caused by expression of uncoupling protein 1 in yeast. *Biochem J* 356: 779-789, 2001.

71. **Sundin U, Moore G, Nedergaard J and Cannon B**. Thermogenin amount and activity in hamster brown fat mitochondria: effect of cold acclimation. *Am J Physiol Regulatory Integrative Comp Physiol* 252: R822-R832, 1987.

72. **Teruel T, Smith SA, Peterson J and Clapham JC**. Synergistic activation of UCP-3 expression in cultured fetal rat brown adipocytes by PPAR alpha and PPAR gamma ligands. *Biochem Biophys Res Commun* 273: 560-564, 2000.

73. **Toien O, Drew KL, Chao ML and Rice ME**. Ascorbate dynamics and oxygen consumption during arousal from hibernation in Arctic ground squirrels. *Am J Physiol Regulatory Integrative Comp Physiol Physiol* 281: R572-R583, 2001.

74. **Trayhurn P and Jennings G**. Nonshivering thermogenesis and the thermogenic capacity of brown fat in fasted and/or refed mice. *Am J Physiol Regulatory Integrative Comp Physiol* 254: R11-R16, 1988.

75. **Van der Lee K, Willemsen PHM, Samec S, Seydoux J, Dulloo AG, Pelsers M, Glatz JFC, Van der Vusse GJ and Van Bilsen M**. Fasting-induced changes in the expression of genes controlling substrate metabolism in the rat heart. *J Lip Res* 42: 1752-1758, 2001.

76. **Van der Lee KAJM, Willemsen PHM, Van der Vusse GJ and Van Bilsen M**. Effects of fatty acids on uncoupling protein-2 expression in the rat heart. *FASEB J* 14: 495-502, 2000.

77. **Vidal-Puig A, Solanes G, Grujic D, Flier JS and Lowell BB**. UCP3: an uncoupling protein homologue expressed preferentially and abundantly in skeletal muscle and brown adipose tissue. *Biochem Biophys Res Commun* 235: 79-82, 1997.

78. **Vidal-Puig AJ, Grujic D, Zhang CY, Hagen T, Boss O, Ido Y, Szczepanik A, Wade J, Mootha V, Cortright R, Muoio DM and Lowell BB**. Energy metabolism in uncoupling protein 3 gene knockout mice. *J Biol Chem* 275: 16258-16266, 2000.

79. **von Praun C, Burkert M, Gessner M and Klingenspor M**. Tissue-specific expression and cold-induced mRNA levels of uncoupling proteins in the Djungarian hamster. *Physiol Biochem Zool* 74: 203-211, 2001.

80. **Weigle DS, Selfridge LE, Schwartz MW, Seeley RJ, Cummings DE, Havel PJ, Kuijper JL and BeltrandelRio H**. Elevated free fatty acids induce uncoupling protein 3 expression in muscle: A potential explanation for the effect of fasting. *Diabetes* 47: 298-302, 1998.

81. **Yu XX, Mao WG, Zhong A, Schow P, Brush J, Sherwood SW, Adams SH and Pan GH**. Characterization of novel UCP5/BMCP1 isoforms and differential regulation of UCP4 and UCP5 expression through dietary or temperature manipulation. *FASEB J* 14: 1611-1618, 2000.

82. **Zhang CY, Hagen T, Mootha VK, Slieker LJ and Lowell BB**. Assessment of uncoupling activity of uncoupling protein 3 using a yeast heterologous expression system. *FEBS Lett* 449: 129-134, 1999.

Table 2.1. Temperatures of various tissues from arctic ground squirrels under hibernating under thermogenic conditions.

Tissue / region	Temperature (°C)
Brain	3.9 ± 0.5^{a}
BAT	3.5 ± 0.7^{a}
Neck	3.4 ± 0.4^{a}
Liver	0.2 ± 0.5^{b}
Rectum	0.2 ± 0.4^{b}
abWAT	$-0.6 \pm 0.4^{b,c}$
SKM	-1.5 ± 0.4^{c}

Arctic ground squirrels (n = 7) were housed at -10°C. BAT, brown adipose tissue; abWAT, abdominal white adipose tissue, SKM, skeletal muscle (gastrocnemius). Values are means ± SE. Tissues/regions with different superscripts are significantly different ($P < 0.01$).

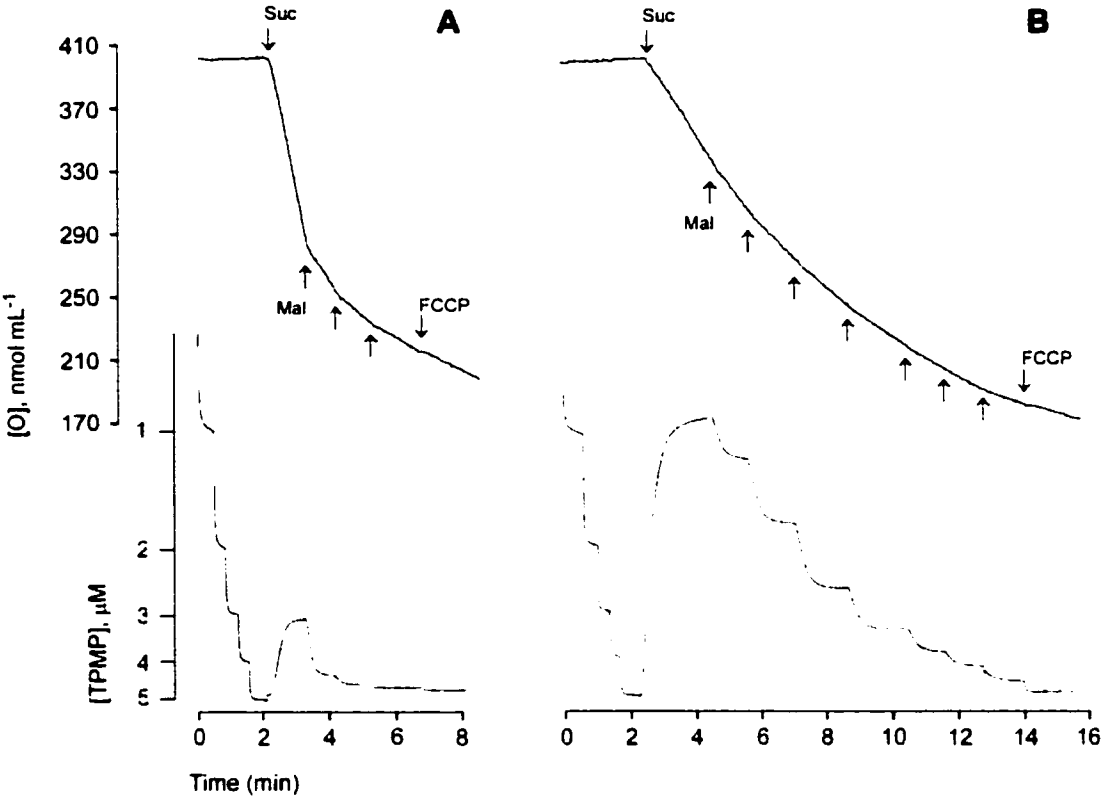

Figure 2.1. Representative traces of the proton leak assay in brown adipose tissue. Representative traces of the proton leak assay in brown adipose tissue showing the relationship between the concentrations of oxygen (upper trace) and TPMP (lower trace) in assay buffer. Mitochondria from each animal were assayed both in the absence (A) and presence (B) of GDP (2 mM). Mitochondria were incubated in assay buffer, rotenone, oligomycin, and nigericin for at least one minute prior to TPMP additions. Arrows designate addition of succinate (Suc), successive additions of malonate (Mal) or the final addition of respiratory uncoupler (FCCP); for clarity, the arrows are only shown in the oxygen trace. The mitochondrial membrane potential is calculated from, and is inversely proportional to, the concentration of TPMP in assay buffer, such that a low concentration of TPMP in the buffer reflects a high $\Delta\psi_m$. See MATERIALS AND METHODS for details.

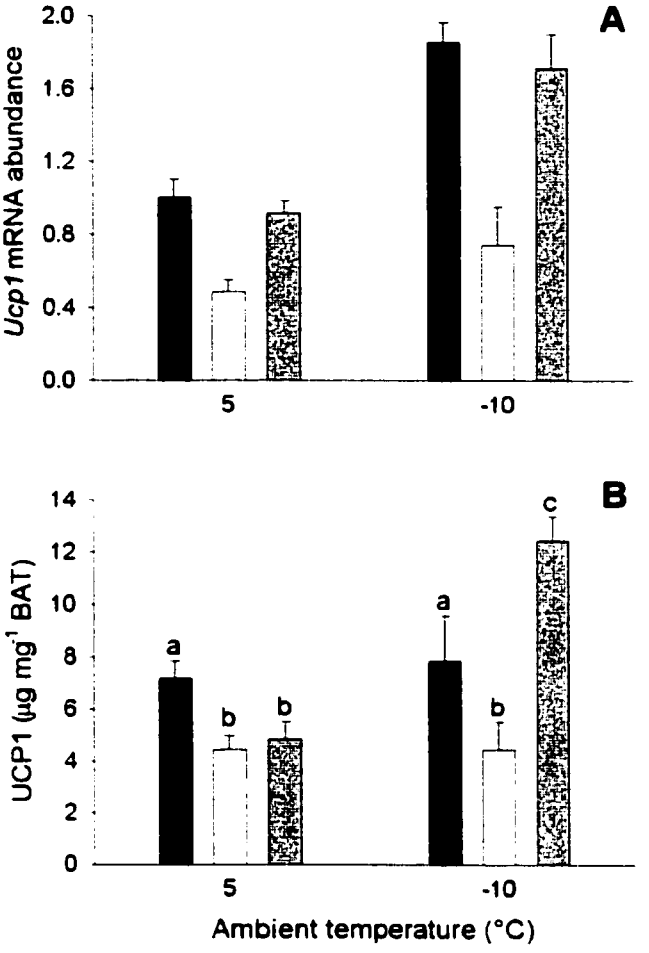

Figure 2.2. Effect of temperature and activity on levels of *Ucp1* mRNA and UCP1. Effect of temperature and activity on levels of brown adipose tissue (BAT) *Ucp1* mRNA standardized to 18S rRNA (A) and UCP1 quantified from BAT homogenates (B) in arctic ground squirrels. Animals were housed at either 5°C or -10°C and were from one of three activity classes: active animals that had not hibernated (ACT, black bars), active animals subjected to a 48 h fast (FAST, white bars), or hibernating animals in deep torpor (HIB, gray bars). Not indicated are significant effects of temperature (-10°C > 5°C, $P < 0.0001$) and activity class (ACT ≥ HIB > FAST, $P < 0.001$) on *Ucp1* mRNA levels. Values are means + SE. Means with different letters are significantly different.

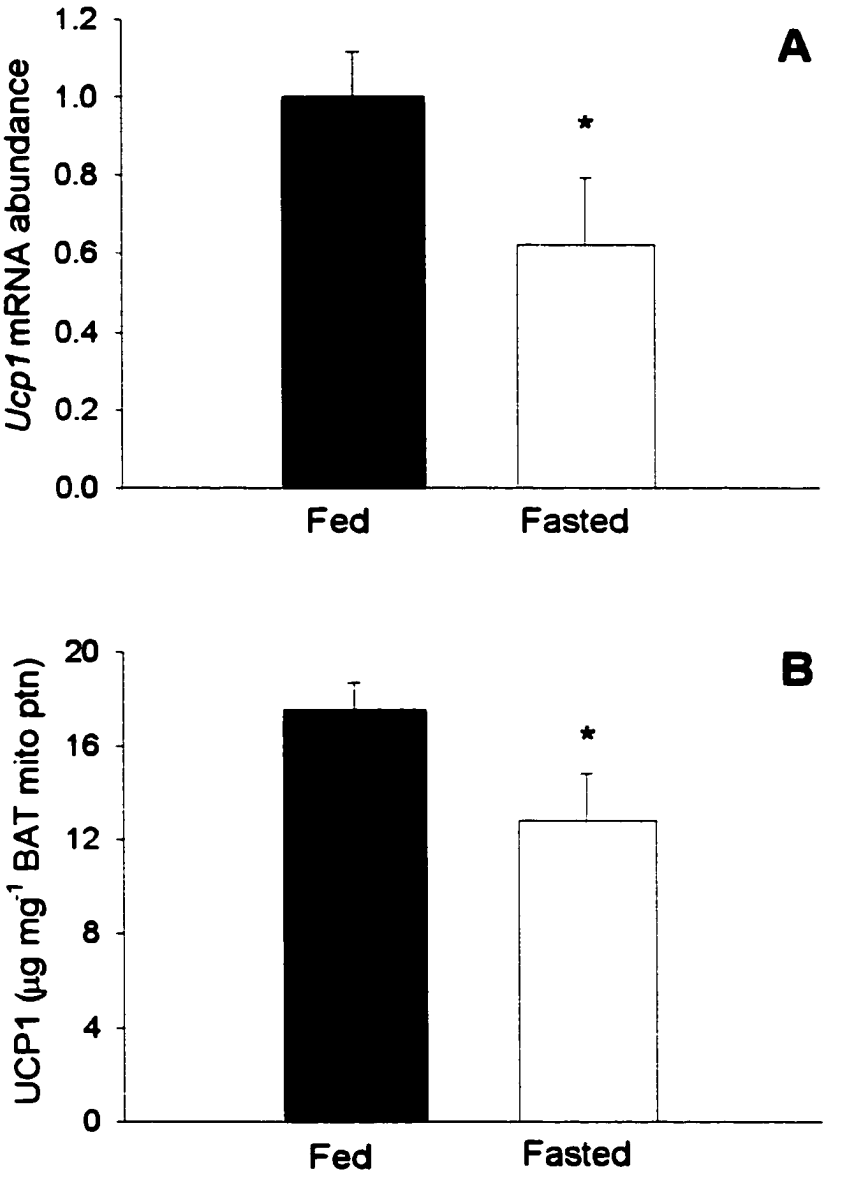

Figure 2.3. Effect of fasting on levels of *Ucp1* mRNA and UCP1.
Levels of brown adipose tissue *Ucp1* mRNA standardized to 18S rRNA (A) and UCP1 quantified from brown adipose tissue mitochondria (B) in fed and fasted arctic ground squirrels housed at 5°C. Values are means + SE. * indicates a significant difference from fed animals ($P \leq 0.05$).

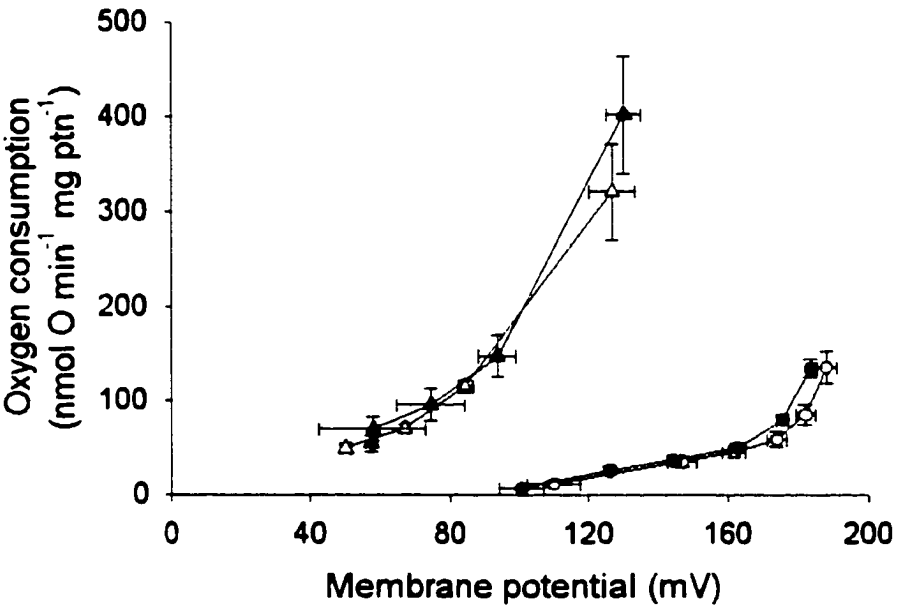

Figure 2.4. Kinetics of the proton leak in brown adipose tissue mitochondria. Kinetics of the proton leak in brown adipose tissue mitochondria isolated from fed (filled symbols) and fasted (open symbols) arctic ground squirrels and assayed in the absence (triangles) or presence (circles) of 2 mM guanosine diphosphate (GDP). The maximal rate of proton leak occurs under state 4 conditions which are shown as the extreme upper-right point for each curve; neither oxygen consumption nor membrane potential were significantly different between treatment at either 0 or 2 mM GDP. Not indicated is a significant effect of GDP on both state 4 oxygen consumption ($P < 0.01$) and membrane potential ($P < 0.001$) for both fed and fasted groups. For details on assay conditions see MATERIALS AND METHODS section.

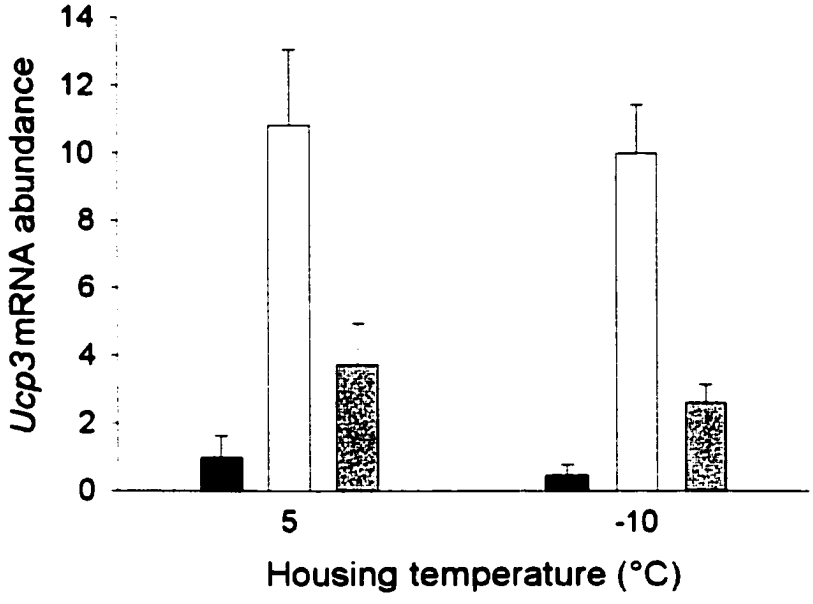

Figure 2.5. Effect of temperature and activity on levels on *Ucp3* mRNA.
Effect of temperature and activity on levels of skeletal muscle *Ucp3* mRNA standardized to 18S rRNA in arctic ground squirrels. Animals were housed at either 5°C or -10°C and were from one of three activity classes: active animals that had not hibernated (ACT, black bars), active animals subjected to a 48 h fast (FAST, white bars), or hibernating animals in deep torpor (HIB, gray bars). Not indicated are significant effects of activity on *Ucp3* mRNA levels (FAST > HIB > ACT, $P < 0.0001$). Values are means + SE.

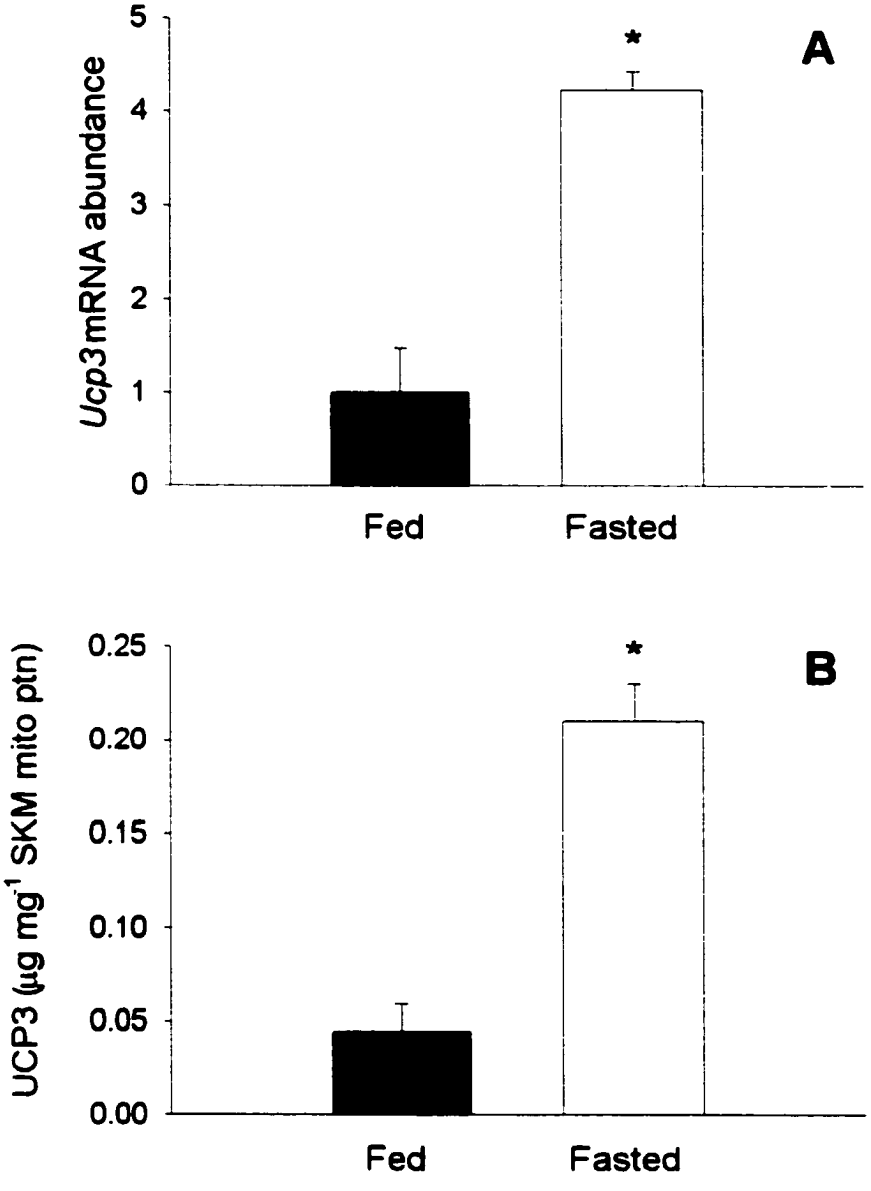

Figure 2.6. Effect of fasting on levels of *Ucp3* mRNA and UCP3.
Levels of skeletal muscle *Ucp3* mRNA standardized to 18S rRNA (A) and UCP3 quantified from skeletal muscle mitochondria (B) in fed and fasted arctic ground squirrels housed at 5°C. Values are means + SE. * designates significant difference from fed animals ($P < 0.01$).

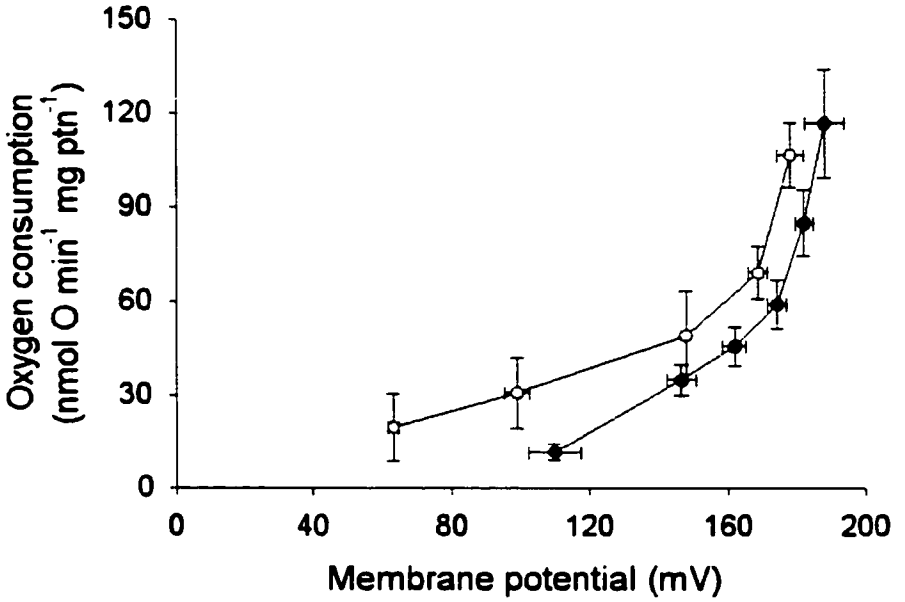

Figure 2.7. Kinetics of the proton leak in skeletal muscle mitochondria.
Kinetics of the proton leak in skeletal muscle mitochondria isolated from fed (filled symbols) and fasted (open symbols) arctic ground squirrels housed at 5°C. The maximal rate of proton leak occurs under state 4 conditions which are shown as the extreme upper-right point for each curve; neither oxygen consumption nor membrane potential were significantly different between treatments.

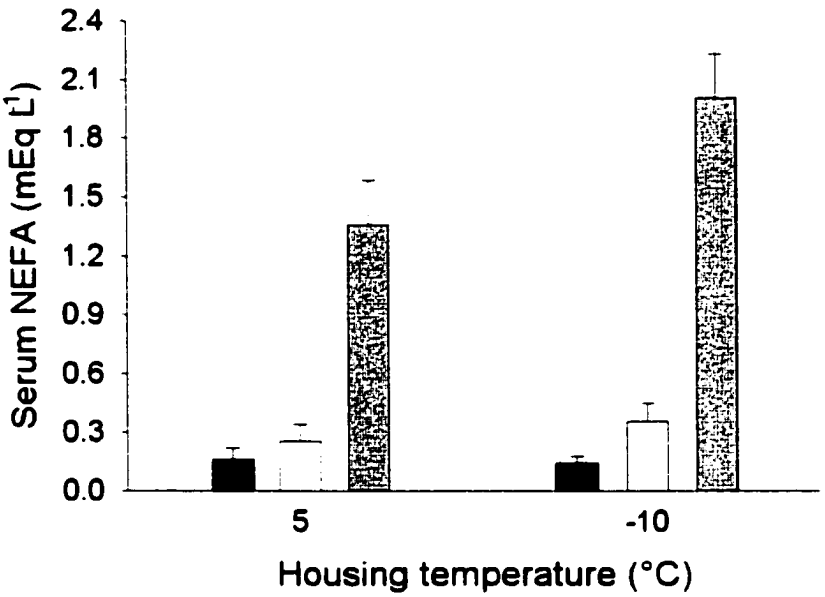

Figure 2.8. Effect of temperature and activity on levels of nonesterified fatty acids. Effect of temperature and activity on serum levels of nonesterified fatty acids (NEFA) in arctic ground squirrels. Animals were housed at either 5°C or -10°C and were from one of three activity classes: active animals that had not hibernated (ACT, black bars), active animals subjected to a 48 h fast (FAST, white bars), or hibernating animals in deep torpor (HIB, gray bars). Not indicated are significant effects of activity on NEFA levels (HIB > ACT ≥ FAST, $P < 0.0001$). Values are means + SE.

CHAPTER 3 - TISSUE-SPECIFIC DEPRESSION OF MITOCHONDRIAL PROTON LEAK AND SUBSTRATE OXIDATION IN HIBERNATING ARCTIC GROUND SQUIRRELS

Barger, J.L., Brand, M.D., Barnes, B.M., Boyer, B.B. Tissue-specific depression of mitochondrial proton leak and substrate oxidation in hibernating arctic ground squirrels. Prepared for submission to the American Journal of Physiology Regulatory, Integrative, and Comparative Physiology subsection.

ABSTRACT

A significant proportion of standard metabolic rate is devoted to driving mitochondrial proton leak, and this futile cycle may be a site of metabolic control during hibernation. To determine if the proton leak pathway is decreased during metabolic depression related to hibernation, mitochondria were isolated from liver and skeletal muscle of non-hibernating (active) and hibernating arctic ground squirrels (*Spermophilus parryii*). At an assay temperature of 37°C, both state 3 and state 4 respiration rates and membrane potentials were significantly depressed in liver mitochondria isolated from hibernators. In contrast, in skeletal muscle mitochondria, only state 3 respiration rate was decreased during hibernation. The decrease in oxygen consumption of liver mitochondria was not achieved by decreased activity of the set of reactions generating the proton gradient and not lowered proton permeability. These results suggest that mitochondrial proton conductance is unchanged during hibernation and that the reduced metabolism in hibernators is a partial consequence of tissue-specific depression of substrate oxidation.

INTRODUCTION

A central question in mammalian hibernation is whether the low metabolic rates observed in hibernating animals are due to active suppression of metabolism or rather are a secondary consequence of slowed enzyme activities at low body temperatures. In general, whole-animal studies that have examined the effect of body temperature on metabolic rate support the temperature-dependent mechanisms of metabolic suppression (19; 36). However, studies of isolated mitochondria have demonstrated that rates of consumption are reduced during hibernation, and that this metabolic depression is independent of assay temperature (11; 18; 21; 23; 27; 29). Most of these latter studies only examined mitochondria isolated from liver, and when additional tissues have been investigated, results have been mixed. Hannon et al. (21) found that respiration of liver and skeletal muscle homogenates was depressed in hibernating arctic ground squirrels (*Spermophilus parryii*), however, Brustovetsky et al. (9) found that heart and skeletal muscle mitochondrial respiration was increased in hibernating compared to active arctic ground squirrels. A tissue-specific depression of metabolism may explain the discrepancy between whole-animal and mitochondrial studies.

Because mitochondria account for ~90% of total cellular oxygen consumption (32), they are a likely site of control during hibernation. State 3 (ADP-stimulated) respiration is reduced during hibernation (11; 18; 23; 25; 29), possibly as a component of the decreased ATP turnover that is characteristic of many species during metabolic depression (20). Alternatively, reversal of state 3 inhibition during arousal from hibernation suggests a need for elevated levels of ATP and/or thermogenesis (25).

Results of state 4 (non-phosphorylating) respiration in mammalian hibernation are equivocal: several studies report a decrease in state 4 respiration in liver mitochondria (11; 16; 18; 27), while two others found no differences between hibernating and active animals (23; 25). State 4 respiration reflects the futile cycling of protons across the mitochondrial inner membrane (5), and it may be depressed during hibernation by a decrease in membrane proton conductance *per se* (22). Depressed proton cycling may also occur as a secondary consequence of decreased activity of the reactions generating the proton gradient, including substrate translocases, dehydrogenases, and enzymes of the respiratory chain (6). Mitochondrial respiration can be divided into sets of reactions that produce the mitochondrial proton gradient (enzymes of substrate oxidation) and those that consume it (proton leak and ATP synthesis). Discerning which sets of reactions are responsible for metabolic control can be accomplished with parallel measurements of mitochondrial respiration and membrane potential (3). A decrease in substrate oxidation kinetics has been proposed to underlie metabolic depression in liver mitochondria of hibernating arctic ground squirrels (10), but no study has been performed to distinguish among the possible sites of control in a mammalian hibernator.

A major goal of this investigation was to examine the control of mitochondrial proton leak and substrate oxidation subsystems during mammalian hibernation. We studied these parameters in mitochondria isolated from the arctic ground squirrel, which has a hibernating metabolic rate less than 1% of the non-hibernating metabolic rate when housed at temperatures near 0°C (12). We isolated mitochondria from liver and skeletal muscle because metabolic activity of these tissues constitutes 35-50% of standard

metabolic rate (30) and the oxygen consumption driving proton leak in these tissues constitutes 15-20% of standard metabolic rate (34); therefore, proton leak in these tissues is a likely site for metabolic control during hibernation.

METHODS

Animals

Adult arctic ground squirrels were trapped in the Alaska Range (64°N 146°W, elevation 850m) in July and maintained at the University of Alaska Fairbanks. Animals were housed at 5 ± 2°C with a 4L:20D photoperiod and were given Mazuri Rodent Chow (St. Louis, MO), sunflower seeds, carrots, apple slices, and water ad libitum. Animals were inspected twice daily, and wood shavings were placed on the dorsal surface of hibernating animals to assess the pattern of hibernation and arousal episodes. Tissues were collected from hibernators after no fewer than five days into at least the third torpor bout; active (non-hibernating) animals had not previously shown torpor as estimated by daily inspection.

Animals were always pair-sampled (active and hibernating) to minimize variation due to isolation techniques; all experiments were performed between 7 November and 22 December. Active animals were anesthetized with Halothane (Halocarbon Products; North Augusta, SC) and rapidly decapitated. Rectal temperature (T_{rect}) was measured in hibernators by inserting a thermocouple 2-3 cm into the rectum and allowing one minute for the reading to stabilize; the average T_{rect} for hibernating animals was 4.2 ± 0.6°C (range 2.1 – 5.7). Hibernators were euthanized by decapitation without anesthesia. Liver

and gastrocnemius muscle (hereafter referred to as skeletal muscle) were rapidly dissected and transferred into ice-cold buffers for isolation of mitochondria.

Isolation of mitochondria

Isolation procedures were performed on ice and all centrifuge spins were conducted at 2 ± 2°C. Unless otherwise mentioned, all reagents were obtained from Sigma-Aldrich (St. Louis, MO). Liver mitochondria were isolated by disrupting tissue using a Dounce homogenizer with a loose-fitting pestle in a buffer containing 250 mM sucrose, 5mM Trizma®, and 2 mM EGTA. The homogenate was spun at 490 *g* for 10 min and the resulting supernatant was subjected to a high-speed spin cycle (10,550 *g* for 10 min). The supernatant was poured off and lipid remaining on the inner surface of the tube was removed using a paper tissue. The crude mitochondrial pellet was resuspended in homogenization buffer containing 0.5% fatty acid-free bovine serum albumin (BSA; Intergen; Purchase, NY) to chelate endogenous fatty acids and subjected to an additional high-speed spin cycle. The resulting pellet was resuspended in homogenization buffer (-BSA) and subjected to a final high-speed spin cycle. The final pellet was resuspended in a minimal volume of homogenization buffer (-BSA) and stored on ice.

Skeletal muscle was trimmed of fat and connective tissue, finely minced with a razor blade on a glass plate over ice, and transferred to a beaker containing ice-cold wash buffer (100 mM KCl, 50 mM Tris-HCl, and 2 mM EGTA). The excess buffer was poured off and replaced with additional buffer; this process was repeated an additional five times to remove any hair, fat, and connective tissue from the preparation. After the final wash, excess buffer was poured off and replaced with a digestion buffer (10 mL · g tissue^{-1})

containing 100 mM KCl, 50 mM Tris-HCl, 2 mM EGTA, 0.5% fatty acid-free BSA, 5 mM $MgCl_2$, 1 mM ATP, and nagarse (18.7 units · g tissue^{-1}). This mixture was kept on ice for 10 min with occasional stirring and then briefly homogenized with a Polytron (2 × 10 s). After an additional 10 min with occasional stirring on ice, the homogenate was spun at 490 *g* for 10 min. The supernatant was filtered through three layers of gauze and spun at 10,500 *g* for 10 min. The crude mitochondrial pellet was resuspended in excess wash buffer and subjected to an additional high-speed spin cycle (10,500 *g* for 10 min). The final pellet was resuspended in a minimal volume of wash buffer and kept on ice.

Protein concentration of all mitochondria preparations was determined in duplicate by the bicinchoninic acid assay (Pierce Chemical BCA Protein Assay Kit; Rockford, IL) with BSA as the standard. Integrity of isolated mitochondria was estimated by calculating the respiratory control ratio for each preparation (state 3 / state 4 respiration rates).

Measurement of mitochondrial bioenergetics

All assays were performed at 37°C in 3 mL of assay buffer containing mitochondria (liver = 1 mg protein · mL^{-1}, skeletal muscle = 0.5 mg protein · mL^{-1}), 120 mM KCl, 5mM KH_2PO_4, 3 mM HEPES, 1 mM EGTA, and 0.5% fatty acid-free BSA, pH 7.2. We chose this temperature because depression of mitochondrial oxygen consumption has been shown to be independent of assay temperature (23; 27) and because slip of the mitochondrial proton pumps may occur at lower temperatures (14). A dual-channel chart recorder (Kipp and Zonen; The Netherlands) was used to record simultaneous measurements of oxygen consumption and membrane potential. Oxygen consumption

was measured using a Rank Brothers Model 10 oxygen electrode (Cambridge, UK) assuming 406 nmol O · mL^{-1} buffer (28). Mitochondrial membrane potential ($\Delta\psi_m$, mV) was estimated by uptake of the lipophilic cation triphenylmethylphosphonium (TPMP) using the following equation:

$$\Delta\psi m = 61.5 \log \left\{ \frac{([\text{TPMP}] \text{ added} - [\text{TPMP}] \text{ external}) \times \text{TPMP binding correction}}{0.001 \times [\text{protein}] \times [\text{TPMP}] \text{ external}} \right\}$$

To estimate the concentration of TPMP in the assay buffer ([TPMP] external), a standard curve of TPMP concentration and chart recorder distance was generated with incremental additions of TPMP (1, 2, 3, 4, 5 μM) for each assay. Electrode drift was corrected after each run by addition of 2 μM carbonyl cyanide *p*-(trifluoromethoxy)phenylhydrazone (FCCP). Mitochondrial TPMP binding corrections were 0.4 and 0.35 for liver and skeletal muscle, respectively (33).

The kinetics of proton leak and substrate oxidation were assayed in triplicate and duplicate, respectively, for each mitochondrial preparation (4). The kinetics of proton leak were measured by titrating state 4 respiration with malonate, a competitive inhibitor of succinate (liver = 0, 0.5, 1, 1.5, 2, 2.5 mM malonate; muscle = 0, 0.3, 0.6, 1, 1.3 mM malonate). The kinetics of substrate oxidation were estimated by the slope of the line defined by oxygen consumption rate and $\Delta\psi_m$ under state 3 and state 4 conditions. State 3 conditions were established by incubating mitochondria in the presence of 5 μM rotenone (to inhibit complex I oxidation of endogenous NADH), 80 ng nigericin · mL^{-1} (to set ΔpH

to zero), 250 μM ADP, and 5 mM succinate. State 4 conditions were obtained by incubating mitochondria in 5 μM rotenone, 80 ng · mL^{-1} nigericin, 5 mM succinate, and 1 μg · mL^{-1} oligomycin, a specific inhibitor of the F_oF_1 ATP synthase.

Statistics

Means for all parameters were compared between active and hibernating groups (n = 5 animals per group) using Student's t-tests.

RESULTS

Bioenergetics of liver mitochondria

Membranes of liver mitochondria did not appear to be physically damaged during isolation as assessed by respiratory control ratios (Table 3.1). Although the mean respiratory control ratio for the hibernating group was significantly lower than the active group, this was due to lower rates of state 3 oxygen consumption in hibernators (decreased to 30% of non-hibernators) rather than disrupted membrane integrity, as all preparations had high values for state 4 $\Delta\psi_m$ (> 170 mV).

Representative traces of the proton leak assay in liver mitochondria for an active and a hibernating arctic ground squirrel are shown in Figure 3.1 and show that mitochondria isolated from hibernating animals had lower rates of state 4 oxygen consumption and were unable to achieve the high $\Delta\psi_m$ of mitochondria isolated from active squirrels. These traces were used to determine the kinetics of the proton leak system which are summarized in Figure 3.2A. Although state 4 oxygen consumption and $\Delta\psi_m$ were significantly different between active and hibernating groups (Table 3.1; $P <$ 0.01), the curves overlapped such that the rate of proton leak was not significantly

different at any common values of $\Delta\psi_m$ (range: 140-180 mV). Specifically, proton conductance, calculated as proton leak rate per mV, was statistically similar between groups for liver mitochondria at a $\Delta\psi_m$ of 180 mV, the highest potential achieved by both groups (Figure 3.3).

A significant depression of substrate oxidation was observed in liver mitochondria during hibernation. State 3 and 4 respiration rates were significantly depressed in hibernators ($P < 0.0001$ and 0.01, respectively), as were state 3 and state 4 $\Delta\psi_m$ ($P < 0.05$ and 0.01, respectively), and across a range of $\Delta\psi_m$ spanning state 3 and state 4 conditions, respiration in liver mitochondria from hibernators was approximately one-third to one-half that of the rate in the active animals at a given value of $\Delta\psi_m$ (Figure 3.2B).

Bioenergetics of skeletal muscle mitochondria

The kinetics of proton leak were virtually identical in mitochondria isolated from skeletal muscle of hibernating and active ground squirrels (Figure 3.4A). Although state 3 respiration of skeletal muscle mitochondria was significantly decreased in hibernators to 80% of the rate of active squirrels (Table 3.1; $P = 0.04$), there was no difference in state 4 respiration or state 3 and 4 $\Delta\psi_m$ between groups (Figure 3.4B), and therefore the slopes of the lines connecting state 3 and state 4 oxygen consumption rate and $\Delta\psi_m$ were not significantly different between treatments.

DISCUSSION

Proton leak across the mitochondrial inner membrane accounts for 20-30% of standard metabolic rate (5) and represents a significant inefficiency because energy released

during substrate oxidation is not conserved as ATP. During hibernation, arctic ground squirrels have a metabolic rate approximately 1% of the resting metabolic rate in non-hibernating animals, and therefore control of proton leak is likely during hibernation. Whether the reduced metabolism is achieved in part by alteration of mitochondrial proton cycling has not been investigated before in a mammalian hibernator. Our study demonstrates that in arctic ground squirrels, hibernation is characterized by an active depression of proton leak in liver mitochondria that persists at high (37°C) assay temperatures. The reduction in proton cycling was not achieved by a reduction in membrane proton conductance. Instead, proton cycling in liver mitochondria was controlled at the level of substrate oxidation, as has been demonstrated in skeletal muscle of frogs (*Rana temporaria*) held under hypoxia (37) and in estivating snail (*Helix aspersa*) hepatopancreas cells (1). In arctic ground squirrels, the reduction of proton cycling was tissue-specific: proton leak was depressed in liver mitochondria of hibernators, but mitochondria isolated from skeletal muscle from hibernating and active animals exhibited nearly identical bioenergetic profiles.

Kinetics of proton leak

Mitochondrial respiration under non-phosphorylating (state 4) conditions is used to drive the leak of protons across the mitochondrial inner membrane. Results from three studies of mitochondria isolated from the liver of hibernating Richardson's (27) and arctic ground squirrels (11; 16) showed lower rates of state 4 respiration compared to non-hibernating animals. This depression was independent of assay temperature and was reversed during arousal from hibernation (16; 27). In contrast, Martin et al. (25) found no

differences in state 4 respiration in liver mitochondria isolated from hibernating, arousing, or summer-active golden-mantled ground squirrels. The results from the present study are in agreement with the former studies: during hibernation, state 4 respiration was decreased by 41% in mitochondria isolated from liver and assayed at 37°C (Table 3.1). Procedural differences may account for the discrepancy between our and previous studies: magnesium inhibits succinate dehydrogenase in rat liver (24; 26) and skeletal muscle (13) mitochondria, and the inclusion of magnesium in the assay buffer (11 mM $MgCl_2$, Ref. 25) may have masked differences in state 4 respiration between hibernating and active animals. This possibility is supported by the finding that the average state 4 oxygen consumption of both active and hibernating liver mitochondria in golden-mantled ground squirrels (25) was less than that measured in hibernators in this study and in Richardson's ground squirrels (27).

State 4 respiration is a crude indicator of proton leak, and parallel measurements of oxygen consumption and membrane potential are required to determine if a change in the magnitude of proton leak is in fact due to a change in membrane proton conductance. Proton conductance can be estimated by comparing rates of proton leak at common values of $\Delta\psi_m$ and is calculated as proton leak rate ÷ membrane potential . Decreased proton conductance has been observed experimentally and accounts for approximately 50% of the decrease in respiration rate between hyperthyroid and euthyroid rat hepatocytes (22). In addition, the difference in mitochondrial respiration between endotherms and ectotherms is also attributable to decreased proton conductance (7; 37). A decrease in proton conductance has not been demonstrated, however, in organisms that

depress metabolic rate. State 4 respiration was decreased in skeletal muscle mitochondria isolated from frogs held under hypoxia versus normoxia, but rates of oxygen consumption did not differ between groups at common values of $\Delta\psi_m$, suggesting that proton conductance was not altered (37). A similar study demonstrated that proton conductance is unchanged in hepatopancreas cells isolated from metabolically-depressed snails (1). The same conclusion was found for liver mitochondria in this study: although state 4 respiration was decreased in hibernators, the rate of proton leak did not differ for values of $\Delta\psi_m$ that were attained by mitochondria in both groups. Specifically, estimated proton conductance did not differ between hibernating and active groups at 180 mV, the highest $\Delta\psi_m$ that was common to both treatments (Figure 3.3). It is possible that this more stringent analysis underestimates the actual response, i.e. fails to identify a decrease in conductance, and therefore some of the decrease in oxygen consumption may be due to a modest depression of proton leak that could not be resolved using our techniques. However, the finding that the maximal (state 4) $\Delta\psi_m$ achieved by hibernators was significantly lower than that of the active animals (Figure 3.2A) corroborates the conclusion that conductance is not decreased during hibernation.

There are few studies of the effect of hibernation on mitochondrial bioenergetics in tissues other than liver. Brustovetsky et al. (9) reported that heart and skeletal muscle mitochondria isolated from hibernating arctic ground squirrels had elevated levels of state 4 respiration compared to non-hibernators. This increase may have been due to fatty acid-induced uncoupling (38), as rates were similar between groups when mitochondria were assayed in the presence of BSA. The present study reports similar findings in

skeletal muscle: state 4 respiration and $\Delta\psi_m$ were identical between hibernators and active squirrels, and the kinetic response of the proton leak was identical across all values of $\Delta\psi_m$ (Figure 3.4A).

Kinetics of substrate oxidation

An alternative means of decreasing proton cycling (other than altering membrane conductance) is by controlling the set of reactions that generate the proton gradient, namely by decreasing the activity of the enzymes of substrate oxidation. A number of studies suggest that substrate oxidation is decreased in liver mitochondria isolated from hibernating arctic ground squirrels (8; 11; 16), but membrane potential was not measured, and it is formally possible that the decreased respiration in these studies was attributable to decreased proton permeability.

The kinetics of substrate oxidation are typically measured by titrating either state 3 respiration with oligomycin or state 4 respiration with a chemical uncoupler; the resulting drop in membrane potential causes a stimulation of mitochondrial respiration, and the magnitude of this increase reflects the activity of the substrate oxidation subsystem (3). This response can also be estimated by plotting respiration rate against $\Delta\psi_m$ measured under state 3 and state 4 conditions. The line generated between these two points estimates the kinetic response of the substrate oxidation system to changes in $\Delta\psi_m$. In liver mitochondria, respiration rate was decreased two- to threefold in hibernators across the range of $\Delta\psi_m$ between state 4 and state 3 conditions, respectively (Figure 3.2B). In the absence of a change in membrane conductance (above), these data suggest that control of substrate oxidation reactions is the means by which mitochondrial proton

cycling is reduced during hibernation in arctic ground squirrels. Decreased activity of the enzymes of substrate oxidation appears to be the predominant mechanism by which proton cycling is reduced during metabolic depression in general, as this pattern was observed in mitochondria isolated from skeletal muscle of frogs housed under hypoxia (37) and snail hepatopancreas cells (1). Although the data from this study do not reveal which components of the substrate oxidation module are depressed, others have suggested that respiratory control of liver mitochondria during hibernation may be attributable to a decreased activity of succinate dehydrogenase (15; 16; 23; 27), a decreased rate of electron transfer in the respiratory chain (8), and altered membrane fluidity due to a lower activity of phospholipase A_2 (11).

In mitochondria isolated from skeletal muscle of arctic ground squirrels, however, it is uncertain if the kinetics of substrate oxidation are decreased during hibernation: respiration rate and $\Delta\psi_m$ were not different under state 4 conditions, but there was a slight depression of state 3 respiration rate (Figure 3.4B), suggesting a slight reduction in the activity of the substrate oxidation module. However, the reduction is significantly smaller than that observed in liver mitochondria (Figure 3.2B). The reason for this tissue-specific difference is not known, although the substrate oxidation module tends to be more active in skeletal muscle than in liver (33) and perhaps is less able to be controlled at the mitochondrial level. Alternatively, it is possible that substrate oxidation kinetics could be controlled *in vivo* at the organ level via decreased perfusion of skeletal muscle during hibernation, which would limit substrate supply. Measurement of proton leak in intact skeletal muscle (31) might resolve this issue.

In summary, this is the first study to investigate the kinetics of proton leak in a hibernating mammal. The results suggest that the decreased proton cycling in liver mitochondria during hibernation is achieved by decreasing the driving force (substrate oxidation reactions) and not due to decreased proton conductance. This depression persists at assay temperatures of 37°C, and adds to the growing body of literature that suggests that metabolic processes are subject to active control during hibernation, and not solely a function of reduced enzyme activity at low body temperatures.

PERSPECTIVES

Active depression of metabolism permits survival during periods of energy limitation and is a wide-spread phenomenon that involves coordinated regulation of ATP supply and demand (20). This can be achieved through decreasing energy-expensive processes such as protein synthesis (17), maintenance of ion gradients (2), and proton leak (1; 37) and this study). To date, all studies of mitochondrial proton cycling during metabolic depression have revealed that decreased proton leak is achieved by decreasing its driving force (substrate oxidation) rather than by decreasing the conductance of the membrane to protons. This similar pattern of control across a diverse range of taxa suggests an evolutionarily conserved means of regulating metabolic depression at the mitochondrial level, although the specific mechanism is unknown. In addition, this study found that metabolic control is tissue-specific, and this could potentially confound analyses of metabolic depression based on whole-animal metabolic rates.

Surprisingly, organisms devote a significant amount of respiration towards driving proton leak even during metabolic depression, suggesting that proton leak serves a critical

function that must be retained despite its cost. Proton leak may ameliorate the formation of reactive oxygen species (ROS) (35), and it is tempting to speculate that the maintenance of proton cycling in skeletal muscle represents a mechanism to prevent oxidative damage during ischemia-reperfusion injury during arousal from hibernation. The fact that inhibition of mitochondrial respiration in other tissues is reversed during arousal from hibernation also supports the hypothesis that proton leak may protect against ROS generation during tissue reperfusion. While there is little evidence that mitochondrial proton leak ameliorates oxidative damage *in vivo*, hibernating animals may be a useful model system towards this end.

ACKNOWLEDGEMENTS

We thank Dr. Paul Brookes for providing the TPMP sleeves used in this study and Drs. Abel Bult-Ito, Kelly Drew, and Dana Thomas for evaluation of the manuscript. Financial support was provided to J.L.B. through a fellowship provided by the Alaska NSF-EPSCoR program and to B.B.B. from DEPSCoR grant #N00014-01-1-0907.

REFERENCES

1. **Bishop T, St-Pierre J and Brand MD**. Primary causes of decreased mitochondrial oxygen consumption during metabolic depression in snail cells. *Am J Physiol Regulatory Integrative Comp Physiol* 282: R372-R382, 2002.

2. **Boutiiier RG**. Mechanisms of cell survival in hypoxia and hypothermia. *J Exp Biol* 204: 3171-3181, 2001.

3. **Brand MD**. The proton leak across the mitochondrial inner membrane. *Biochim Biophys Acta* 1018: 128-133, 1990.

4. **Brand MD**. Measurement of mitochondrial protonmotive force. In: *Bioenergetics: a practical approach*. Oxford: Oxford University Press, 1995, p. 39-62.

5. **Brand MD, Chien LF, Ainscow EK, Rolfe DF and Porter RK**. The causes and functions of mitochondrial proton leak. *Biochim Biophys Acta* 1187: 132-139, 1994.

6. **Brand MD, D'Alessandri L, Reis HM and Hafner RP**. Stimulation of the electron transport chain in mitochondria isolated from rats treated with mannoheptulose or glucagon. *Arch Biochem Biophys* 283: 278-284, 1990.

7. **Brookes PS, Buckingham JA, Tenreiro AM, Hulbert AJ and Brand MD**. The proton permeability of the inner membrane of liver mitochondria from ectothermic and endothermic vertebrates and from obese rats: correlations with standard metabolic rate and phospholipid fatty acid composition. *Comp Biochem Physiol* 119B: 325-334, 1998.

8. **Brustovetsky NN, Amerkhanov ZG, Popova E and Konstantinov AA**. Reversible inhibition of electron transfer in the ubiquinol. Cytochrome c reductase segment of the

mitochondrial respiratory chain in hibernating ground squirrels. *FEBS Lett* 263: 73-76, 1990.

9. **Brustovetsky NN, Egorova MV, Gnutov D, Gogvadze VG, Mokhova EN and Skulachev VP**. Thermoregulatory, carboxyatractylate-sensitive uncoupling in heart and skeletal muscle mitochondria of the ground squirrel correlates with the level of free fatty acids. *FEBS Lett* 305: 15-17, 1992.

10. **Brustovetsky NN, Egorova MV and Mayevsky EI**. Regulation of oxidative activity and $\Delta\Psi$ of liver mitochondria of active and hibernating gophers. The role of phospholipase A_2. *Comp Biochem Physiol* 102B: 635-638, 1992.

11. **Brustovetsky NN, Mayevsky EI, Grishina EV, Gogvadze VG and Amerkhanov ZG**. Regulation of the rate of respiration and oxidative phosphorylation in liver mitochondria from hibernating ground squirrels, *Citellus undulatus*. *Comp Biochem Physiol* 94B: 537-541, 1989.

12. **Buck CL and Barnes BM**. Effects of ambient temperature on metabolic rate, respiratory quotient, and torpor in an arctic hibernator. *Am J Physiol Regulatory Integrative Comp Physiol* 279: R255-R262, 2000.

13. **Cadenas S and Brand MD**. Effects of magnesium and nucleotides on the proton conductance of rat skeletal-muscle mitochondria. *Biochem J* 348: 209-213, 2000.

14. **Canton M, Luvisetto S, Schmehl I and Azzone GF**. The nature of mitochondrial respiration and discrimination between membrane and pump properties. *Biochem J* 310: 477-481, 1995.

15. **Chaffee RRJ, Hoch FL and Lyman CP**. Mitochonrial oxidative enzymes and phosphorylations in cold exposure and hibernation. *Am J Physiol* 201: 29-32, 1961.

16. **Fedotcheva NJ, Sharyshev AA, Mironova GD and Kondrashova MN**. Inhibition of succinate oxidation and K+ transport in mitochondria during hibernation. *Comp Biochem Physiol* 82B: 191-195, 1985.

17. **Frerichs KU, Smith CB, Brenner M, DeGracia DJ, Krause GS, Marrone L, Dever TE and Hallenbeck JM**. Suppression of protein synthesis in brain during hibernation involves inhibition of protein initiation and elongation. *Proc Natl Acad Sci USA* 95: 14511-14516, 1998.

18. **Gehnrich SC and Aprille JR**. Hepatic gluconeogenesis and mitochondrial function during hibernation. *Comp Biochem Physiol* 91B: 11-16, 1988.

19. **Geiser F**. Reduction of metabolism during hibernation and daily torpor in mammals and birds: temperature effect or physiological inhibition? *J Comp Physiol [B]* 158: 25-37, 1988.

20. **Hand SC and Hardewig I**. Downregulation of cellular metabolism during environmental stress: mechanisms and implications. *Annu Rev Physiol* 58: 539-563, 1996.

21. **Hannon JP, Vaughn DA and Hock RJ**. The endogenous tissue respiration of the arctic ground squirrels as affected by hibernation and season. *J Cellular Comp Physiol* 57: 5-10, 1961.

22. **Harper ME and Brand MD**. The quantitative contributions of mitochondrial proton leak and ATP turnover reactions to the changed respiration rates of hepatocytes from rats of different thyroid status. *J Biol Chem* 268: 14850-14860, 1993.

23. **Liu CC, Frehn JL and LaPorta AD**. Liver and brown fat mitochondrial response to cold in hibernators and nonhibernators. *J Appl Physiol* 27: 83-89, 1969.

24. **Lund P and Wiggins D**. Maintenance of energy-linked functions in rat liver mitochondria. *Biochim Biophys Acta* 1018: 98-102, 1990.

25. **Martin SL, Maniero GD, Carey S and Hand SC**. Reversible depression of oxygen consumption in isolated liver mitochondria during hibernation. *Physiol Biochem Zool* 72: 255-264, 1999.

26. **Panov A and Scarpa A**. Mg^{2+} control of respiration in isolated rat liver mitochondria. *Biochemistry* 35: 12849-12856, 1996.

27. **Pehowich DJ and Wang LCH**. Seasonal changes in mitochondrial succinate dehydrogenase activity in a hibernator, *Spermophilus richardsonii. J Comp Physiol [B]* 154: 495-501, 1984.

28. **Reynafarje B, Costa LE and Lehninger AL**. O_2 solubility in aqueous media determined by a kinetic method. *Anal Biochem* 145: 406-418, 1985.

29. **Roberts JC and Chaffee RRJ**. Suppression of mitochondrial respiration in hibernation and its reversal in arousal. In: *Proceedings of the International Symposia on Environmental Physiology: Bioenergetics and Temperature Regulation*, edited by Smith RE, Shields JL, Hannon JP and Horwitz BA. Bethesda, MD: FASEB, 1972, p. 101-107.

30. **Rolfe DFS and Brand MD**. Contribution of mitochondrial proton leak to skeletal muscle respiration and to standard metabolic rate. *Am J Physiol Cell Physiol* 271: C1380-C1389, 1996.

31. **Rolfe DFS and Brand MD**. Proton leak and control of oxidative phosphorylation in perfused, resting rat skeletal muscle. *Biochim Biophys Acta* 1276: 45-50, 1996.

32. **Rolfe DFS and Brown GC**. Cellular energy utilization and molecular origin of standard metabolic rate in mammals. *Physiol Rev* 77: 731-758, 1997.

33. **Rolfe DFS, Hulbert AJ and Brand MD**. Characteristics of mitochondrial proton leak and control of oxidative phosphorylation in the major oxygen-consuming tissues of the rat. *Biochim Biophys Acta* 1188: 405-416, 1994.

34. **Rolfe DFS, Newman JMB, Buckingham JA, Clark MG and Brand MD**. Contribution of mitochondrial proton leak to respiration rate in working skeletal muscle and liver and to SMR. *Am J Physiol Cell Physiol* 276: C692-C699, 1999.

35. **Skulachev VP**. Uncoupling: new approaches to an old problem of bioenergetics. *Biochim Biophys Acta* 1363: 100-124, 1998.

36. **Snapp BD and Heller HC**. Suppression of metabolism during hibernation in ground squirrels (*Citellus lateralis*). *Physiol Zool* 54: 297-307, 1981.

37. **St-Pierre J, Brand MD and Boutilier RG**. The effect of metabolic depression on proton leak rate in mitochondria from hibernating frogs. *J Exp Biol* 203: 1469-1476, 2000.

38. **Sultan A and Sokolove PM**. Free fatty acid effects on mitochondrial permeability: An overview. *Archiv Biochem Biophys* 386: 52-61, 2001.

Table 3.1. Respiratory properties of liver and skeletal muscle mitochondria.

	Liver		Skeletal muscle	
	Active	Hibernating	Active	Hibernating
State 3 respiration	253.1 ± 18.7	76.9 ± 10.4 *	602.3 ± 36.7	481.9 ± 25.8 *
State 4 respiration	33.0 ± 2.9	19.4 ± 2.0 *	107.9 ± 5.2	95.6 ± 7.3
Respiratory control ratio	7.8 ± 0.5	4.3 ± 0.9 *	5.6 ± 0.2	5.2 ± 0.2

Respiratory rates are shown as nmol O · min^{-1} · mg^{-1} mitochondrial protein; see MATERIALS AND METHODS for specific assay conditions. Respiratory control ratios were calculated as state 3 respiration ÷ state 4 respiration. * Significantly different compared to active value ($P < 0.01$). Values are means ± SE.

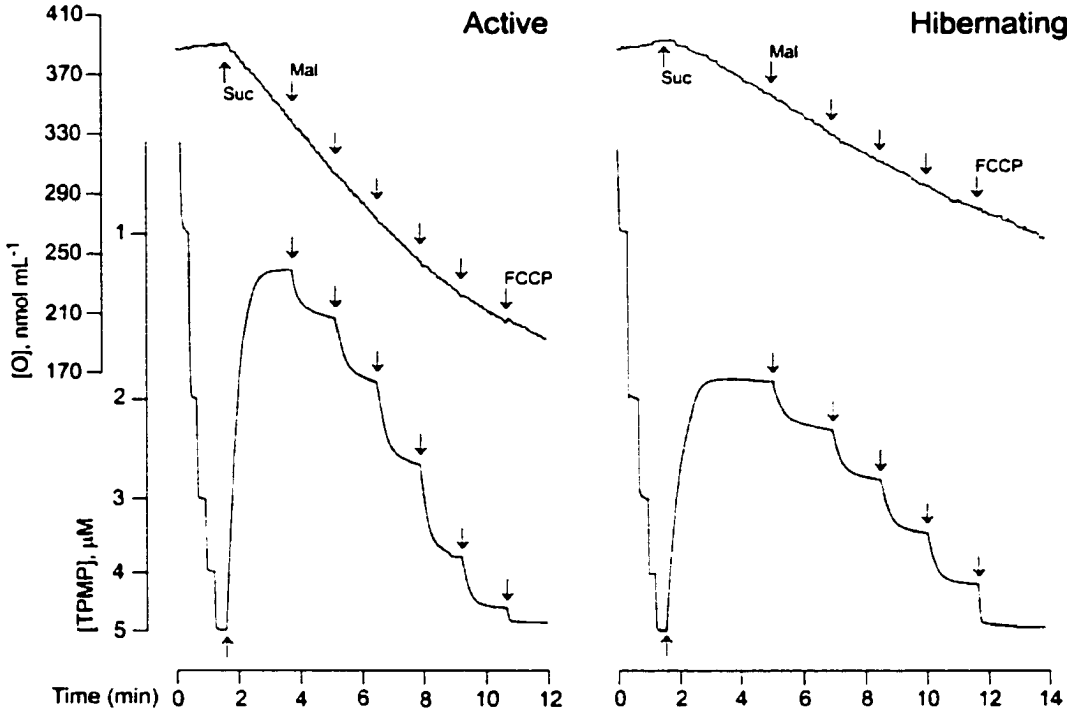

Figure 3.1. Representative traces of the proton leak assay in liver mitochondria. Representative traces showing the relationship between the concentrations of oxygen (upper trace) and TPMP (lower trace) in assay buffer containing mitochondria isolated from the livers of an active (left panel) and a hibernating (right panel) arctic ground squirrel sampled on the same day. Mitochondria were incubated in assay buffer, rotenone, oligomycin, and nigericin for at least one minute prior to TPMP additions. Upward arrows designate addition of succinate (Suc) and downward arrows designate the successive additions of malonate (Mal) or the final addition of a chemical uncoupler (FCCP); arrows on the TPMP traces correspond with those on the oxygen traces. The mitochondrial membrane potential is calculated from, and is an inverse function of, the concentration of TPMP in assay buffer, such that a low concentration of TPMP in the buffer reflects a high $\Delta\psi_m$. See MATERIALS AND METHODS for details.

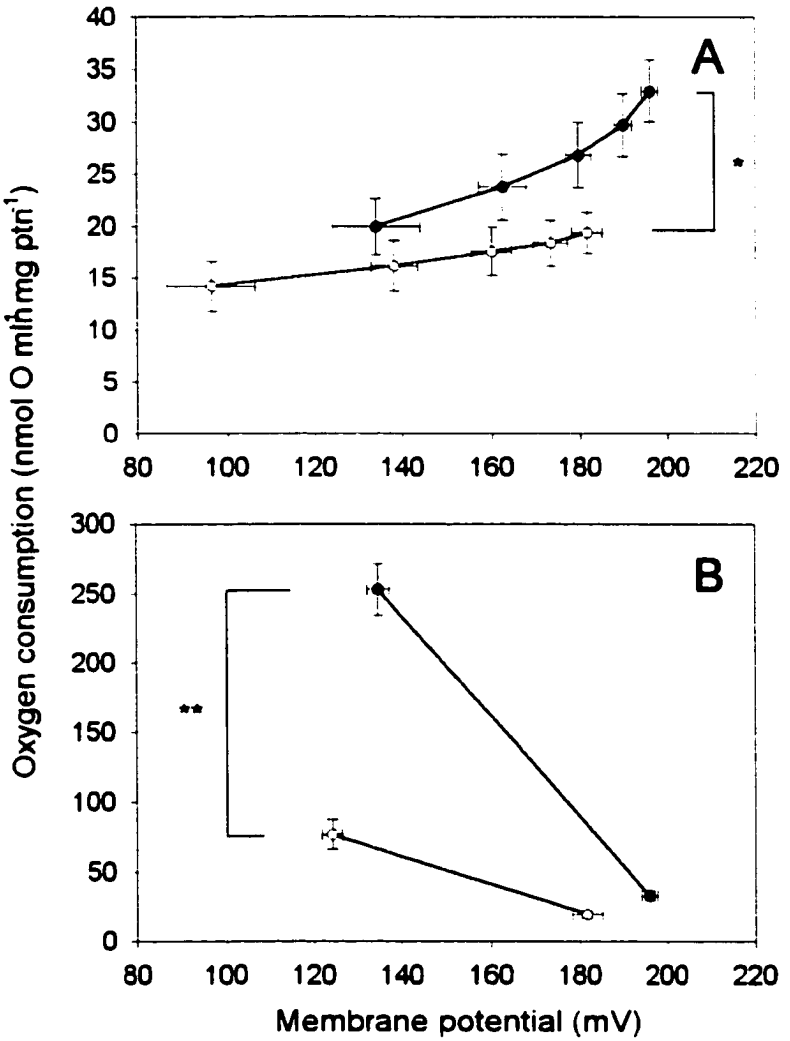

Figure 3.2. Kinetics of the proton leak and substrate oxidation systems in liver mitochondria.

Kinetic response of the proton leak (A) and substrate oxidation system (B) to $\Delta\psi_m$ in liver mitochondria isolated from active and hibernating arctic ground squirrels. *Filled symbols*, active animals; *open symbols*, hibernating animals. * designates a significant difference between active and hibernating groups for both state 4 respiration rate and state 4 $\Delta\psi_m$ ($P < 0.01$); ** designates a significant difference between active and hibernating groups for both state 3 respiration rate and state 3 $\Delta\psi_m$ ($P < 0.001$). Values are means ± SE; $n = 5$ animals per treatment.

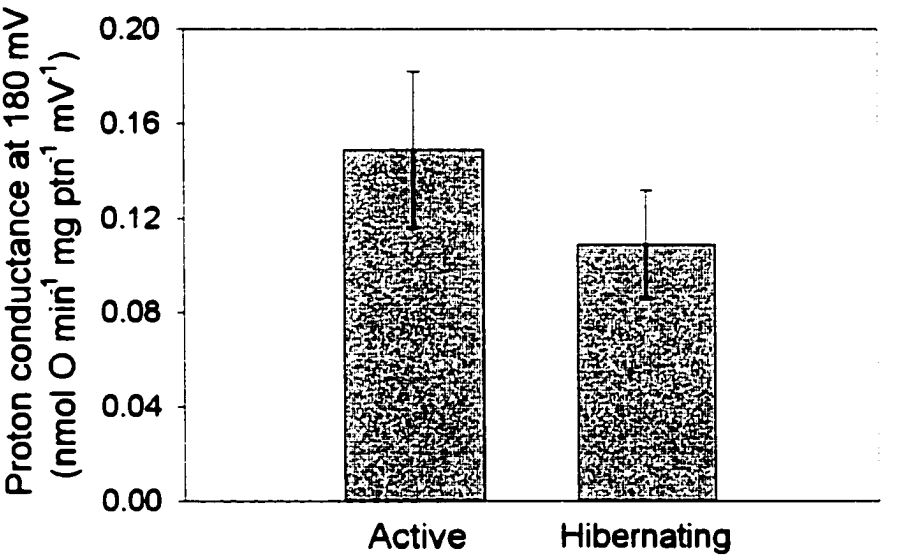

Figure 3.3. Estimated proton conductance of liver mitochondria.
Estimated proton conductance of mitochondria isolated from liver of arctic ground squirrels at a $\Delta\psi_m$ of 180 mV. Proton conductance is defined as proton leak rate per mV and was calculated as proton leak rate ÷ 180 (the highest $\Delta\psi_m$ common to both active and hibernating groups) and was not significantly different between active and hibernating groups. Values are means ± 95% confidence intervals.

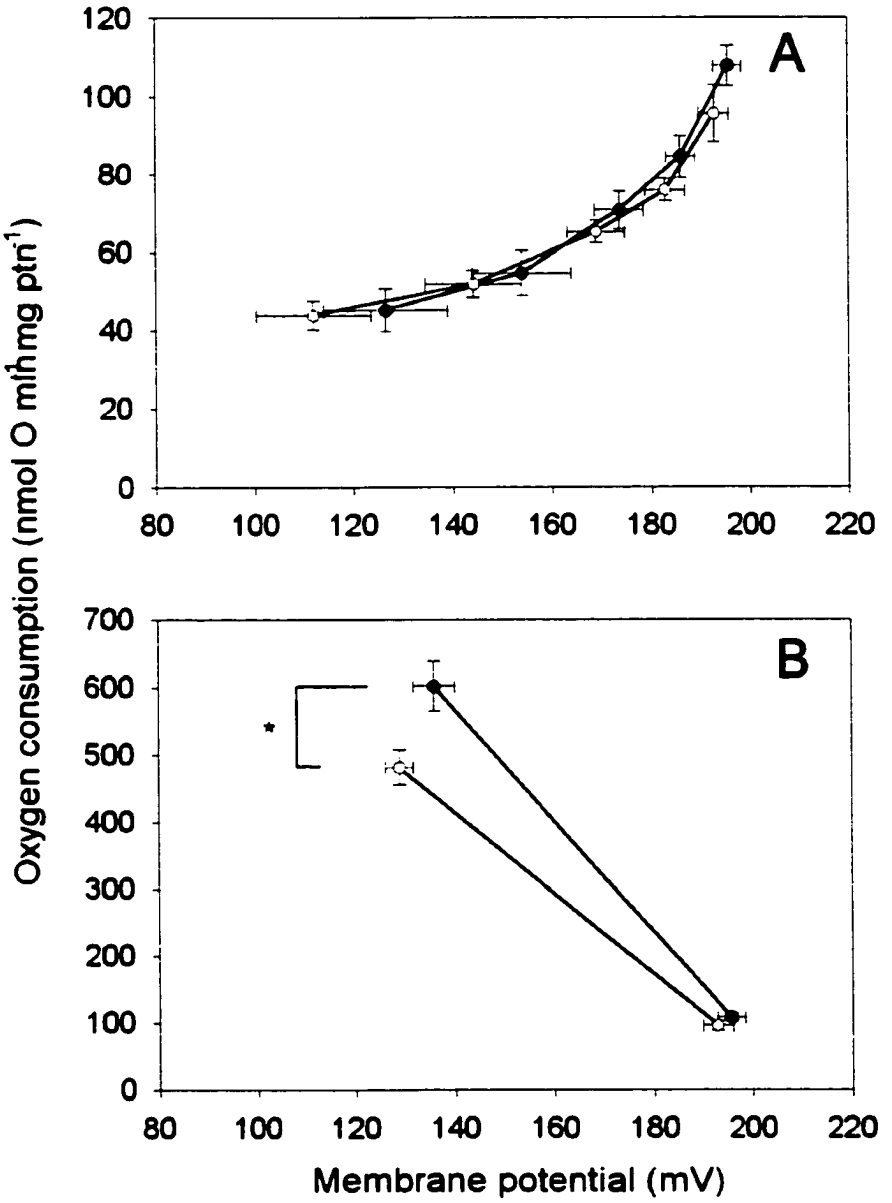

Figure 3.4. Kinetics of the proton leak and substrate oxidation systems in skeletal muscle mitochondria.

Kinetic response of the proton leak (A) and substrate oxidation system (B) to $\Delta\psi_m$ in skeletal muscle mitochondria isolated from active and hibernating arctic ground squirrels. *Filled symbols*, active animals; *open symbols*, hibernating animals. * designates a significant difference between active and hibernating groups for state 3 respiration rate (P = 0.04).Values are means ± SE; n = 5 animals per treatment.

CONCLUSIONS

The hormone leptin was initially proposed to serve as a negative feedback signal to counter obesity, as demonstrated in an inbred mouse strain deficient for leptin production (Pelleymounter et al. 1995; Zhang et al. 1994). However, leptin failed to elicit marked decreases in food intake and body mass in later studies using outbred rodent strains (Harris et al. 1998), humans (Heymsfield et al. 1999), and wild species (Baker et al. 2000; Boyer et al. 1997; Klingenspor et al. 1996; Ormseth et al. 1996). In a review of leptin research, these seemingly paradoxical results led one investigator to conclude that if the primary physiological role of leptin is to prevent obesity, than "it must rank as the least effective hormone in all of endocrinology" (Unger 2000). I hypothesized that leptin serves as a reliable index of adiposity and acts to regulate food intake, adiposity, and timing of immergence into hibernation in a seasonally-fattening species, the arctic ground squirrel. However, during prehibernation fattening, all of these parameters were unaffected by administration of mouse recombinant leptin. Accumulating evidence in an array of species suggests that leptin controls metabolism when found at physiological concentrations in the blood, but that its effects do not increase in magnitude when leptin is found at extremely high levels in the circulation (Flier 1998). Similarly, I found that administration of a low dose of leptin resulted in moderate increases in serum leptin levels and tended to promote mass gain by concomitantly increasing serum insulin levels and minimizing energy expenditure via uncoupling proteins (UCPs); in general, this pattern was reversed when animals were administered a high dose of leptin that elevated plasma levels 14-fold above the physiological range. Coordination of seasonal activities

prior to hibernation probably depends on a complex interaction between environmental factors as well as other hormones and neuropeptides with redundant control mechanisms. While leptin may play a role in this intricate system, the balance of experimental evidence does not support the notion that leptin functions to prevent obesity.

After prehibernation fattening, arctic ground squirrels commence a prolonged hibernation season during which animals defend a high body temperature by invoking nonshivering thermogenesis (NST). Uncoupling protein 1 (UCP1) is a mitochondrial inner membrane protein in brown adipose tissue (BAT) and mediates NST by uncoupling oxidative phosphorylation (Nicholls and Locke 1984). Tissues other than BAT have been reported to show NST, but because UCP1 is found almost exclusively in BAT a molecular mechanism for this process was not clear. Recently, several genes have been identified whose protein sequences are homologous to UCP1 and are expressed in a manner suggesting that they may mediate NST in multiple tissues. I investigated the possibility that UCP3 mediates NST in skeletal muscle (SKM) of the arctic ground squirrel by comparing its expression and activity to that of UCP1 under a variety of experimental regimes. Consistent with a thermoregulatory role, UCP1 was elevated by cold exposure, increased in animals hibernating at low temperatures, and was decreased during fasting. However, levels of *Ucp3* mRNA were not elevated by cold but were paradoxically increased during fasting. Furthermore, a fivefold increase in UCP3 levels did not catalyze mitochondrial uncoupling in vitro, suggesting that UCP3 does not mediate NST. Levels of *Ucp3* mRNA were elevated during hibernation, and because levels of fatty acids circulate at high concentrations during this time, these results agree

with the developing hypothesis that UCP3 may function to protect mitochondria from lipotoxicity when fatty acids circulate at high levels in the blood (Himms-Hagen and Harper 2001).

Extending my investigation into the control of metabolism at the mitochondrial level, I conducted an experiment to determine if the magnitude of the endogenous proton leak, an inherent inefficiency found in all mitochondria (Brand 1990), is reduced during hibernation as a means of actively depression metabolism. To date, only two studies have investigated the control of this pathway during metabolic depression: mitochondria isolated from frogs housed under anoxia (St-Pierre et al. 2000) and hepatopancreas cells isolated from estivating snails (Bishop et al. 2002). Both studies show a decreased activity of the proton leak pathway; however, the decrease in proton cycling is not due to decreased proton permeability of the mitochondrial inner membrane but rather to a decreased activity of the upstream block of reactions generating the proton gradient. I found that mitochondria isolated from the liver of hibernating arctic ground squirrels showed an identical pattern of control, but that the bioenergetic profile of mitochondria isolated from skeletal muscle were unchanged during hibernation. This is the first study to identify the mitochondrial basis for active metabolic depression in a hibernating mammal. Because mitochondrial activity during metabolic depression is controlled by a similar mechanism in diverse taxa, this suggests that there is an evolutionarily conserved means for metabolic depression. The finding that proton cycling is not affected by hibernation in skeletal muscle mitochondria was unexpected; however, maintenance of proton cycling has been proposed to prevent the formation of reactive oxygen species

(Skulachev 1998), and may therefore be a mechanism to protect against oxidative damage during ischemia/reperfusion injury that may occur in skeletal muscle during hibernation.

The underlying premise of all of these studies was that the newly identified mechanisms of metabolic control would be most pronounced in a model system which shows high amplitude changes in energy balance. In general, this was not the case: the role of leptin and uncoupling protein homologues was similar to that observed in numerous species which do not show dramatic increases in adiposity or possess a large thermogenic capacity. Similarly, the mechanism for depression of respiration in mitochondria isolated from the liver of arctic ground squirrels is similar to that observed in frogs and snails. At first blush, these findings undermine the supposed advantages of using a comparative approach to elucidate mechanisms of metabolic control. However, I would argue that using the comparative approach offers perhaps the most effective means of elucidating metabolic control, because, as in these studies, using a comparative approach fails to show metabolic control in a model system where one would expect it to be most pronounced.

APPENDIX – IMPACT OF ENDOTOXIN ON UCP HOMOLOGUE mRNA ABUNDANCE, THERMOREGULATION, AND MITOCHONDRIAL PROTON LEAK KINETICS

Published in the American Journal of Physiology as: Yu XX, Barger JL, Boyer BB, Brand MD, Pan G and Adams SH. Impact of endotoxin on UCP homolog mRNA abundance, thermoregulation, and mitochondrial proton leak kinetics. American Journal of Physiology – Endocrinology and Metabolism 279: E433-E446, 2000. Reprinted with permission from the American Physiological Society.

ABSTRACT

Linking tissue uncoupling protein (UCP) homologue abundance with functional metabolic outcomes and with expression of putative genetic regulators promises to better clarify UCP homologue physiological function. A murine endotoxemia model characterized by marked alterations in thermoregulation was employed to examine the association between heat production, *Ucp* homologue expression, and mitochondrial proton leak ("uncoupling"). After intraperitoneal lipopolysaccharide (LPS, ~6 mg · kg^{-1}) injection, colonic temperature (T_c) in adult female C57BL6/J mice dropped to a nadir of ~30°C by 8 h, preceded by a four- to fivefold drop in liver *Ucp2* and *Ucp5* / brain mitochondrial carrier protein 1 mRNA levels, with no change in their hindlimb skeletal muscle (SKM) expression. SKM *Ucp3* mRNA rose fivefold during development of hypothermia and was correlated with an LPS-induced increase in plasma free fatty acid concentration. *Ucp2* and *Ucp5* transcripts recovered about three- to sixfold in both tissues starting at 6-8 h, preceding a recovery of T_c between 16 and 24 h. SKM *Ucp3* followed an opposite pattern. Such results are not consistent with an important influence of UCP3 in driving heat production but do not preclude a role for UCP2 or UCP5 in this process. The transcription coactivator *Pgc-1* displayed a transient LPS-evoked rise (threefold) or drop (two- to fivefold) in SKM and liver expression, respectively. No differences between control and LPS-treated mouse liver or SKM in vitro mitochondrial proton leak were evident at time points corresponding to large differences in *Ucp* homologue expression.

INTRODUCTION

Maintenance of a stable body temperature involves a precise balance between heat acquisition and loss, driven by a complex interaction of physiological, behavioral, and environmental processes. The ability to generate and regulate metabolic heat is a hallmark of endothermy and a critical adjunct to other events which contribute to efficient thermoregulation (physiological control of convective and conductive heat loss, heat- or cold-seeking behavior, etc.). Heat production in endotherms is in part ascribed to global energetic inefficiency inherent to cellular biochemical reactions augmented by additional energy-consuming mechanisms, including protein turnover and futile cycling, which drive ATP consumption (8). The relative contribution of these and other mechanisms toward establishment of metabolic rate is the subject of active research. Identification of the molecular and biochemical components underlying regulation of heat balance has important ramifications for the development of pharmaceutical intervention strategies to treat metabolic disorders, and for clarifying regulation of adaptational thermoregulation in nature.

One potential locus of thermoregulatory control is proton flux across the inner mitochondrial membrane. It is now apparent that the inward flow of protons via mechanisms independent of F_1F_o ATP synthase (termed "proton leak") is not insignificant and would act to dissipate fuel-derived energy as heat (8; 36). In rodents, this process is modified by changes in thyroid status (18; 25) and in some forms of obesity (11), and it may account for ~20% to 40% of tissue metabolic rate under normal conditions (8). The underpinnings of proton leak remain to be established. The characterization and cloning

of *Ucp1* (7; 19), a specific uncoupling protein (UCP) that facilitates accelerated proton leak in stimulated rodent brown adipose tissue (BAT), have supported the notion that bodywide proton leak may be regulated by specific mitochondrial proteins. Recent descriptions of putative UCP homologues residing in various tissues (3; 15-17; 27; 39; 41; 45) have sparked interest in exploring whether these proteins influence tissue-specific or whole animal heat production. Some studies examining homologue mRNA abundance are consistent with a role for UCP homologues in modifying proton leak and metabolic rate, whereas other results may point to additional metabolic roles for these proteins.

Supportive of an uncoupling role for UCP homologues, there are certain conditions in which *Ucp2* or *Ucp3* mRNAs appear to correlate with in vitro determinations of mitochondrial proton leak (11; 25). Furthermore, expression of *Ucp2* and *Ucp3* in rodent BAT rises in response to cold exposure (6), concurrent with increased proton leak in this tissue. Thyroid hormone administration to rodents, a condition in which tissue proton leak has been shown to rise (18; 25), increases *Ucp3* mRNA in muscle (17; 21; 25) and up-regulates *Ucp2* in a tissue-specific manner (21; 24). *Ucp5* [also termed brain mitochondrial carrier protein 1 (BMCP1) (39)] is widely expressed, and its liver mRNA level is altered in parallel with metabolism during fasting, cold challenge, and a high-fat diet in obesity-resistant mice; cold also induces its expression in the brain (45). Brain-specific *Ucp4* mRNA is upregulated in this organ upon exposure of mice to cold (45), consistent with the hypothesis that UCP4 could be involved in localized adaptational thermoregulation (28). Results that do not support a classic thermogenic uncoupling role for UCP2 and UCP3 include reports of a rise in their

skeletal muscle (SKM) transcript levels during fasting or food restriction (5; 9; 17; 20; 29; 30; 37; 43) despite a lack of change of in vitro SKM proton leak (9), the higher abundance of *Ucp2* mRNA sometimes observed in obesity (11; 16; 29), and the lack of a consistent demonstration for a robust rise in SKM mRNAs upon cold exposure (3; 5; 15; but also see (4) for induction of *Ucp2* by cold).

Divergent tissue expression patterns (*Ucp2* is widely expressed, whereas *Ucp3* is most abundant in SKM and BAT, but without expression in liver) and differential modification after certain experimental manipulations (17; 43; 44) indicate that some differences in gene regulation exist when *Ucp2* and *Ucp3* are compared. Often, however, patterns of expression for these homologues converge (6). The association between their expression and that of *Ucp5*, and the differential expression of *Ucp5* in SKM have not been reported.

Animal models that display broad alterations in heat production serve as valuable tools to better understand cellular mechanisms that drive metabolic rate, including the role of UCP homologues. The murine model of endotoxemia provides an interesting system in this regard, because administration of lipopolysaccharide (LPS) elicits a range of thermoregulatory responses, including acute hypothermia usually followed by temperature recovery (23; 32). It is plausible that LPS-induced changes in *Ucp* homologue expression and uncoupling activity in metabolically relevant tissues underlie the decline and/or rebound of body temperature in this model. Indeed, it has been reported that liver *Ucp2* mRNA is increased at 12-24 h after LPS administration in rodents (11; 12; 14), leading to the speculation that this rise may signal an increase in

active uncoupling and thermogenesis in this organ (14). However, no physiological or biochemical correlates were presented, and studies investigating the temporal effects of LPS on *Ucp* homologue expression in SKM have not been reported. In this study, we examined the degree to which *Ucp* homologue mRNA abundance correlates with observed changes in functional metabolic outcomes (body temperature, mitochondrial proton leak, and metabolic rate) after a hypothermia-inducing dose of LPS, focusing on the liver and SKM which are estimated to contribute over one-half of the metabolic rate under normal conditions (8). In an effort to better understand the regulatory factors driving observed *Ucp* homologue expression changes, the association between such changes with those of the recently characterized peroxisome proliferator-activated receptor-γ (PPARγ) coactivator 1 (PGC-1) (33; 44) was assessed. PGC-1 has been implicated in the induction of genes encoding UCP1, UCP2, and other metabolically relevant proteins (33; 44). In addition, the idea was explored that core body temperature-sensing pathways trigger alterations in *Ucp* homologue gene expression in LPS-treated mice. Despite large changes in liver and SKM *Ucp* homologue mRNA abundance, *Pgc-1* expression, and evidence for remarkable metabolic shifts after LPS, no association of these parameters with mitochondrial proton leak could be discerned. A disconnect between *Pgc-1* and *Ucp2* expression (particularly evident in SKM) after LPS indicated that under these conditions regulatory factors distinct from PGC-1 modulated *Ucp2* transcription.

MATERIALS AND METHODS

Animals

All animal studies conformed to the "Guiding Principles for Research Involving Animals and Human Beings" and were done in accordance with guidelines set forth by the Institutional Animal Care and Use Committee at Genentech. Female C57BL6/J mice (Jackson Labs, Bar Harbor, ME) aged 54–63 days and weighing 16–18 g were used for all studies. Mice were received 1 wk before experimentation and, unless otherwise noted, were housed on a 12:12-h light-dark cycle (lights on at 0600) at 22°C and were fed normal rodent chow (Ralston Purina Chow 5010, St. Louis, MO). Where indicated, heparinized blood was obtained by heart puncture from CO_2-anesthetized mice and was promptly centrifuged to obtain plasma, after which free fatty acid (FFA) concentrations were measured (NEFA C kit, Wako Chemicals, Richmond, VA).

Reagents

LPS was a Westphal preparation from *Escherichia coli* 055:B5 (Lot 121379JD, Difco Laboratories, Detroit, MI). Methyltriphenylphosphonium bromide (TPMP) was purchased from Aldrich Chemicals (Milwaukee, WI). Collagenase Type IV was obtained from Worthington Biochemical (Lakewood, NJ). Other chemicals were from Sigma (St. Louis, MO).

LPS administration

To best compare results with those reported by Faggioni et al. (14), conditions used herein were generally similar to those used by that group. A working stock of LPS was prepared in sterile PBS, and aliquots were frozen at 220°C and thawed once on the day of the experiment. For all LPS experiments, LPS was injected intraperitoneally at 100 mg · mouse^{-1} (5.6–6.2 mg · kg^{-1}) in a volume of 100 mL between 1430 and 1630. Preliminary

experiments indicated that this dosage elicited a marked hypothermia compared with doses 10- to 100-fold lower (not shown) and was similar in magnitude to the amount given by Faggioni et al. Control mice received 100 mL PBS intraperitoneally. After injection, mice were given access to water but were fasted to account for the effects of LPS-induced cachexia (14). Various parameters hypothesized to be influenced by endotoxemia were monitored for up to 48 h (see below). Unless otherwise noted (see *study 2*), mice were housed at 22°C for the duration of each experiment.

Body temperature and Ucp homologue mRNA after LPS (studies 1 and 2)

An initial experiment (*study 1*) was designed to ascertain whether mRNAs encoding UCP homologues track metabolism after LPS. At intervals of 0, 2, 4, 6, 8, 16, 24, and 48 h after injection, body temperatures in groups of control or LPS-treated mice (n = 3–5 per treatment per time point) were determined as follows. Mice were removed from the cage with minimal disturbance, and colonic temperature (T_c) was rapidly measured with a mouse rectal thermocouple (Physitemp BAT-10 recorder/RET-3 thermocouple, Clifton, NJ). Mice were then killed under CO_2, and tissues were harvested and snap-frozen. For studies of SKM, whole hindlimb SKM was excised, and visible fat and nervous tissue were removed before freezing. In *study 2*, a new group of mice were subjected to the same protocol but were placed in a warm (34°C) room after injection to test the effects of core temperature maintenance on LPS-altered parameters.

Total RNA preparations from liver or pulverized SKM of individual mice were made (Ultraspec reagent, Biotecx Laboratories, Houston, TX) and were assayed for

mRNA abundance with quantitative real time RT-PCR after digestion of samples with DNAse per manufacturer's instructions (GIBCO BRL, Grand Island, NY). This system employed primers and probes specific to murine *Ucp2*, total *Ucp5*, *Ucp3*, *Pgc-1*, and macrophage-specific marker F4/80 (Table A.1). 18S primers/probes were purchased from Perkin-Elmer Applied Biosystems (Foster City, CA). Specificity of *Ucp* primers/probes was confirmed by testing against a panel of plasmids containing cDNAs encoding *Ucp2-5*, and the amount of RNA analyzed was in the linear range of the assay (not shown). Reactions and detection were carried out with the use of a model 7700 sequence detector and TaqMan reagents (PE Applied Biosystems) in a volume of 50 mL and containing 100 ng RNA, 3 mM $MgCl_2$, reaction buffer A (13), 12.5 U MuLV reverse transcriptase, 1.25 U TaqGold, forward and reverse primers (0.01 OD each), and 0.1 mM probe (18S analyses utilized 240 pg RNA, 5.5 mM $MgCl_2$, and 0.05 mM probe/primer). Cycling conditions were 50°C for 15 min and 95°C for 10 min, followed by 40 cycles of 95°C for 15 s and 60°C for 1 min. Putative housekeeping gene mRNAs (β-actin, GAPDH, RPL19) tested in a subset of LPS liver samples indicated that their levels declined over time after injection (14); thus 18S mRNA abundance was used as a loading control, and all values reported herein represent 18S-corrected values. Based on established tissue distribution patterns for the *Ucp* homologues (see the introductory section of this paper), analyses focused on *Ucp3* in SKM and *Ucp2*/*Ucp5* in SKM and liver.

Mitochondrial proton leak measurements (study 3)

In *study 3*, examining the correlation between *Ucp* homologue mRNA and mitochondrial proton leak in liver and SKM, a new set of mice was used (injection protocol identical to that of *study 1*). At certain times after injection, mitochondria were prepared from control or LPS-injected animals and assayed in parallel. Protocols for mitochondria isolation and measurement of proton leak were patterned after those reported elsewhere (36). After measuring T_c, mice were killed under CO_2, livers were removed, a fraction was snap-frozen for mRNA analysis, and the remainder was placed in ice-cold STE buffer (250 mM sucrose, 5 mM Tris, 2 mM EGTA, pH 7.4). For mitochondria, livers from 3–5 mice per treatment were pooled and minced on ice in a small volume of STE. Samples were then processed by standard homogenization and centrifugation methods (36), with the final mitochondrial pellet resuspended in 500 mL STE and kept on ice until analysis. Hindlimb SKM was obtained from a separate set of mice. For these studies, muscle from a single mouse per treatment was obtained and snap-frozen for RNA, after which hindlimb muscles from each of 5–6 mice per treatment were pooled to obtain mitochondria. Samples were processed by use of a slight modification of the protocols employed by Rolfe et al. (36): after removal of visible fat and nervous tissue, samples in the current study were placed in ice-cold CP1 buffer (100 mM KCl, 50 mM Tris · HCl, 2 mM EGTA, pH 7.4), minced on an ice-cold glass plate, and added to 50 mL of pH 7.4 CP2 buffer (100 mM KCl, 50 mM Tris · HCl, 2 mM EGTA, 0.5% FFA-free BSA, 5 mM $MgCl_2$, 1 mM ATP, 2.1 U nagarse · mL; ATP/nagarse added on day of experiment). Samples were kept on ice for 10 min with occasional agitation and then subjected to a brief (10 s, 20,000 rpm) polytron on ice (PowerGen 700, Fisher Scientific, Santa Clara,

CA) and an additional 10-min cold incubation before differential centrifugation and washes at 4°C (36). Supernatants from the initial 10-min/500-*g* centrifugation were poured through two layers of gauze before the high-speed spins/washes. Resulting pellets were resuspended in 200–300 mL CP1 and kept on ice until assay. Mitochondria prepared in this way yielded respiratory control ratios (state 3/state 4 respiration with succinate as substrate) of >5 (liver) or >3 (SKM). Protein concentrations were determined by the bicinchoninic acid assay (BCA kit, Pierce, Rockford, IL).

For proton leak assays, mitochondria were introduced at ~1 mg protein · mL^{-1} to a water-jacketed chamber containing 3.5 mL pH 7.2 KHE buffer (120 mM KCl, 5 mM KH_2PO_4, 3 mM HEPES, 1 mM EGTA, 0.3% fatty acid-free BSA) containing rotenone (5 μM), oligomycin (1 μg · mL^{-1}), and nigericin (80 ng · mL^{-1}). Oxygen consumption of mitochondria was monitored by a Clark-type model 300 oxygen electrode/Type 1 electronic stirring head (Rank Brothers, Cambridge, UK) interfaced with a Unit DW4 oxygen back-off system (Gritech Engineering, UK) and a chart recorder (Kipp and Zonen). Oxygen saturation values of 471 nmol O · mL^{-1} and 406 nmol O · mL^{-1} were used to calculate oxygen consumption of preparations assayed at 26 and 37°C, respectively (34). Measurements of mitochondrial TPMP1 uptake were made with a TPMP1-sensitive electrode (36) referenced with a semimicro CE2 pH electrode (Unicam, Cambridge, UK) and interfaced with a back-off box, pH meter, and chart recorder. Within each individual run, a standard curve of recorder distance vs. [TPMP] was calculated using 1-μM additions of TPMP to 5 μM (liver) or 0.5-μM additions to 2 μM (SKM). After addition of Na2-succinate (4 μM), respiration was titrated by additions of

Na_2-malonate (≤7.9 μM and 4.5 μM in liver and SKM, respectively). Drift was determined by addition of 2 μM carbonyl cyanide *p*-(trifluoromethoxy)phenylhydrazone to abolish membrane potential at the end of each assay run. Mitochondrial membrane potential ($\Delta\psi$, in mV) was calculated with the equation:

$$\Delta\psi = 61.5 \log\left\{\frac{([\text{TPMP}]\ \text{added} - [\text{TPMP}]\ \text{external}) \times \text{TPMP binding correction}}{0.001 \times [\text{protein}] \times [\text{TPMP}]\ \text{external}}\right\}$$

where the TPMP binding corrections are 0.4 and 0.35 for liver and SKM, respectively (36).

Hepatocyte isolation (study 4)

Changes in *Ucp* homologue and *Pgc-1* expression in hepatocytes isolated from control and LPS-treated mice (injection protocols identical to that in *study 1*) were assessed with the following procedure. At certain times after injection, mice were anesthetized by intraperitoneal injection of 100 μL ketamine-xylazine-saline (2:1:10) and immobilized, and the inferior vena cava was exposed. With introduction of air bubbles avoided at all steps, a 22-gauge Angiocath catheter (Becton-Dickinson, Rutherford, NJ) was placed below the liver, with clotting avoided by injection of 200 μL 1,000 U heparin · mL^{-1}. An infusion line containing 37°C *buffer I* (142 mM NaCl, 6.7 mM KCl, 100 mM HEPES, 5.3 mM EGTA, pH 7.4) was attached, flow was initiated at 4 mL · min^{-1}, the portal vein was severed, and the inferior vena cava below the heart was ligated. After 5 min, flow was switched to 37°C *buffer II* (66.7 mM NaCl, 6.7 mM KCl, 100 mM HEPES, 4.8 mM $CaCl_2$, 1% FFA-free BSA, 77 U Type IV collagenase · mL^{-1}, pH 7.6) for 20–30 min. Perfused livers were excised, the gall bladder was removed, and cells were dissociated by

cutting the liver capsule and agitating the tissue in a small volume of *buffer II* with mincing. The preparation was poured into a 50-mL conical tube through a 250 μM filter and then a 40 mM filter. The preparation was brought to ~20 mL with cold HBSS and then centrifuged at ~50 *g* for 3 min. The supernatant containing nonparenchymal cells (NPCs) with nonpelleted hepatocytes was withdrawn and saved on ice (cells in supernatants from this and subsequent washes are termed the "NPC-enriched fraction"). Cells were resuspended in 20 mL cold HBSS via gentle rocking and recentrifuged at 50 *g* for 1 min, and the supernatant was withdrawn. This step was repeated, and the resulting hepatocyte-enriched pellet was snap-frozen. The pooled supernatants were centrifuged at 5,000 *g* for 10 min, and the NPC-enriched pellet was snap-frozen. This protocol using repeated washes yields a low-speed pellet containing >95% hepatocytes (1).

Indirect calorimetry (study 5)

Twelve ad libitum-fed mice were acclimated for 24 h to respiration chambers (Oxymax System, Columbus Instruments, Columbus, OH). After acclimation, one-half of the mice were injected with LPS, and one-half served as PBS-injected controls (injection protocol as in *study 1*). The first postinjection measurement of oxygen consumption occurred; 1 h after injection and was followed hourly thereafter. T_c was determined immediately after the 24-h postinjection chamber measurement. Mice were fasted after injection but were allowed free access to water.

Statistics

Changes in mRNA abundance and Tc over time after injection were assessed by use of the general linear models procedure of SAS (SAS Institute, Cary, NC) as a 2 × 8 factorial

design analyzing the effects of treatment (LPS vs. controls), time, and treatment × time interactions. Significant ($P < 0.05$) time or treatment × time interactions were observed for all parameters; however, individual comparisons between time-matched control vs. LPS-treated mice (see figure legends) were made only if treatment × time effects were significant. Means ± SE are reported.

RESULTS

Study 1: LPS-evoked temperature, Ucp homologue, and Pgc-1 mRNA changes

The administration of a ~6 mg · kg^{-1} dose of endotoxin induced a profound hypothermia in mice (Figure A.1A). T_c fell to 34°C by 4 h after injection, dropping further to a nadir of ~30°C by 8 h after injection. Although there was a decline in T_c by 2 h, this change was not statistically significant. Individuals sampled at 24 and 48 h after injection displayed a robust recovery of T_c, with a slight overshoot above time-matched controls by 48 h (Figure A.1A). Both control and LPS-treated mice were fasted after injection, and this led to a significant drop in T_c in controls by 16 h, remaining low through 48 h.

Ucp homologue mRNA abundance in the liver was blunted sharply and rapidly after LPS administration (Figure A.1, B and C), with 2 h postinjection values only ~20–25% of controls. Transcript amount for each began to rise between 6 and 8 h after injection and were no different from time-matched controls at the 16-h time point. Hepatic *Ucp2* mRNA levels rose further between 16 and 24 h, remaining elevated compared with time-matched controls (Figure A.1B). In the latter, fasting elicited a significant drop in *Ucp2* and *Ucp5* mRNA by 16–24 h (Figure A.1, B and C). Based on real-time RT-PCR analysis of time-zero control samples, whole liver mRNA expression

of *Ucp2* was about twofold higher than *Ucp5* (not shown). The magnitude of change in rodent liver *Ucp2* mRNA after LPS in the current study using quantitative RT-PCR is less than that reported by researchers who used Northern blot analysis (11; 12; 14), likely caused by differences in experimental regimens and our use of a more sensitive analytical methodology.

Skeletal muscle patterns of *Ucp2* and *Ucp5* mRNA abundance after LPS administration differed substantially compared with liver (Figure A.2, A-C). For instance, the decline in *Ucp5* mRNA over the first 4 h after injection was not statistically significant (Figure A.2C), and an LPS-induced decline in *Ucp2* expression was not apparent (Figure A.2A). In contrast to the liver pattern, SKM *Ucp5* mRNA in LPS-treated mice rose significantly above controls, reaching levels more than threefold higher than time-zero amounts by 48 h after injection (Figure A.2C). Furthermore, a fasting-induced drop in *Ucp2* or *Ucp5* transcript was not seen in SKM from control mice (Figure A.2, A and C). Interestingly, however, the mRNA levels for *Ucp2* and *Ucp5* began to rise between 6 and 8 h after LPS (Figure A.2, A and C), an induction reminiscent of that seen in liver (Figure A.1, B and C). As in liver, SKM *Ucp2* mRNA increased significantly above control values between 16 and 48 h in LPS-treated mice (Figure A.2A).

The *Ucp3* mRNA changes observed in SKM after LPS were markedly different relative to those observed for *Ucp2* and *Ucp5* (Figure A.2, A-C). After injection, there was an immediate and substantial induction of the *Ucp3* gene as judged by mRNA abundance, reaching levels more than fivefold above time-zero controls by 6 h (Figure

A.2B). Levels tapered off over the remaining hours to equal those of time-matched controls by 24 h after injection, an event concurrent with time-dependent increases in *Ucp2* and *Ucp5* mRNA (see above). The rise in *Ucp3* mRNA in fasted controls was transient. In data not shown, RT-PCR detection values in SKM from time-zero controls revealed that expression of *Ucp3* exceeded that of *Ucp2* and *Ucp5* by ~4- and >30-fold, respectively. *Ucp2* mRNA abundance was about fourfold higher in SKM than liver, whereas *Ucp5* was similar between tissues.

Exploration of the molecular basis of the remarkable *Ucp* homologue expression changes noted over the first 24 h after injection of LPS (see above) prompted analysis of *Pgc-1* mRNA abundance in a subset of samples from these same mice. In liver, LPS significantly depressed *Pgc-1* up to fivefold in a time-dependent manner, with eventual recovery of transcript levels between 8 and 16 h after injection (Figure A.3). In contrast, *Pgc-1* mRNA abundance had risen more than threefold by 2 h after injection in SKM from LPS-treated mice, falling significantly to reach levels not statistically different from time-zero controls between 4 and 16 h (Figure A.3). In time-zero control tissues, mRNA abundance for *Pgc-1* in whole liver was ~2- and ~10-fold lower than that determined in SKM and BAT, respectively (not shown).

Study 2: effect of core body temperature clamp on LPS-induced expression changes

It was intriguing to note that induction of *Ucp* homologue expression in liver and SKM in *study 1*, clear by 6–8 h after injection of LPS, occurred when core body temperature had approached or reached its nadir (see Figures A.1 and A.2). Although these events may simply be coincidental, one may consider a paradigm in which signals emanating

from core body temperature (T_{core})-sensitive neurons in the brain act to modulate peripheral cellular heat production. Were the delayed *Ucp* homologue gene expression increases observed after LPS "triggered" by low T_{core}, and would such increases be blunted should T_{core} be clamped to near-control temperature? As an initial test of this hypothesis, a second set of LPS and control mice was placed in a warm room (34°C) after injection, thus preventing the large drop in T_c displayed in *study 1* (compare Figures A.1A and A.4A).

This treatment did not alter most patterns of *Ucp* homologue mRNA changes (Figures A.4 and A.5). For example, liver *Ucp2* and *Ucp5* mRNAs in LPS-treated mice dropped and then recovered to exceed or equal control values, respectively (Figure A.4, B and C), similar to what was observed at 22°C (Figure A.1, B and C). As in studies performed at 22°C (Figure A.2B), SKM *Ucp3* transcript in temperature-clamped LPS-treated mice increased significantly (albeit with more of a delay) and then fell in a time-dependent manner (Figure A.5B). Generally, control patterns of *Ucp* homologue expression were similar in both studies, although the increase in *Ucp3* mRNA in fasted control SKM appeared to be higher and of longer duration at 34°C (compare Figures A.2B and A.5B). Despite such similarities, there were notable differences in expression between the studies. Although a significant and delayed induction of *Ucp2* mRNA in SKM in LPS-treated mice was seen in both 22°C and 34°C studies (compare Figures A.2A and A.5A), a substantial transient fall in *Ucp2* expression was observed only at 34°C (Figure A.5A). The pattern for *Ucp5* mRNA in the mice given LPS was generally

similar (compare Figures A.2C and A.5C); however, the magnitude of the delayed induction in *Ucp5* mRNA abundance was blunted at 34°C (Figure A.5C).

Study 3: mitochondrial proton leak after LPS treatment

Marked alterations in body temperature and *Ucp* homologue gene expression after LPS treatment (Figures A.1 and A.2) suggested that significant time-dependent changes in mitochondrial uncoupling kinetics, an expected functional correlate of UCP activity, could have occurred in endotoxin-challenged mice. To assess this possibility, mitochondrial proton leak in LPS-injected mouse liver was assayed in parallel with control liver mitochondria at time points corresponding to diminution and recovery of *Ucp2* and *Ucp5* expression (4 and 16 h, respectively; Figure A.1, B and C). Liver samples used for proton leak measurements yielded an expression pattern matching that of the initial study (significant drop in *Ucp2* and *Ucp5* mRNA at 4 h post-LPS, recovery to control levels by 16 h; not shown). An LPS-induced T_c decline was again observed at 4 h (controls, 37.0 ± 0.18°C; LPS, 34.9 ± 0.34°C; n = 9/treatment) and 16 h (controls, 34.5 ± 0.32°C; LPS, 25.8 ± 0.41°C; n = 24/treatment) resembling that of the initial study (Figure A.1A). Despite large changes in mRNA abundance and T_c in this group of mice (similar to mice in *study 1*), no significant difference in liver mitochondrial respiration due to proton leak between treatments was discernible under our assay conditions (Figure A.6, A and B). Similarly, no suggestion of proton leak differences was evident in SKM mitochondria at 16 h after injection (not shown).

To gather additional insight into the physiological relevance of proton leak in hypothermic mice, a subset of LPS mitochondria used for the 16-h analyses described

above was also assayed at 26°C. This temperature corresponds to the average T_c of LPS-treated mice (see above) and is therefore more likely to reflect the kinetics of proton leak in mitochondria from these animals in situ compared with assays performed at 37°C. At this cooler temperature, oxygen consumption due to proton leak was a fraction of that observed in control or LPS mitochondria assayed at 37°C, despite increased estimated membrane potentials overall (Figure A.6C).

Study 4: hepatocyte expression of Ucp homologues

It has been reported that, in rodent liver, *Ucp2* expression in hepatocytes is minor compared with that in the far less abundant Kupffer cells (11; 12; 26). This issue is relevant to interpretation of correlations between proton leak and whole liver *Ucp* homologue mRNA abundance, because the contribution of NPC mitochondria to preparations used for proton leak is vanishingly small compared with the contribution from hepatocytes (2). In addition, the cell-specific expression of *Ucp5* or *Pgc-1* in liver has not been reported. To address these issues, mRNA was analyzed from hepatocyte-enriched preparationsI derived from a separate set of control or LPS-treated mice at time points corresponding to proton leak measurements made in mice used for *study 3*. As seen for whole liver (Figure A.1, B and C), hepatocyte *Ucp2* and *Ucp5* mRNA dropped substantially by 4 h after injection of LPS, with *Ucp5* mRNA recovering to control values by 16 h (Figure A.7, A and B). However, hepatocyte *Ucp2* expression was not increased by 16 h in this group of mice. Hepatocytes expressed *Pgc-1* (Figure A.7C), with the drop in mRNA after LPS administration similar to the pattern observed in whole liver (Figure A.3).

Study 5: oxygen consumption after LPS administration

The profound hypothermic response and subsequent body temperature recovery in LPS-treated mice (Figure A.1A) indicated that substantial changes in metabolic heat production occur in these animals over the first 24 h after LPS. As a functional corollary to in vitro observations of *Ucp* homologue expression and mitochondrial proton leak, metabolic rate was assessed by indirect calorimetry in mice injected with saline or LPS. Compared with mice from *study 1* (e.g., Figure A.1A), animals from this group displayed substantial variation in their metabolic response to endotoxin (Figure A.8). In all but one animal (*cage 2*, see Figure A.8 legend), oxygen consumption began to diverge from control mice between 3 and 4 h after injection with a progressive and marked hypometabolism occurring from 4 h onward. One animal (*cage 12*) exhibited a partial recovery of oxygen consumption beginning by ~16 h (Figure A.8). Importantly, differences in oxygen consumption were reflected by T_c measures taken at 24 h after injection: controls (33.9 ± 0.6°C, n = 6), hypometabolic mice (24.6 ± 0.22°C, n = 4), the *cage 2* mouse (34.2°C), and the *cage 12* mouse (28.6°C).

DISCUSSION

Association of Ucp homologue expression and metabolic outcomes

Whether newly described or still undiscovered mitochondrial carrier proteins act to uncouple mitochondrial respiration analogous to UCP1 is actively being investigated. There is an abundance of information regarding *Ucp* homologue expression changes under various metabolic conditions, but few studies have correlated such changes with functional metabolic outcomes in rodents (11; 21; 25; 37; 38). The current set of

experiments centered on the premise that, should a particular UCP homologue act as an uncoupler in situ, robust modulation of its expression in vivo should elicit concurrent detectable changes in functional outcomes, including metabolic heat production and mitochondrial proton leak. Analyses described herein focused on liver and SKM, which are believed to account for over one-half of the metabolic rate of rodents (8).

Based on mRNA patterns alone, certain aspects of *Ucp2* and *Ucp5* expression in the current model are consistent with the view that these homologues contribute to heat production in vivo. First, development of hypothermia in LPS-treated mice was preceded by a drop in liver *Ucp2* and *Ucp5* mRNA abundance (Figure A.1), and under normal conditions the liver's contribution to metabolic rate is significant (8). The failure of LPS to diminish *Ucp2* or *Ucp5* expression in SKM during hypothermia (Figure A.2), however, suggests that any putative impact of these homologues on diminution of heat production would not have been manifested in SKM. Second, recovery of T_c was preceded by significant increases in *Ucp2* and *Ucp5* expression in liver and SKM (Figures A.1 and A.2), consistent with the hypothesis that increased activity of these homologues contributed to reestablishment of T_c after LPS. The significant lag between *Ucp2* and *Ucp5* expression changes (beginning at ~6-8 h after injection, Figures A.1 and A.2) and the recovery of T_c to control levels (between 16 and 24 h after injection, Figure A.1) do not preclude the possibility that these proteins are involved in T_c recovery following LPS, because a sustained rise in energy expenditure would have been required to normalize the T_c of hypothermic mice. For example, an increase of 4°C in a 17-g mouse over a period of 8 h (Figure A.1) would have required the generation and full

sequestration of ~60 calories just to account for the temperature rise (13). This is an underestimate of the actual energy needs to accomplish this feat, because it does not take into account the loss of metabolic heat via respiration and other routes. Furthermore, mitochondrial proton leak kinetics slow considerably at cooler temperatures (Figure A.6C). Thus truly effective activities of putative UCP homologues are not likely to parallel expression changes in hypothermic animals, and would only manifest themselves fully as mice begin to warm.

Expression patterns of *Ucp3* in SKM (Figure A.2B) raise questions about the relevance of *Ucp3* toward driving truly meaningful heat production changes in LPS-treated mice, and they lend support to the idea that this homologue has other primary functions in vivo (37; 38; 43). For instance, *Ucp3* transcript levels in SKM were rapidly triggered fivefold by LPS administration (Figure A.2), rising concurrent with the drop in body temperature (the latter tracked metabolic rate, see RESULTS). On the other hand, T_c recovery was accompanied by diminishing *Ucp3* mRNA levels.

Regardless of the roles of UCP homologues in modifying in situ uncoupling, tissue proton leak could not have been the only factor contributing to hypometabolism following LPS. The four- to eightfold drop in oxygen consumption (Figure A.8) and the magnitude of decline in T_c (Figure A.1) due to LPS appear too large to be accounted for by changes in proton leak alone, which under basal conditions may represent up to ~20%-40% of tissue oxygen consumption in rodents (8). Global depression of metabolism, including a diminution of reactions generating and consuming the mitochondrial electrochemical gradient, likely occurs after high-dose LPS administration

to mice. For example, although not measured in the current study, endotoxin has been shown to increase nitric oxide (NO) production (28; 40), and NO or its derivatives powerfully inhibit the electron transport chain (35). Furthermore, mice developing hypothermia after LPS (Figure A.1) displayed a marked reduction in motor activity (23). Thus, regardless of any possible changes in proton leak, LPS-induced diminution of ATP consumption or depression of the $\Delta\psi$ generating pathways would contribute to alterations of metabolic rate and body temperature.

Despite large alterations of T_c (Figure A.1), metabolic rate (Figure A.8), and *Ucp* homologue mRNA in liver (Figures A.1 and A.7) and SKM (Figure A.2), no discernible difference in proton leak could be detected in mitochondria prepared from liver (Figure A.6) or SKM (see RESULTS). Recently, a lack of correlation was reported between leak and liver/SKM *Ucp2* and SKM *Ucp3* mRNA in mice administered thyroid hormone or after a fast (9; 21). A lack of correlation between in vitro proton leak assays and *Ucp* homologue mRNA abundance could signal that the primary physiological role of UCP2, UCP3, and UCP5 is not to catalyze mitochondrial proton leak per se but rather to serve as carriers for fatty acids or other moieties. Alternatively, it is possible that the commonly used assay conditions for measurement of mitochondrial proton leak employed in the current study do not adequately reflect leak kinetics in vivo under every condition and may therefore lead to negative interpretations of UCP homologue activity. In a recent study, Lanni et al. (24) noted that proton leak differences in SKM mitochondria derived from rats differing in thyroid status were observed only when assays were carried out free of BSA, suggesting involvement of fatty acids with proton leak. As noted by Porter et al.

(31), higher proton leak was observed in hepatocytes from aged rats compared with young rats, but such a difference was not apparent with the use of isolated mitochondria. Thus various factors, including fatty acids or purine nucleotides (6; 19; 39), and perhaps protein modulators, may regulate UCPs in the context of the cell in situ. In addition, it is possible that changes in protein levels in the tissues examined herein were too small to enable detection of differences in proton leak despite alterations of mRNA. Finally, the possibility cannot be discounted that still uncharacterized mitochondrial carriers exist and importantly influenced proton leak in these tissues.

The variable results to date regarding *Ucp* homologue expression and functional outcomes highlight the necessity for research to clarify further the metabolic roles of these proteins. Although we observed no differences in mitochondrial proton leak, despite remarkable alterations of *Ucp* homologue gene expression in LPS-treated mice, increased proton leak was observed in mitochondria prepared from *ob/ob* mouse liver and hyperthyroid rat SKM that displayed increased hepatocyte *Ucp2* and SKM *Ucp3* expression, respectively (11; 24). Samec et al. (38) did not observe a correlation between *Ucp* homologue mRNA abundance and whole animal oxygen consumption in a high-fat/low-fat model, whereas Jekabsons et al. (21) presented evidence of a positive association between muscle *Ucp2* and *Ucp3* expression changes and whole animal oxygen consumption. Our correlative data on T_c recovery and *Ucp2/Ucp5* mRNA (Figures A.1 and A.2) concur with this latter finding, because Tc tracks changes in oxygen consumption (see RESULTS), but they differ in that *Ucp3* mRNA changes generally followed a pattern opposite that of T_c (Figure A.2). Finally, others have

reported increased rodent SKM *Ucp2* and *Ucp3* mRNA with fasting or food restriction (4; 5; 9; 17; 20; 37; 43), but our results in fasting control mice indicated that *Ucp2* and *Ucp3* mRNA changes were transient and varied between *studies 1* and *2* (Figures A.2 and A.5). Differences between our study and those of others could be related to our use of analytical mRNA methodology or to the fact that we initiated the injection and fasting regimen in late afternoon, a time point preceded by low food intake relative to the dark cycle.

Gene regulation of Ucp homologues

LPS administration initiates a complex cascade of events in which an array of cytokines, prostaglandins, and other factors change temporally to influence metabolism (27). With respect to humoral, paracrine, or autocrine components that influenced *Ucp* homologue expression in the first hours after LPS (Figures A.1 and A.2), factors such as tumor necrosis factor-α (TNF-α) and interleukin-1β that emerge early in the cascade are good candidates. Faggioni et al. (14) reported that a single injection of TNF-α to mice caused a two- to threefold increase in liver, SKM, and WAT *Ucp2* mRNA levels at 12 h, but changes at earlier time points were not reported. Indeed, a delay in liver *Ucp2* induction after LPS or TNF-α treatment has been consistently observed [(11; 12; 14), this study]. Thus a direct stimulation of *Ucp2* or *Ucp5* genes in mouse liver or SKM by TNF-α does not appear possible, because the transient nature of this cytokine dictates that its direct effects must occur in the first ~2 h after LPS (46), when *Ucp2* and *Ucp5* mRNA levels were stable or falling (Figures A.1 and A.2). Cytokines induced later in the LPS-induced cascade (28) or other humoral factors, such as the newly described high mobility group 1

(42), might have influenced the delayed induction of *Ucp2* and *Ucp5* in liver and SKM after LPS (Figures A.1 and A.2).

The current study illustrates that, under certain conditions, the mechanisms controlling *Ucp2* and *Ucp5* genes may converge and that genetic regulation of *Ucp3* is markedly different from that of *Ucp2* or *Ucp5* after high-dose endotoxin in mice. For instance, LPS evoked a similar repression and recovery of *Ucp2* and *Ucp5* expression in liver (Figures A.1 and A.4) plus a delayed induction in SKM (Figures A.2 and A.5), contrasting with the early and transient induction of SKM *Ucp3* (Figures A.2 and A.5). There is evidence that the availability of fatty acid-associated moieties (20; 43) stimulates expression of UCPs. Indeed, the availability of fatty acids likely influenced the expression of SKM *Ucp3* in the current study, as evidenced by a separate experiment in which plasma FFA levels plus *Ucp3* mRNA were determined at 0, 2, and 6 h after injection of LPS or PBS. A strong correlation between plasma FFA concentration and *Ucp3* expression was observed in LPS-treated mice (Figure A.9). Compared with time-matched controls, the 6-h post-injection FFA concentration (1.20 ± 0.12 mM) and SKM *Ucp3* expression ($600 \pm 32\%$ of *time 0*) in LPS-treated mice was approximately two- and threefold greater. The mechanisms underlying the LPS-induced rise in circulating FFA levels and their association with *Ucp3* gene expression remain unknown.

Activation of PPARγ and/or PPARα (10; 20; 22), and tissue-specific upregulation of the coactivator *Pgc-1* (33; 44), could influence *Ucp* homologue expression. Studies examining the role of ectopic PGC-1 in C_2C_{12} cells and other in vitro preparations suggested that this coactivator is critical for the activation of the *Ucp1* and *Ucp2* genes,

with little to no impact on *Ucp3* gene expression (33; 44). Interestingly, LPS sparked a significant increase in SKM *Pgc-1* expression (Figure A.3), which correlated well with initiation of *Ucp3* expression but was not associated with a change in *Ucp2* or *Ucp5* mRNA (Figure A.2). Thus it is intriguing to postulate that SKM PGC-1 activity may influence the *Ucp3* gene in the context of the whole animal and may have influenced changes in *Ucp3* gene expression in LPS-treated mice. There was some disconnect between *Pgc-1* and *Ucp2* or *Ucp5* expression in whole liver, such that *Ucp* homologue mRNA levels rose well before recovery of *Pgc-1* expression (Figures A.1 and A.3). Recently, Boss et al. (3) reported that administration of β-adrenergic agonists or exposure to cold in wild-type or β3-receptor knock-out mice could lead to increases in SKM *Ucp2* and *Ucp3* expression without concomitant changes in *Pgc-1* mRNA. Such examples of minimal correlation are not consistent with the idea that PGC-1 changes alone drive *Ucp2* or *Ucp5* expression in vivo, with the caveat that PGC-1 protein abundance was not measured (Ref. 3, this study). Using quantitative PCR, we found *Pgc-1* to be expressed in whole liver, hepatocytes, and SKM (Figures A.3 and A.7), at odds with the data of Puigserver et al. (33), which indicated nominal expression in liver or SKM (*Pgc-1* could be induced by cold in the latter tissue) using Northern analysis. These discrepancies are likely explained by technical differences in sensitivity, because *Pgc-1* expression using real time RT-PCR was far greater (10-fold) in mouse BAT than liver (see RESULTS), consistent with Puigserver et al. Results to date [(3; 33; 44), this study] indicate that the relative impact of PGC-1 activity on genes encoding UCP family members largely depends on the specific cell type, UCP homologue, and biological context of the system

in study (i.e., whether or not PPARγ is activated by ligand). It is clear that additional regulatory mechanisms exist that modify *Ucp* genes independently of changes in *Pgc-1* expression alone.

Exposure to cold ambient temperature (T_a) is a powerful stimulus that engages the metabolic machinery of mammals, including β-adrenergic stimulation of BAT thermogenic activity (4). There is some evidence that a cold T_a induces *Ucp* homologue expression in a tissue-dependent manner (reviewed in Ref. 4; see also Ref. 45). We are unaware of any reports that have studied the effects of core body temperature (T_{core}) on UCP homologues, and we wondered whether experimental modulation of T_{core} would elicit changes in their expression levels. One hypothesis, for instance, is that the drop in T_{core} after LPS administration in mice (Figure A.1) may have stimulated the genes encoding UCP2 and UCP5 (Figures A.1 and A.2) via T_{core} sensors that communicate with the brain. Teleologically, a hypothermia induced enhancement of thermogenic uncoupling activity via UCP homologues could help counteract an excessive T_{core} drop. Artificial maintenance of T_{core} after LPS would be expected to dampen any cold-stimulated rise in *Ucp* homologue expression. In an initial test of this hypothesis, clamping of T_{core} after LPS challenge generally failed to blunt the delayed stimulation of *Ucp2* and *Ucp5* gene expression, with the possible exception of SKM *Ucp5*, whose induction was lower compared with that seen at 22°C (Figures A.3 and A.4). These findings indicate that regulatory factors independent of T_{core} were at play in our LPS model.

In summary, some aspects of the current set of experiments are supportive of the idea that UCP2 and UCP5 are involved in metabolic changes occurring in LPS-treated mice. mRNA for these homologues was induced in whole liver and SKM during recovery from LPS-induced hypothermia, and in liver, their transcript levels dropped during the onset of hypothermia. Despite these patterns, no difference was observed in vitro mitochondrial proton leak. Alterations in SKM *Ucp3* mRNA after endotoxin were distinctly different from those observed for *Ucp2* or *Ucp5*, changing in the opposite direction from body temperature. These data point to different mechanisms of gene regulation and suggest that UCP3 does not serve in a thermogenic capacity under these conditions. Changes in expression of the transcription coactivator *Pgc-1* in muscle appeared to correlate with *Ucp3* expression, whereas the association between *Pgc-1* and *Ucp2* was less compelling. Further study is warranted to assess the possibility that LPS-induced increases in *Ucp* homologue expression/activity help minimize LPS-associated reactive oxygen species production and damage. Ultimately, titration of UCP homologue abundance through gene delivery, transgenic construction, and knock-out technologies promises to clarify further the physiological roles of these proteins.

ACKNOWLEDGEMENTS

The authors thank E. Filvaroff and T. A. Stewart for helpful discussions of the manuscript, M. Renz for significant technical input, and C. Galindo and M. Ostland for statistical assistance.

REFERENCES

1. **Berry MN, Edwards AM and Barritt GJ**. *Isolated Hepatocytes. Preparation, Properties, and Applications*. New York: Elsevier, 1991.

2. **Blouin A, Bolender RP and Weibel ER**. Distribution of organelles and membranes between hepatocytes and nonhepatocytes in the rat liver parenchyma. A stereological study. *J Cell Biol* 72: 441-455., 1977.

3. **Boss O, Bachman E, Vidal-Puig A, Zhang CY, Peroni O and Lowell BB**. Role of the beta(3)-adrenergic receptor and/or a putative beta(4)- adrenergic receptor on the expression of uncoupling proteins and peroxisome proliferator-activated receptor-gamma coactivator-1. *Biochem Biophys Res Commun* 261: 870-876., 1999.

4. **Boss O, Muzzin P and Giacobino JP**. The uncoupling proteins, a review. *Eur J Endocrinology* 139: 1-9, 1998.

5. **Boss O, Samec S, Dulloo A, Seydoux J, Muzzin P and Giacobino JP**. Tissue-dependent upregulation of rat uncoupling protein-2 expression in response to fasting or cold. *FEBS Lett* 412: 111-114., 1997.

6. **Boss O, Samec S, Kuhne F, Bijlenga P, AssimacopoulosJeannet F, Seydoux J, Giacobino JP and Muzzin P**. Uncoupling protein-3 expression in rodent skeletal muscle is modulated by food intake but not by changes in environmental temperature. *J Biol Chem* 273: 5-8, 1998.

7. **Bouillaud F, Weissenbach J and Ricquier D**. Complete cDNA-derived amino acid sequence of rat brown fat uncoupling protein. *J Biol Chem* 261: 1487-1490., 1986.

8. **Brand MD, Chien LF, Ainscow EK, Rolfe DF and Porter RK**. The causes and functions of mitochondrial proton leak. *Biochim Biophys Acta* 1187: 132-139, 1994.

9. **Cadenas S, Buckingham JA, Samec S, Seydoux J, Din N, Dulloo AG and Brand MD**. UCP2 and UCP3 rise in starved rat skeletal muscle but mitochondrial proton conductance is unchanged. *Febs Lett* 462: 257-260, 1999.

10. **Camirand A, Marie V, Rabelo R and Silva JE**. Thiazolidinediones stimulate uncoupling protein-2 expression in cell lines representing white and brown adipose tissues and skeletal muscle. *Endocrinology* 139: 428-431, 1998.

11. **Chavin KD, Yang S, Lin HZ, Chatham J, Chacko VP, Hoek JB, Walajtys-Rode E, Rashid A, Chen CH, Huang CC, Wu TC, Lane MD and Diehl AM**. Obesity induces expression of uncoupling protein-2 in hepatocytes and promotes liver ATP depletion. *J Biol Chem* 274: 5692-5700., 1999.

12. **Cortez-Pinto H, Yang SQ, Lin HZ, Costa S, Hwang CS, Lane MD, Bagby G and Diehl AM**. Bacterial lipopolysaccharide induces uncoupling protein-2 expression in hepatocytes by a tumor necrosis factor-alpha-dependent mechanism. *Biochem Biophys Res Commun* 251: 313-319., 1998.

13. **Faber P and Garby L**. Fat content affects heat capacity: a study in mice. *Acta Physiol Scand* 153: 185-187., 1995.

14. **Faggioni R, Shigenaga J, Moser A, Feingold KR and Grunfeld C**. Induction of UCP2 gene expression by LPS: A potential mechanism for increased thermogenesis during infection. *Biochem Biophys Res Commun* 244: 75-78, 1998.

15. **Fleury C, Neverova M, Collins S, Raimbault S, Champigny O, Levi-Meyrueis C, Bouillaud F, Seldin MF, Surwit RS, Ricquier D and Warden CH**. Uncoupling protein-2: a novel gene linked to obesity and hyperinsulinemia. *Nat Genet* 15: 269-272, 1997.

16. **Gimeno RE, Dembski M, Weng X, Deng N, Shyjan AW, Gimeno CJ, Iris F, Ellis SJ, Woolf EA and Tartaglia LA**. Cloning and characterization of an uncoupling protein homolog: a potential molecular mediator of human thermogenesis. *Diabetes* 46: 900-906, 1997.

17. **Gong DW, He YF, Karas M and Reitman M**. Uncoupling protein-3 is a mediator of thermogenesis regulated by thyroid hormone, beta 3-adrenergic agonists, and leptin. *J Biol Chem* 272: 24129-24132, 1997.

18. **Harper ME and Brand MD**. The quantitative contributions of mitochondrial proton leak and ATP turnover reactions to the changed respiration rates of hepatocytes from rats of different thyroid status. *J Biol Chem* 268: 14850-14860, 1993.

19. **Heaton GM, Wagenvoord RJ, Kemp A, Jr. and Nicholls DG**. Brown-adipose-tissue mitochondria: photoaffinity labelling of the regulatory site of energy dissipation. *Eur J Biochem* 82: 515-521., 1978.

20. **Hwang CS and Lane MD**. Up-regulation of uncoupling protein-3 by fatty acid in C2C12 myotubes. *Biochem Biophys Res Commun* 258: 464-469, 1999.

21. **Jekabsons MB, Gregoire FM, SchonfeldWarden NA, Warden CH and Horwitz BA**. T_3 stimulates resting metabolism and UCP-2 and UCP-3 mRNA but not

nonphosphorylating mitochondrial respiration in mice. *Amer J Physiol Endocrinol Met* 40: E380-E389, 1999.

22. **Kelly LJ, Vicario PP, Thompson GM, Candelore MR, Doebber TW, Ventre J, Wu MS, Meurer R, Forrest MJ, Conner MW, Cascieri MA and Moller DE.** Peroxisome proliferator-activated receptors gamma and alpha mediate in vivo regulation of uncoupling protein (UCP-1, UCP-2, UCP-3) gene expression. *Endocrinology* 139: 4920-4927, 1998.

23. **Kozak W, Conn CA and Kluger MJ**. Lipopolysaccharide induces fever and depresses locomotor activity in unrestrained mice. *Am J Physiol* 266: R125-135., 1994.

24. **Lanni A, Beneduce L, Lombardi A, Moreno M, Boss O, Muzzin P, Giacobino JP and Goglia F**. Expression of uncoupling protein-3 and mitochondrial activity in the transition from hypothyroid to hyperthyroid state in rat skeletal muscle. *Febs Lett* 444: 250-254, 1999.

25. **Lanni A, DeFelice M, Lombardi A, Moreno M, Fleury C, Ricquier D and Goglia F**. Induction of UCP2 mRNA by thyroid hormones in rat heart. *FEBS Lett* 418: 171-174, 1997.

26. **Larrouy D, Laharrague P, Carrera G, Viguerie-Bascands N, Levi-Meyrueis C, Fleury C, Pecqueur C, Nibbelink M, Andre M, Casteilla L and Ricquier D**. Kupffer cells are a dominant site of uncoupling protein 2 expression in rat liver. *Biochem Biophys Res Commun* 235: 760-764, 1997.

27. **Mao WG, Yu XX, Zhong A, Li WL, Brush J, Sherwood SW, Adams SH and Pan GH**. UCP4, a novel brain-specific mitochondrial protein that reduces membrane potential in mammalian cells. *Febs Lett* 443: 326-330, 1999.

28. **Marsh CB and Wewers MD**. The pathogenesis of sepsis. Factors that modulate the response to gram- negative bacterial infection. *Clin Chest Med* 17: 183-197., 1996.

29. **Millet L, Vidal H, Andreelli F, Larrouy D, Riou JP, Ricquier D, Laville M and Langin D**. Increased uncoupling protein-2 and -3 mRNA expression during fasting in obese and lean humans. *J Clin Invest* 100: 2665-2670, 1997.

30. **Millet L, Vidal H, Larrouy D, Andreelli F, Laville M and Langin D**. mRNA expression of the long and short forms of uncoupling protein-3 in obese and lean humans. *Diabetologia* 41: 829-832, 1998.

31. **Porter RK, Joyce OJP, Farmer MK, Heneghan R, Tipton KF, Andrews JF, McBennett SM, Lund MD, Jensen CH and Melia HP**. Indirect measurement of mitochondrial proton leak and its application. *Int J Obesity* 23: S12-S18, 1999.

32. **Prashker D and Wardlaw AC**. Temperature responses of mice to Escherichia coli endotoxin. *Br J Exp Pathol* 52: 36-46., 1971.

33. **Puigserver P, Wu Z, Park CW, Graves R, Wright M and Spiegelman BM**. A cold-inducible coactivator of nuclear receptors linked to adaptive thermogenesis. *Cell* 92: 829-839., 1998.

34. **Reynafarje B, Costa LE and Lehninger AL**. O_2 solubility in aqueous media determined by a kinetic method. *Anal Biochem* 145: 406-418, 1985.

35. **Richter C, Schweizer M and Ghafourifar P**. Mitochondria, nitric oxide, and peroxynitrite. *Methods Enzymol* 301: 381-393, 1999.

36. **Rolfe DFS, Hulbert AJ and Brand MD**. Characteristics of mitochondrial proton leak and control of oxidative phosphorylation in the major oxygen-consuming tissues of the rat. *Biochim Biophys Acta* 1188: 405-416, 1994.

37. **Samec S, Seydoux J and Dulloo AG**. Role of UCP homologues in skeletal muscles and brown adipose tissue: mediators of thermogenesis or regulators of lipids as fuel substrate? *Faseb J* 12: 715-724, 1998.

38. **Samec S, Seydoux J and Dulloo AG**. Post-starvation gene expression of skeletal muscle uncoupling protein 2 and uncoupling protein 3 in response to dietary fat levels and fatty acid composition - A link with insulin resistance. *Diabetes* 48: 436-441, 1999.

39. **Sanchis D, Fleury C, Chomiki N, Goubern M, Huang Q, Neverova M, Gregoire F, Easlick J, Raimbault S, Levi-Meyrueis C, Miroux B, Collins S, Seldin M, Richard D, Warden C, Bouillaud F and Ricquier D**. BMCP1, a novel mitochondrial carrier with high expression in the central nervous system of humans and rodents, and respiration uncoupling activity in recombinant yeast. *J Biol Chem* 273: 34611-34615, 1998.

40. **Shiomi M, Wakabayashi Y, Sano T, Shinoda Y, Nimura Y, Ishimura Y and Suematsu M**. Nitric oxide suppression reversibly attenuates mitochondrial dysfunction and cholestasis in endotoxemic rat liver. *Hepatology* 27: 108-115., 1998.

41. **Vidal-Puig A, Solanes G, Grujic D, Flier JS and Lowell BB**. UCP3: an uncoupling protein homologue expressed preferentially and abundantly in skeletal muscle and brown adipose tissue. *Biochem Biophys Res Commun* 235: 79-82, 1997.

42. **Wang H, Bloom O, Zhang M, Vishnubhakat JM, Ombrellino M, Che J, Frazier A, Yang H, Ivanova S, Borovikova L, Manogue KR, Faist E, Abraham E, Andersson J, Andersson U, Molina PE, Abumrad NN, Sama A and Tracey KJ**. HMG-1 as a late mediator of endotoxin lethality in mice. *Science* 285: 248-251, 1999.

43. **Weigle DS, Selfridge LE, Schwartz MW, Seeley RJ, Cummings DE, Havel PJ, Kuijper JL and BeltrandelRio H**. Elevated free fatty acids induce uncoupling protein 3 expression in muscle: A potential explanation for the effect of fasting. *Diabetes* 47: 298-302, 1998.

44. **Wu ZD, Puigserver P, Andersson U, Zhang CY, Adelmant G, Mootha V, Troy A, Cinti S, Lowell B, Scarpulla RC and Spiegelman BM**. Mechanisms controlling mitochondrial biogenesis and respiration through the thermogenic coactivator PGC-1. *Cell* 98: 115-124, 1999.

45. **Yu XX, Mao WG, Zhong A, Schow P, Brush J, Sherwood SW, Adams SH and Pan GH**. Characterization of novel UCP5/BMCP1 isoforms and differential regulation of UCP4 and UCP5 expression through dietary or temperature manipulation. *Faseb Journal* 14: 1611-1618, 2000.

46. **Zanetti G, Heumann D, Gerain J, Kohler J, Abbet P, Barras C, Lucas R, Glauser MP and Baumgartner JD**. Cytokine production after intravenous or peritoneal gram-negative bacterial challenge in mice. Comparative protective efficacy of antibodies to tumor necrosis factor-alpha and to lipopolysaccharide. *J Immunol* 148: 1890-1897., 1992.

Table A.1. Murine-specific primer/probe sequences used for real-time RT-PCR analyses

Gene	Forward Primer	Probe	Reverse Primer
Ucp2	TACCAGAGCACTGTCGAAGCC	ACAAGACCATTGCACGAGAGGAAGGGAT	AGTCCCTTTCCAGAGGCCC
Ucp3	AGAGGGTGGCTCAGGAGGG	CCCACGGCCTTCTACAAAGGATTTGTG	CCCAGACGCAGAAAGGAGG
Ucp5	GGGTGTGGTCCCAACTGCT	CGTGCTGCAATCGTTGTGGGAGTAGAG	TTCTTGGTAATATCATAAACGGGCA
Pgc-1	GTAGGCCCAGGTACGACAGC	TGAAGCCTATGAGCACGAAAGGCTCAA	GCTCTTTGCGGTATTCATCCC
F4/80	TCTGAGGCAGAAGCTCTGCA	AGAAGTCTCTAAACTCAAGGACACGAGGTTGCTG	ATCTGGGCAATGGCCTTGA

Ucp, uncoupling protein; PGC-1, peroxisome proliferator-activated receptor-γ coactivator 1; F4/80, a macrophage-specific marker. Sequences are 5' to 3'; probes were labeled with 5'FAM/3'TAMRA.

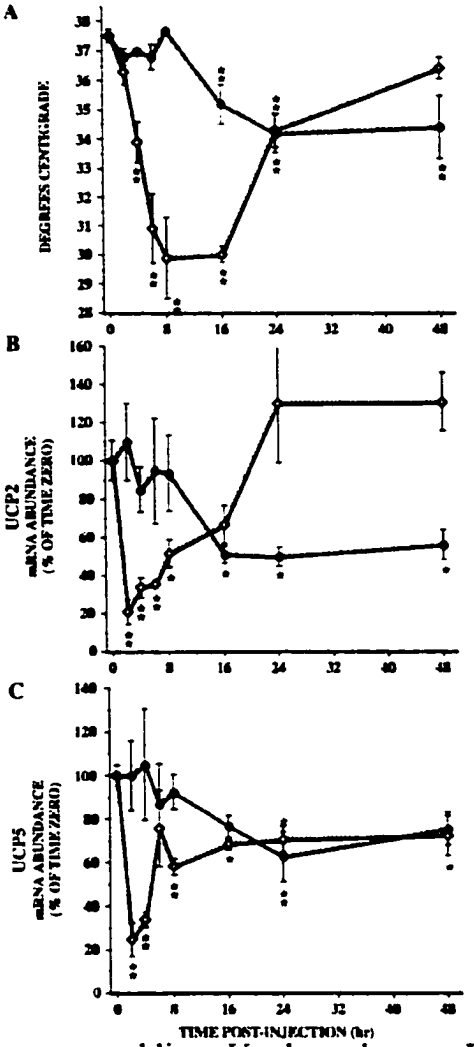

Figure A.1. Body temperature and liver *Ucp* homologue mRNA abundance following LPS treatment.

Marked hypothermia and large changes in whole liver uncoupling protein (*Ucp*) homologue mRNA abundance in mice treated with lipopolysaccharide (LPS). Adult female C57BL6/J mice were treated with a single ip dose of PBS (controls, filled circles) or LPS (~6 mg · kg^{-1}, open diamonds), after which colonic temperature (A),whole liver I mRNA abundance (B), and whole liver *Ucp5* mRNA abundance (C) were determined over 48 h postinjection (study 1, see MATERIALS AND METHODS). Animals were injected (0 h) between 1530 and 1630, fasted after treatment, and housed at 22°C for the duration of the study (see MATERIALS AND METHODS for details). Each point represents the mean ± SE of 3-5 independent measurements (**P* 0.05, ***P* < 0.01 vs. time 0 values); some error bars are within the symbol. Not indicated are significant differences (*P* < 0.05) between LPS mice and time-matched controls, occurring at 4-8, 16, and 48 h (temperature), 2-6, 24, and 48 h (*Ucp2*), and 2, 4, and 8 h (*Ucp5*).

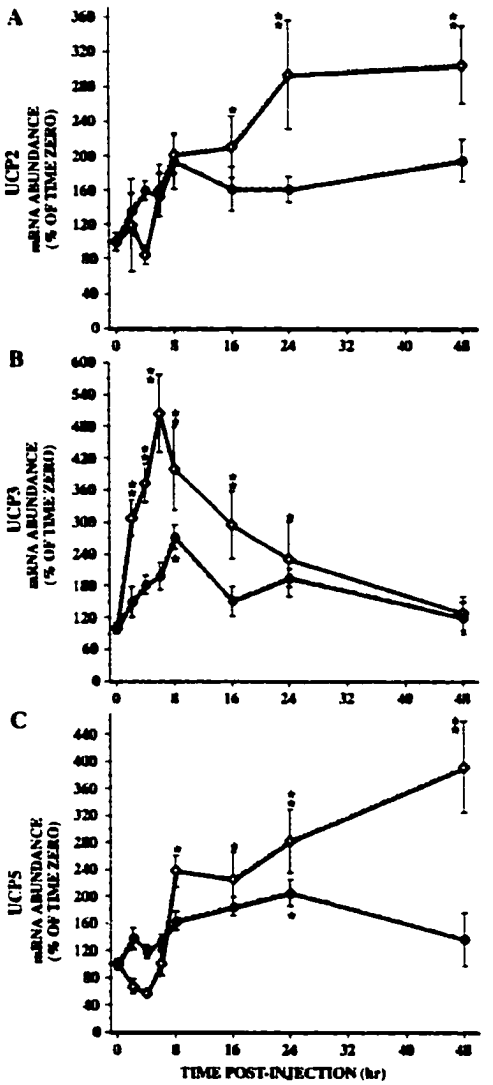

Figure A.2. Stimulation of *Ucp* homologue expression in skeletal muscle following LPS treatment.

Time-dependent stimulation of *Ucp* homologue expression in hindlimb skeletal muscle (SKM) of LPS-treated mice. Determinations of *Ucp2* (A), *Ucp3* (B), and *Ucp5* mRNA abundance (C) were made on SKM derived from control (filled circles) or LPS-treated (open diamonds) mice housed at 22°C (see Figure A.1 legend). Each point represents the mean ± SE of 3-5 independent measurements, derived from mice depicted in Figure A.1 (*$P < 0.05$, **$P < 0.01$ vs. time 0 values); some error bars are within the symbol. Values for *Ucp2* mRNA at 8 h tended to be higher relative to time 0 ($P < 0.1$). Not indicated are significant differences ($P < 0.05$) between LPS mice and time-matched controls, occurring at 2-6 and 16 h (*Ucp3*), and at 48 h (*Ucp5*) (no significant treatment × time interaction for *Ucp2*).

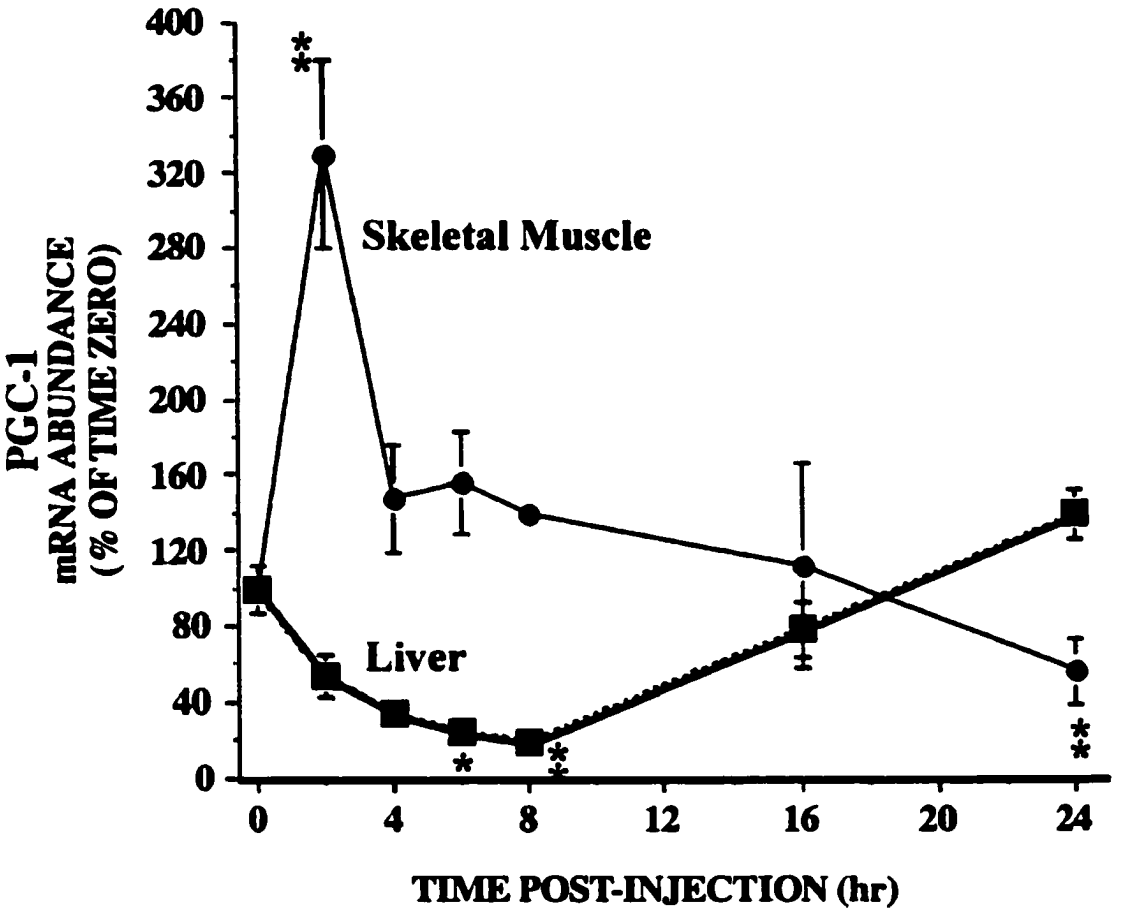

Figure A.3. Changes in *Pgc-1* mRNA following LPS treatment.
Tissue-dependent stimulation or repression of peroxisome proliferator-activated receptor-γ (*Pgc-1*) expression in mice administered LPS. *Pgc-1* mRNA abundance was determined in a subset of SKM (filled circles) and whole liver (filled squares) samples from mice treated with LPS (samples are the same as those whose data are presented in Figures A.1 and A.2). Three independent samples were used at each timepoint (*$P <$ 0.05, **$P < 0.01$ vs. time 0 values); some error bars are within the symbol. The drop in liver mRNA was apparent by 2 h ($P = 0.06$). Not shown are PBS-injected control values, which were not altered significantly relative to time 0.

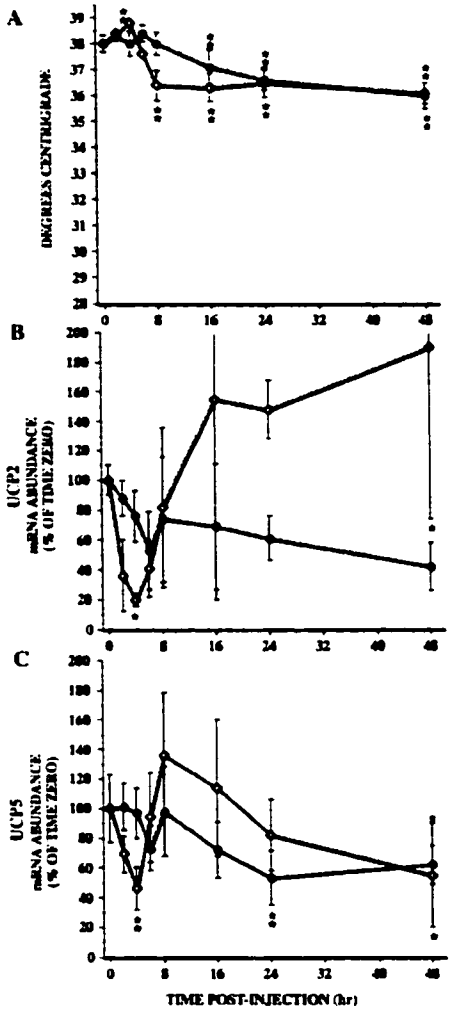

Figure A.4. Body temperature and liver *Ucp* homologue mRNA abundance following LPS treatment with prevention of hypothermia.
Whole liver patterns of *Ucp* homologue mRNA abundance after prevention of hypothermia in LPS-treated mice. Adult female C57BL6/J mice were treated in the between 15:30-16:30 with a single ip dose of PBS (controls, filled circles) or LPS (open diamonds) and housed at an ambient temperature of 34°C with fasting (study 2, see MATERIALS AND METHODS). Colonic temperature (A), liver *Ucp2* mRNA abundance (B), and liver *Ucp5* mRNA abundance (C) were determined in groups of mice through 48 h postinjection. Each point represents the mean ± SE of 3-4 independent measurements (*$P < 0.05$, ** $P < 0.01$ vs. time 0 values); some error bars are within the symbol. The lower values for *Ucp2* at 2 and 6 h after LPS ($P < 0.1$) did not achieve statistical significance. Not indicated are significant differences ($P < 0.05$) between LPS mice and time-matched controls, occurring at: 4-16 h (body temperature), 16-48 h (*Ucp2*), and 2 h (*Ucp5*).

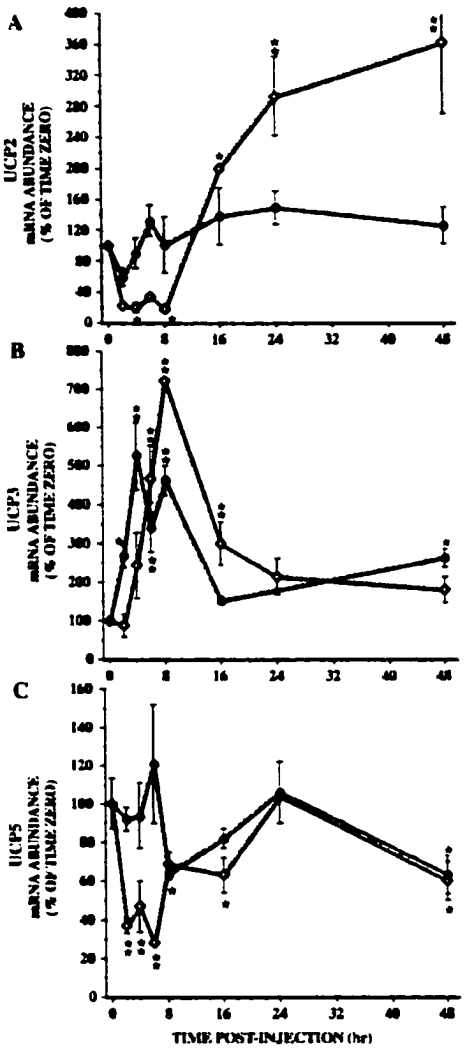

Figure A.5. Changes in SKM *Ucp* homologue mRNA abundance following LPS treatment with prevention of hypothermia.
Hindlimb SKM patterns of *Ucp* homologue mRNA abundance after prevention of hypothermia in LPS-treated mice. Determinations of *Ucp2* (A), *Ucp3* (B), and *Ucp5* mRNA abundance (C) were made on SKM derived from control (filled circles) or LPS-treated (open diamonds) mice housed at 34°C (see Figure A.4 Legend for details). Each point represents the mean ± SE of 3-4 independent measurements (*$P < 0.05$, **$P < 0.01$ vs. time 0 values); some error bars are within the symbol. Values for *Ucp2* at 2 and 6 h ($P < 0.1$), *Ucp5* at 8 h ($P = 0.06$), and increased *Ucp3* at 4 h ($P = 0.06$) post-LPS clearly differed from time 0 values, but did not achieve statistical significance at $P < 0.05$. Not indicated are significant differences ($P < 0.05$) between LPS mice and time-matched controls which occurred at: 6-8 and 24-48 h (*Ucp2*), 2-4 and 8 h (*Ucp3*), and 2-6 h (*Ucp5*).

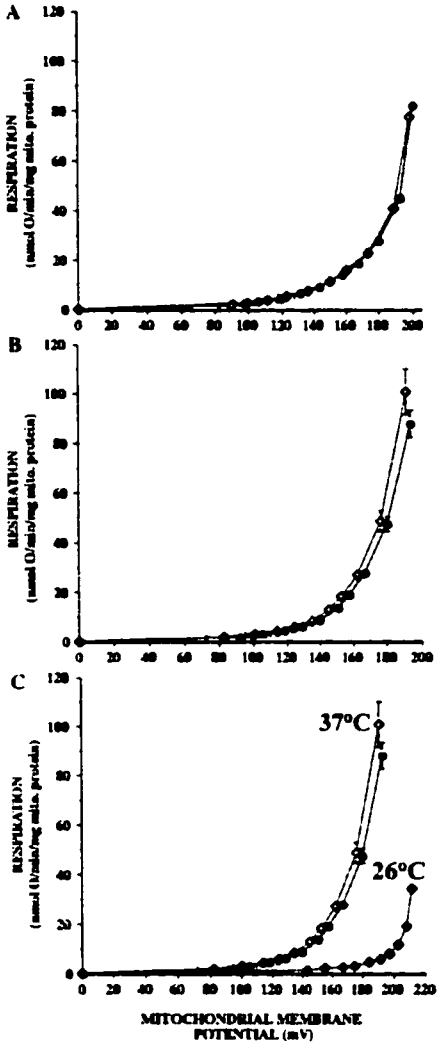

Figure A.6. Effect of in vivo LPS treatment on proton leak in liver mitochondria. Lack of effect of in vivo LPS treatment on liver mitochondrial proton leak kinetics in mice. Respiration attributable to liver mitochondrial proton leak was measured at various titrations of mitochondrial membrane potential in isolated organelles derived from adult female C57BL6/J mice injected ip with PBS (controls, filled circles) or LPS (open diamonds) between 1530 and 1630 (study 3, see MATERIALS AND METHODS). Graphs correspond to measurements taken at 4 h (A) or at 16 h (B and C) postinjection. Data in (C) illustrate the alteration of proton leak which occurred in a subset (n = 3) of 16-h LPS-treated mouse preparations assayed at 26°C (filled diamonds) compared with kinetics of mitochondria assayed at the typical 37°C [data from (B) are reproduced in (C) for comparison]. Symbols represent mean values for independent experiments at any given titration point in the assay (n = 3/treatment at 4 h, n = 7/treatment at 16 h), with SEs for respiration and membrane potentials indicated by vertical and horizontal error bars, respectively; some errors are within the symbol.

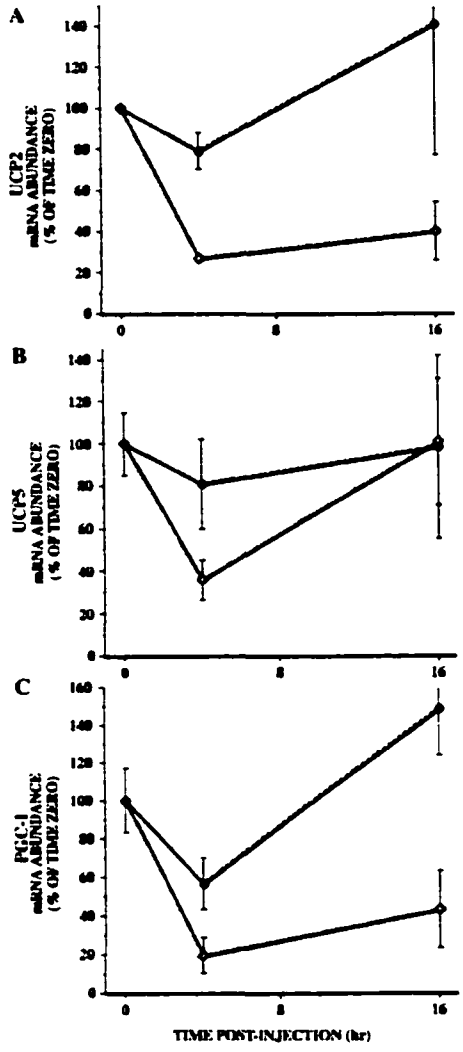

Figure A.7. Levels of hepatocyte *Ucp* homologue and *Pgc-1* mRNA following LPS treatment.

Depression of *Ucp* homologue and *Pgc-1* mRNA in hepatocytes isolated from LPS-treated mice. At each timepoint depicted, hepatocyte-enriched cell fractions were obtained from adult female C57BL6/J mice injected with PBS (controls, filled circles) or LPS (open diamonds)(study 4, see MATERIALS AND METHODS). Values at each timepoint represent the mean mRNA abundance of *Ucp2* (A), *Ucp5* (A), or *Pgc-1* (C) from two independent preparations/treatment.

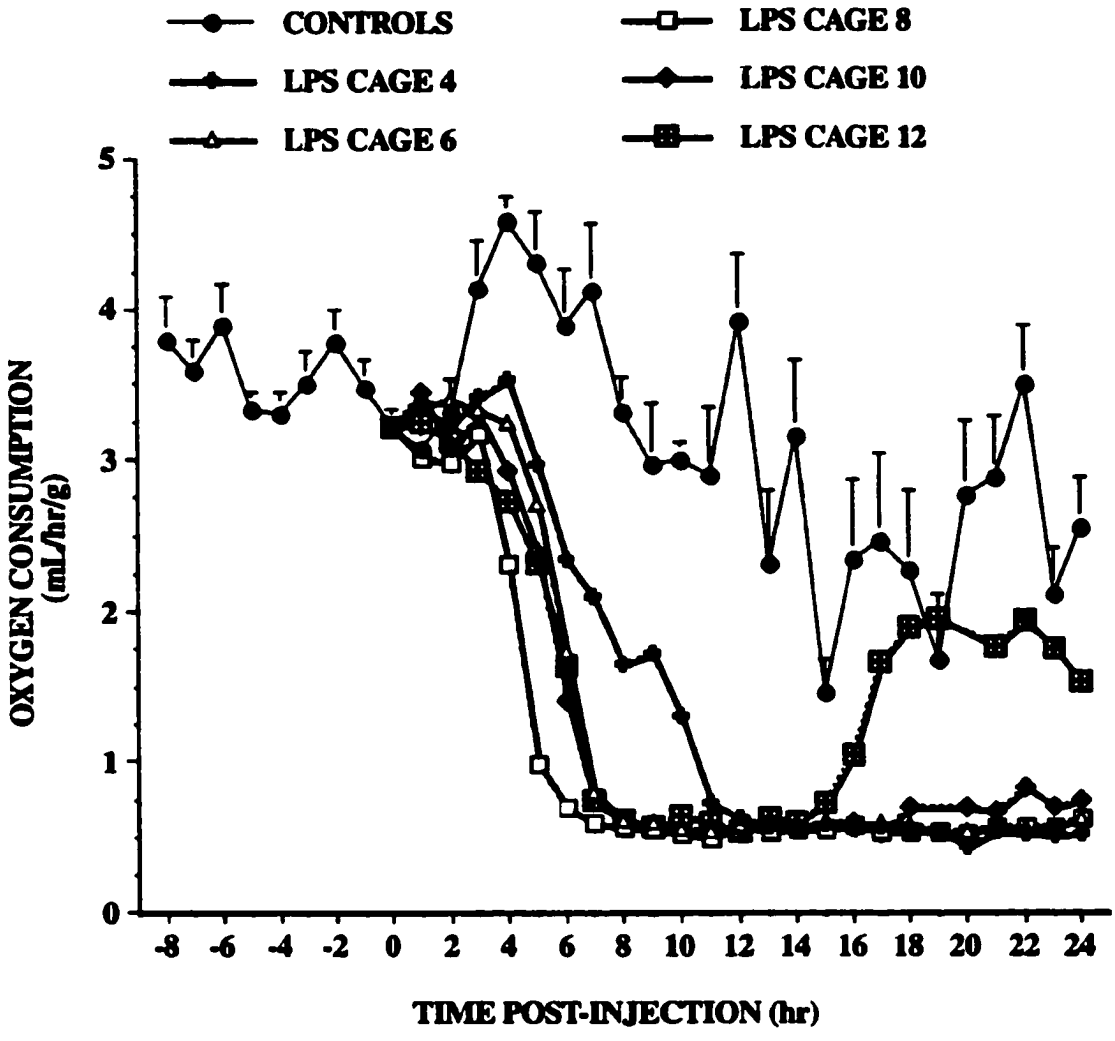

Figure A.8. Metabolic depression in mice injected with endotoxin.
Metabolic depression in mice injected with endotoxin. Metabolic rate was determined via indirect calorimetry in adult female C57BL6/J mice before and after ip injection of PBS (controls, filled circles) or LPS (other symbols) between 1430 and 1530 (0 h), after which animals were fasted (study 5, see MATERIALS AND METHODS). Control values represent the mean ± SE of all mice at –8 to 0 h (n = 12) or those injected with PBS at 1-h postinjection onward (n = 6). Data on individual LPS-treated mice are shown separately to highlight individual variation observed after treatment in this particular group of animals. Not shown is a single LPS-treated mouse (cage 2) who for unclear reasons did not display a drop in metabolic rate following injection (see RESULTS).

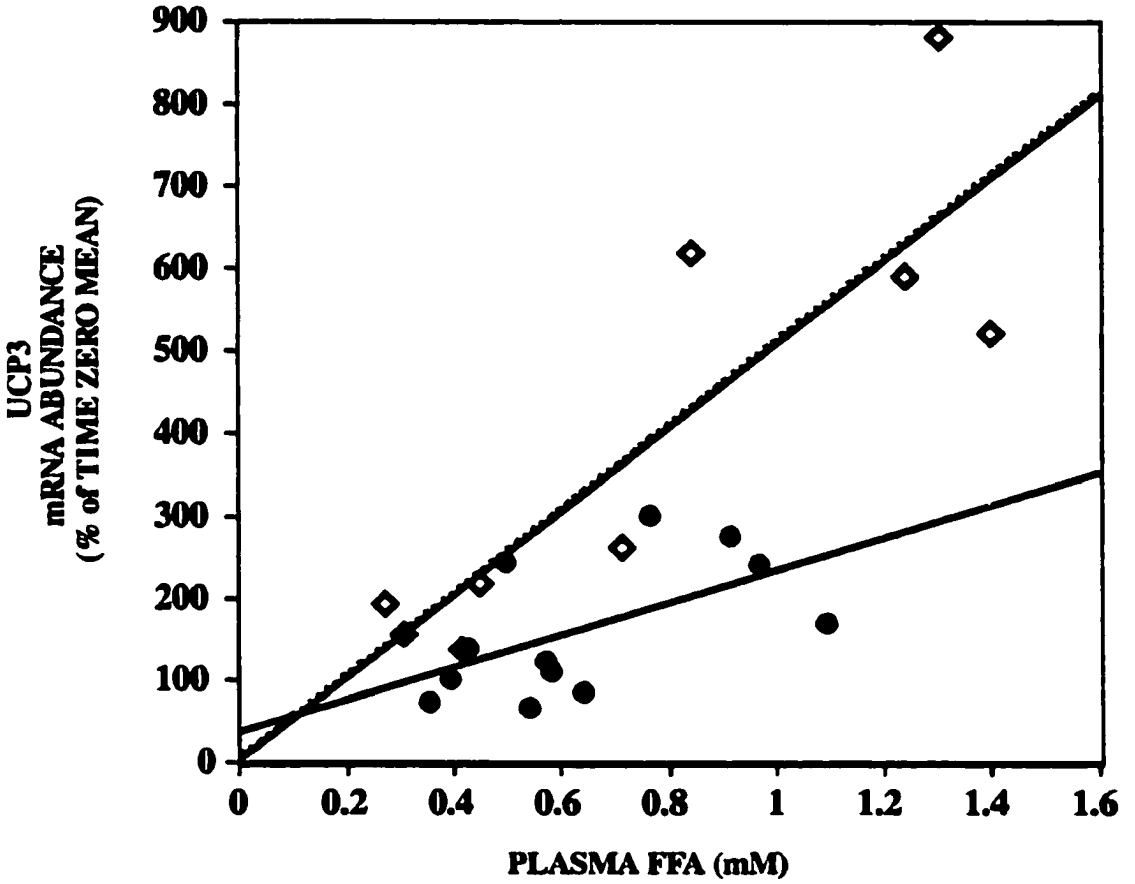

Figure A.9. Relationship between *Ucp3* mRNA and free fatty acids.
Ucp3 expression in SKM of LPS-treated mice correlates with a rise in plasma free fatty acid (FFA) concentration. Determinations of circulating FFA and hindlimb SKM *Ucp3* mRNA abundance were made in samples derived from adult female C57BL6/J mice injected ip with PBS (controls, filled circles) or LPS (open diamonds). *Ucp3* mRNA was strongly correlated with plasma FFA in LPS mice ($r^2 = 0.75$, $P < 0.001$ / slope different from zero), whereas this relationship was not as apparent in controls $r^2 = 0.33$, $P = 0.05$ / slope different from zero). Data points represent matched samples across all timepoints measured (0, 2, and 6 h postinjection; see DISCUSSION).

REFERENCES

Ahima RS, Prabakaran D, Mantzoros C, Qu D, Lowell B, Maratos-Flier E, Flier JS. 1996. Role of leptin in the neuroendocrine response to fasting. Nature 382:250-252.

Baker DM, Larsen DA, Swanson P, Dickhoff WW. 2000. Long-term peripheral treatment of immature coho salmon (*Oncorhynchus kisutch*) with human leptin has no clear physiologic effect. General and Comparative Endocrinology 118:134-138.

Banks WA, DiPalma CR, Farrell CL. 1999. Impaired transport of leptin across the blood-brain barrier in obesity. Peptides 20:1341-1345.

Barnes BM. 1989. Freeze avoidance in a mammal: body temperatures below 0°C in an Arctic hibernator. Science 244:1593-1595.

Barre H, Cohen-Adad F, Rouanet JL. 1987. Two daily glucagon injections induce nonshivering thermogenesis in Muscovy ducklings. American Journal of Physiology 252:E616-E620.

Berry MN, Edwards AM, Barritt GJ. 1991. Isolated Hepatocytes. Preparation, Properties, and Applications. New York: Elsevier.

Bezaire V, Hofmann W, Kramer JK, Kozak LP, Harper ME. 2001. Effects of fasting on muscle mitochondrial energetics and fatty acid metabolism in *Ucp3(-/-)* and wild-type mice. American Journal of Physiology 281:E975-E982.

Billington CJ, Briggs JE, Harker S, Grace M, Levine AS. 1994. Neuropeptide Y in hypothalamic paraventricular nucleus: a center coordinating energy metabolism. American Journal of Physiology 266:R1765-R1770.

Bishop T, St-Pierre J, Brand MD. 2002. Primary causes of decreased mitochondrial oxygen consumption during metabolic depression in snail cells. American Journal of Physiology 282:R372-R382.

Bjorbaek C, El-Haschimi K, Frantz JD, Flier JS. 1999. The role of SOCS-3 in leptin signaling and leptin resistance. Journal of Biological Chemistry 274:30059-30065.

Blouin A, Bolender RP, Weibel ER. 1977. Distribution of organelles and membranes between hepatocytes and nonhepatocytes in the rat liver parenchyma. A stereological study. Journal of Cell Biology 72:441-455.

Boss O, Bachman E, Vidal-Puig A, Zhang CY, Peroni O, Lowell BB. 1999. Role of the β_3-adrenergic receptor and/or a putative β_4-adrenergic receptor on the expression of uncoupling proteins and peroxisome proliferator-activated receptor-γ coactivator-1. Biochemical and Biophysical Research Communications 261:870-876.

Boss O, Muzzin P, Giacobino JP. 1998a. The uncoupling proteins, a review. European Journal of Endocrinology 139:1-9.

Boss O, Samec S, Kuhne F, Bijlenga P, Assimacopoulos-Jeannet F, Seydoux J, Giacobino JP, Muzzin P. 1998b. Uncoupling protein-3 expression in rodent skeletal muscle is modulated by food intake but not by changes in environmental temperature. Journal of Biological Chemistry 273:5-8.

Boss O, Samec S, Dulloo A, Seydoux J, Muzzin P, Giacobino JP. 1997a. Tissue-dependent upregulation of rat uncoupling protein-2 expression in response to fasting or cold. FEBS Letters 412:111-4.

Boss O, Samec S, Paoloni-Giacobino A, Rossier C, Dulloo A, Seydoux J, Muzzin P, Giacobino JP. 1997b. Uncoupling protein-3: a new member of the mitochondrial carrier family with tissue-specific expression. FEBS Letters 408:39-42.

Boswell T, Woods SC, Kenagy GJ. 1994. Seasonal changes in body mass, insulin, and glucocorticoids of free-living golden-mantled ground squirrels. General and Comparative Endocrinology 96:339-346.

Bouillaud F, Weissenbach J, Ricquier D. 1986. Complete cDNA-derived amino acid sequence of rat brown fat uncoupling protein. Journal of Biological Chemistry 261:1487-1490.

Boutilier RG. 2001. Mechanisms of cell survival in hypoxia and hypothermia. Journal of Experimental Biology 204:3171-3181.

Boyer BB, Barnes BM, Kopecky J, Jacobsson A, Hermanska J. 1993. Molecular control of prehibernation brown fat growth in arctic ground squirrels. In: Carey C, Florant GL, Wunder BA, Horwitz B, editors. Life in the Cold: Ecological, Physiological, and Molecular Mechanisms. Boulder: Westview Press. p 483-492.

Boyer BB, Barnes BM, Lowell BB, Grujic D. 1998. Differential regulation of uncoupling protein gene homologues in multiple tissues of hibernating ground squirrels. American Journal of Physiology 44:R1232-R1238.

Boyer BB, Ormseth OA, Buck L, Nicolson M, Pelleymounter MA, Barnes BM. 1997. Leptin prevents posthibernation weight gain but does not reduce energy expenditure in arctic ground squirrels. Comparative Biochemistry and Physiology 118C:405-412.

Brand MD. 1990. The proton leak across the mitochondrial inner membrane. Biochimica et Biophysica Acta 1018:128-133.

Brand MD. 1995. Measurement of mitochondrial protonmotive force. Bioenergetics: a practical approach. Oxford: Oxford University Press. p 39-62.

Brand MD, Chien LF, Ainscow EK, Rolfe DF, Porter RK. 1994. The causes and functions of mitochondrial proton leak. Biochimica et Biophysica Acta 1187:132-139.

Brand MD, D'Alessandri L, Reis HM, Hafner RP. 1990. Stimulation of the electron transport chain in mitochondria isolated from rats treated with mannoheptulose or glucagon. Archives of Biochemistry and Biophysics 283:278-284.

Brander F, Keith JS, Trayhum PA. 1993. A 27-mer oligonucleotide probe for the detection and measurement of the mRNA for uncoupling protein in brown adipose tissue of different species. Comparative Biochemistry and Physiology 104B:125-131.

Bray GA. 1997. Obesity and reproduction. Human Reproduction 12 Supplement 1:26-32.

Brookes PS, Buckingham JA, Tenreiro AM, Hulbert AJ, Brand MD. 1998. The proton permeability of the inner membrane of liver mitochondria from ectothermic and endothermic vertebrates and from obese rats: correlations with standard metabolic

rate and phospholipid fatty acid composition. Comparative Biochemistry and Physiology 119B:325-334.

Brown SDM. 1998. Mouse models of genetic disease: New approaches, new paradigms. Journal of Inherited Metabolic Disorders 21:532-539.

Brustovetsky NN, Amerkhanov ZG, Popova E, Konstantinov AA. 1990. Reversible inhibition of electron transfer in the ubiquinol. Cytochrome c reductase segment of the mitochondrial respiratory chain in hibernating ground squirrels. FEBS Letters 263:73-6.

Brustovetsky NN, Egorova MV, Gnutov D, Gogvadze VG, Mokhova EN, Skulachev VP. 1992a. Thermoregulatory, carboxyatractylate-sensitive uncoupling in heart and skeletal muscle mitochondria of the ground squirrel correlates with the level of free fatty acids. FEBS Letters 305:15-7.

Brustovetsky NN, Egorova MV, Mayevsky EI. 1992b. Regulation of oxidative activity and $\Delta\psi$ of liver mitochondria of active and hibernating gophers. The role of phospholipase A_2. Comparative Biochemistry and Physiology 102B:635-638.

Brustovetsky NN, Mayevsky EI, Grishina EV, Gogvadze VG, Amerkhanov ZG. 1989. Regulation of the rate of respiration and oxidative phosphorylation in liver mitochondria from hibernating ground squirrels, *Citellus undulatus*. Comparative Biochemistry and Physiology 94B:537-541.

Buck CL, Barnes BM. 1999a. Annual cycle of body composition and hibernation in free-living arctic ground squirrels. Journal of Mammalogy 80:430-442.

Buck CL, Barnes BM. 1999b. Temperatures of hibernacula and change in body composition of Arctic ground squirrels over winter. Journal of Mammalogy 80:1264-1276.

Buck CL, Barnes BM. 2000. Effects of ambient temperature on metabolic rate, respiratory quotient, and torpor in an arctic hibernator. American Journal of Physiology 279:R255-R262.

Cabrero A, Alegret M, Sanchez RM, Adzet T, Laguna JC, Vazquez M. 2000. Down-regulation of uncoupling protein-3 and -2 by thiazolidinediones in C_2C_{12} myotubes. FEBS Letters 484:37-42.

Cadenas S, Brand MD. 2000. Effects of magnesium and nucleotides on the proton conductance of rat skeletal-muscle mitochondria. Biochemical Journal 348:209-213.

Cadenas S, Buckingham JA, Samec S, Seydoux J, Din N, Dulloo AG, Brand MD. 1999. UCP2 and UCP3 rise in starved rat skeletal muscle but mitochondrial proton conductance is unchanged. FEBS Letters 462:257-260.

Cadenas S, Echtay KS, Harper JA, Jekabsons MB, Buckingham JA, Grau E, Abuin A, Chapman H, Clapham JC, Brand MD. 2002. The basal proton conductance of skeletal muscle mitochondria from transgenic mice overexpressing or lacking uncoupling protein-3. Journal of Biological Chemistry 277:2773-2778.

Camirand A, Marie V, Rabelo R, Silva JE. 1998. Thiazolidinediones stimulate uncoupling protein-2 expression in cell lines representing white and brown adipose tissues and skeletal muscle. Endocrinology 139:428-431.

Cannon B, Matthias A, Golozoubova V, Ohlson KBE, Andersson U, Jacobsson A, Nedergaard J. 1999. Unifying and distinguishing features of brown and white adipose tissues: UCP1 versus other UCPs. In: Guy-Grand B, Ailhaud G, editors. Progress in obesity research. John Libbey & Company, Ltd./8th International Congress on Obesity. p 13-26.

Cannon B, Nedergaard J. 2001. Respiratory and thermogenic capacities of cells and mitochondria from brown and white adipose tissue. Methods in Molecular Biology 155:295-303.

Canton M, Luvisetto S, Schmehl I, Azzone GF. 1995. The nature of mitochondrial respiration and discrimination between membrane and pump properties. Biochemical Journal 310:477-481.

Ceddia RB, William WN, Lima FB, Flandin P, Curi R, Giacobino JP. 2000. Leptin stimulates uncoupling protein-2 mRNA expression and krebs cycle activity and inhibits lipid synthesis in isolated rat white adipocytes. European Journal of Biochemistry 267:5952-5958.

Celis JE, Kruhoffer M, Gromova I, Frederiksen C, Ostergaard M, Thykjaer T, Gromov P, Yu J, Palsdottir H, Magnusson N, Orntoft TF. 2000. Gene expression profiling: monitoring transcription and translation products using DNA microarrays and proteomics. FEBS Letters 480:2-16.

Chaffee RRJ, Hoch FL, Lyman CP. 1961. Mitochondrial oxidative enzymes and phosphorylations in cold exposure and hibernation. American Journal of Physiology 201:29-32.

Champigny O, Ricquier D. 1990. Effects of fasting and refeeding on the level of uncoupling protein mRNA in rat brown adipose tissue: evidence for diet-induced and cold- induced responses. Journal of Nutrition 120:1730-6.

Chavin KD, Yang S, Lin HZ, Chatham J, Chacko VP, Hoek JB, Walajtys-Rode E, Rashid A, Chen CH, Huang CC, Wu TC, Lane MD, Diehl AM. 1999. Obesity induces expression of uncoupling protein-2 in hepatocytes and promotes liver ATP depletion. Journal of Biological Chemistry 274:5692-5700.

Chehab FF, Mounzih K, Lu R, Lim ME. 1997. Early onset of reproductive function in normal female mice treated with leptin. Science 275:88-90.

Chen G, Koyama K, Yuan X, Lee Y, Zhou YT, O'Doherty R, Newgard CB, Unger RH. 1996. Disappearance of body fat in normal rats induced by adenovirus-mediated leptin gene therapy. Proceedings of the National Academy of Sciences of the United States of America 93:14795-14799.

Clapham JC, Arch JR, Chapman H, Haynes A, Lister C, Moore GB, Piercy V, Carter SA, Lehner I, Smith SA and others. 2000. Mice overexpressing human uncoupling protein-3 in skeletal muscle are hyperphagic and lean. Nature 406:415-418.

Cline GW, Vidal-Puig AJ, Dufour S, Cadman KS, Lowell BB, Shulman GI. 2001. In vivo effects of uncoupling protein-3 gene disruption on mitochondrial energy metabolism. Journal of Biological Chemistry 276:20240-20244.

Combatsiaris TP, Charron MJ. 1999. Downregulation of uncoupling protein 2 mRNA in white adipose tissue and uncoupling protein 3 mRNA in skeletal muscle during the early stages of leptin treatment. Diabetes 48:128-133.

Commins SP, Watson PM, Padgett MA, Dudley A, Argyropoulos G, Gettys TW. 1999. Induction of uncoupling protein expression in brown and white adipose tissue by leptin. Endocrinology 140:292-300.

Concannon P, Levac K, Rawson R, Tennant B, Bensadoun A. 2001. Seasonal changes in serum leptin, food intake, and body weight in photoentrained woodchucks. American Journal of Physiology 281:R951-R959.

Considine RV, Sinha MK, Heiman ML, Kriauciunas A, Stephens TW, Nyce MR, Ohannesian JP, Marco CC, McKee LJ, Bauer TL, Caro JF. 1996. Serum immunoreactive-leptin concentrations in normal-weight and obese humans. New England Journal of Medicine 334:292-295.

Cortez-Pinto H, Yang SQ, Lin HZ, Costa S, Hwang CS, Lane MD, Bagby G, Diehl AM. 1998. Bacterial lipopolysaccharide induces uncoupling protein-2 expression in hepatocytes by a tumor necrosis factor-alpha-dependent mechanism. Biochemical and Biophysical Research Communications 251:313-319.

Dark J, Forger NG, Stern JS, Zucker I. 1985. Recovery of lipid mass after removal of adipose tissue in ground squirrels. American Journal of Physiology 249:R73-R78.

Dark J, Forger NG, Zucker I. 1984. Rapid recovery of body mass after surgical removal of adipose tissue in ground squirrels. Proceedings of the National Academy of Sciences of the United States of America 81:2270-2272.

Drew KL, Osborne PG, Frerichs KU, Hu Y, Koren RE, Hallenbeck JM, Rice ME. 1999. Ascorbate and glutathione regulation in hibernating ground squirrels. Brain Research 851:1-8.

Duchamp C, Barre H, Rouanet JL, Lanni A, Cohen-Adad F, Berne G, Brebion P. 1991. Nonshivering thermogenesis in king penguin chicks. I. Role of skeletal muscle. American Journal of Physiology 261:R1438-R1445.

Echtay KS, Brand MD. 2001. Coenzyme Q induces GDP-sensitive proton conductance in kidney mitochondria. Biochemical Society Transactions 29:763-768.

Echtay KS, Roussel D, St-Pierre J, Jekabsons MB, Cadenas S, Stuart JA, Harper JA, Roebuck SJ, Morrison A, Pickering S and others. 2002. Superoxide activates mitochondrial uncoupling proteins. Nature 415:96-9.

Echtay KS, Winkler E, Frischmuth K, Klingenberg M. 2001. Uncoupling proteins 2 and 3 are highly active H+ transporters and highly nucleotide sensitive when activated by coenzyme Q (ubiquinone). Proceedings of the National Academy of Sciences of the United States of America 98:1416-1421.

Elbein SC. 2002. Perspective: the search for genes for type 2 diabetes in the post-genome era. Endocrinology 143:2012-2018.

Faber P, Garby L. 1995. Fat content affects heat capacity: a study in mice. Acta Physiologica Scandinavica 153:185-187.

Fabris R, Nisoli E, Lombardi AM, Tonello C, Serra R, Granzotto M, Cusin I, Rohner-Jeanrenaud F, Federspil G, Carruba MO, Vettor R. 2001. Preferential channeling of energy fuels toward fat rather than muscle during high free fatty acid availability in rats. Diabetes 50:601-608.

Faggioni R, Shigenaga J, Moser A, Feingold KR, Grunfeld C. 1998. Induction of UCP2 gene expression by LPS: a potential mechanism for increased thermogenesis

during infection. Biochemical and Biophysical Research Communications 244:75-78.

Farooqi IS, Jebb SA, Langmack G, Lawrence E, Cheetham CH, Prentice AM, Hughes IA, McCamish MA, O'Rahilly S. 1999. Effects of recombinant leptin therapy in a child with congenital leptin deficiency. New England Journal of Medicine 341:879-884.

Fedotcheva NJ, Sharyshev AA, Mironova GD, Kondrashova MN. 1985. Inhibition of succinate oxidation and K+ transport in mitochondria during hibernation. Comparative Biochemistry and Physiology 82B:191-195.

Feist DD, Florant G, Greenwood MRC, Feist C. 1986. Regulation of energy stores in arctic ground squirrels: brown fat thermogenic capacity, lipoprotein lipase, and pancreatic hormones during fat deposition. In: Heller HC, editor. Living in the Cold:Physiological and Biochemical Adaptations. New York: Elsevier Press. p 281-285.

Fleury C, Neverova M, Collins S, Raimbault S, Champigny O, Levi-Meyrueis C, Bouillaud F, Seldin MF, Surwit RS, Ricquier D and others. 1997. Uncoupling protein-2: a novel gene linked to obesity and hyperinsulinemia. Nature Genetics 15:269-272.

Flier JS. 1998. What's in a name? In search of leptin's physiologic role. Journal of Clinical Endocrinology and Metabolism 83:1407-1413.

Foster DO, Frydman ML. 1978. Nonshivering thermogenesis in the rat. II. Measurements of blood flow with microspheres point to brown adipose tissue as the dominant

site of the calorigenesis induced by noradrenaline. Canadian Journal of Physiology and Pharmacology 56:110-122.

Frederich RC, Hamann A, Anderson S, Lollmann B, Lowell BB, Flier JS. 1995. Leptin levels reflect body lipid content in mice: evidence for diet-induced resistance to leptin action. Nature Medicine 1:1311-1314.

Frerichs KU, Smith CB, Brenner M, DeGracia DJ, Krause GS, Marrone L, Dever TE, Hallenbeck JM. 1998. Suppression of protein synthesis in brain during hibernation involves inhibition of protein initiation and elongation. Proceedings of the National Academy of Sciences of the United States of America 95:14511-14516.

Galster W, Morrison P. 1976. Seasonal changes in body composition of the arctic ground squirrel, *Citellus undulatus*. Canadian Journal of Zoology 54:74-78.

Garlid KD, Jaburek M, Jezek P, Varecha M. 2000. How do uncoupling proteins uncouple? Biochimica et Biophysica Acta 1459:383-389.

Gehnrich SC, Aprille JR. 1988. Hepatic gluconeogenesis and mitochondrial function during hibernation. Comparative Biochemistry and Physiology 91B:11-16.

Geiser F. 1988. Reduction of metabolism during hibernation and daily torpor in mammals and birds: temperature effect or physiological inhibition? Journal of Comparative Physiology B 158:25-37.

Gimeno RE, Dembski M, Weng X, Deng N, Shyjan AW, Gimeno CJ, Iris F, Ellis SJ, Woolf EA, Tartaglia LA. 1997. Cloning and characterization of an uncoupling

protein homologue: a potential molecular mediator of human thermogenesis. Diabetes 46:900-906.

Gong DW, He YF, Karas M, Reitman M. 1997. Uncoupling protein-3 is a mediator of thermogenesis regulated by thyroid hormone, β_3-adrenergic agonists, and leptin. Journal of Biological Chemistry 272:24129-24132.

Gong DW, Monemdjou S, Gavrilova O, Leon LR, Marcus-Samuels B, Chou CJ, Everett C, Kozak LP, Li CL, Deng CX, Harper ME, Reitman ML. 2000. Lack of obesity and normal response to fasting and thyroid hormone in mice lacking uncoupling protein-3. Journal of Biological Chemistry 275:16251-16257.

Grav HI, Blix AS. 1979. A source of nonshivering thermogenesis in fur seal skeletal muscle. Science 204:87-89.

Hagen T, Zhang CY, Slieker LJ, Chung WK, Leibel RL, Lowell BB. 1999. Assessment of uncoupling activity of the human uncoupling protein 3 short form and three mutants of the uncoupling protein gene using a yeast heterologous expression system. FEBS Letters 454:201-206.

Halaas JL, Gajiwala KS, Maffei M, Cohen SL, Chait BT, Rabinowitz D, Lallone RL, Burley SK, Friedman JM. 1995. Weight-reducing effects of the plasma protein encoded by the obese gene. Science 269:543-6.

Hand SC, Hardewig I. 1996. Downregulation of cellular metabolism during environmental stress: mechanisms and implications. Annual Review of Physiology 58:539-563.

Hannon JP, Vaughn DA, Hock RJ. 1961. The endogenous tissue respiration of the arctic ground squirrels as affected by hibernation and season. Journal of Cellular and Comparative Physiology 57:5-10.

Harper JA, Stuart JA, Jekabsons MB, Roussel D, Brindle KM, Dickinson K, Jones RB, Brand MD. 2002. Artifactual uncoupling by uncoupling protein 3 in yeast mitochondria at the concentrations found in mouse and rat skeletal-muscle mitochondria. Biochemical Journal 361:49-56.

Harper ME, Brand MD. 1993. The quantitative contributions of mitochondrial proton leak and ATP turnover reactions to the changed respiration rates of hepatocytes from rats of different thyroid status. Journal of Biological Chemistry 268:14850-14860.

Harris RBS, Zhou J, Redmann SM, Smagin GN, Smith SR, Rodgers E, Zachwieja JJ. 1998. A leptin dose-response study in obese *(ob/ob)* and lean *(+/?)* mice. Endocrinology 139:8-19.

Hayashi M, Nagasaka T. 1983. Suppression of norepinephrine-induced thermogenesis in brown adipose tissue by fasting. American Journal of Physiology 245:E582-E586.

Heaton GM, Wagenvoord RJ, Kemp A, Jr., Nicholls DG. 1978. Brown-adipose-tissue mitochondria: photoaffinity labelling of the regulatory site of energy dissipation. European Journal of Biochemistry 82:515-521.

Heymsfield SB, Greenberg AS, Fujioka K, Dixon RM, Kushner R, Hunt T, Lubina JA, Patane J, Self B, Hunt P and others. 1999. Recombinant leptin for weight loss in

obese and lean adults - A randomized, controlled, dose-escalation trial. Journal of the American Medical Association 282:1568-1575.

Himms-Hagen J, Harper ME. 2001. Physiological role of UCP3 may be export of fatty acids from mitochondria when fatty acid oxidation predominates: An hypothesis. Experimental Biology and Medicine 226:78-84.

Hinz W, Faller B, Gruninger S, Gazzotti P, Chiesi M. 1999. Recombinant human uncoupling protein-3 increases thermogenesis in yeast cells. FEBS Letters 448:57-61.

Hirsch J, Gallian E. 1968. Methods for the determination of adipose cell size in man and animals. Journal of Lipid Research 9:110-119.

Huang SG, Klingenberg M. 1995. Nature of the masking of nucleotide-binding sites in brown adipose tissue mitochondria. Involvement of endogenous adenosine triphosphate. European Journal of Biochemistry 229:718-725.

Hwang CS, Lane MD. 1999. Up-regulation of uncoupling protein-3 by fatty acid in C_2C_{12} myotubes. Biochemical and Biophysical Research Communications 258:464-469.

Iossa S, Lionetti L, Mollica MP, Crescenzo R, Botta M, Samec S, Dulloo AG, Liverini G. 2001. Differences in proton leak kinetics, but not in UCP3 protein content, in subsarcolemmal and intermyofibrillar skeletal muscle mitochondria from fed and fasted rats. FEBS Letters 505:53-56.

Ishida K, Murakami T, Mizuno A, Iida M, Kuwajima M, Shima K. 1997. Leptin suppresses basal insulin secretion from rat pancreatic islets. Regulatory Peptides 70:179-182.

Jacobsson A, Muhleisen M, Cannon B, Nedergaard J. 1994. The uncoupling protein thermogenin during acclimation: indications for pretranslational control. American Journal of Physiology 267:R999-R1007.

Jekabsons MB, Gregoire FM, SchonfeldWarden NA, Warden CH, Horwitz BA. 1999. T_3 stimulates resting metabolism and UCP-2 and UCP-3 mRNA but not nonphosphorylating mitochondrial respiration in mice. American Journal of Physiology 277:E380-E389.

Kelly LJ, Vicario PP, Thompson GM, Candelore MR, Doebber TW, Ventre J, Wu MS, Meurer R, Forrest MJ, Conner MW, Cascieri MA, Moller DE. 1998. Peroxisome proliferator-activated receptors γ and α mediate in vivo regulation of uncoupling protein (UCP-1, UCP-2, UCP-3) gene expression. Endocrinology 139:4920-4927.

Khalfallah Y, Fages S, Laville M, Langin D, Vidal H. 2000. Regulation of uncoupling protein-2 and uncoupling protein-3 mRNA expression during lipid infusion in human skeletal muscle and subcutaneous adipose tissue. Diabetes 49:25-31.

Klingenberg M, Huang SG. 1999. Structure and function of the uncoupling protein from brown adipose tissue. Biochimica et Biophysica Acta Biomembranes 1415:271-296.

Klingenspor M, Dickopp A, Heldmaier G, Klaus S. 1996. Short photoperiod reduces leptin gene expression in white and brown adipose tissue of Djungarian hamsters. FEBS Letters 399:290-294.

Klingenspor M, Niggemann H, Heldmaier G. 2000. Modulation of leptin sensitivity by short photoperiod acclimation in the Djungarian hamster, *Phodopus sungorus*. Journal of Comparative Physiology B 170:37-43.

Kozak W, Conn CA, Kluger MJ. 1994. Lipopolysaccharide induces fever and depresses locomotor activity in unrestrained mice. American Journal of Physiology 266:R125-R135.

Lahlou N, Clement K, Carel JC, Vaisse C, Lotton C, Le Bihan Y, Basdevant A, Lebouc Y, Froguel P, Roger M and others. 2000. Soluble leptin receptor in serum of subjects with complete resistance to leptin: relation to fat mass. Diabetes 49:1347-1352.

Lanni A, Beneduce L, Lombardi A, Moreno M, Boss O, Muzzin P, Giacobino JP, Goglia F. 1999. Expression of uncoupling protein-3 and mitochondrial activity in the transition from hypothyroid to hyperthyroid state in rat skeletal muscle. FEBS Letters 444:250-254.

Lanni A, DeFelice M, Lombardi A, Moreno M, Fleury C, Ricquier D, Goglia F. 1997. Induction of UCP2 mRNA by thyroid hormones in rat heart. FEBS Letters 418:171-174.

Larkin S, Mull E, Miao W, Pittner R, Albrandt K, Moore C, Young A, Denaro M, Beaumont K. 1997. Regulation of the third member of the uncoupling protein family, UCP3, by cold and thyroid hormone. Biochemical and Biophysical Research Communications 240:222-7.

Larrouy D, Laharrague P, Carrera G, Viguerie-Bascands N, Levi-Meyrueis C, Fleury C, Pecqueur C, Nibbelink M, Andre M, Casteilla L, Ricquier, D. 1997. Kupffer cells are a dominant site of uncoupling protein 2 expression in rat liver. Biochemical and Biophysical Research Communications 235:760-764.

Liu CC, Frehn JL, LaPorta AD. 1969. Liver and brown fat mitochondrial response to cold in hibernators and nonhibernators. Journal of Applied Physiology 27:83-89.

Liu QY, Bai C, Chen F, Wang RP, MacDonald T, Gu MC, Zhang Q, Morsy MA, Caskey CT. 1998. Uncoupling protein-3: a muscle-specific gene upregulated by leptin in ob/ob mice. Gene 207:1-7.

Liu XT, Lin QS, Li QF, Huang CX, Sun RY. 1998. Uncoupling protein mRNA, mitochondrial GTP-binding, and T-4 5'-deiodinase activity of brown adipose tissue in Daurian ground squirrel during hibernation and arousal. Comparative Biochemistry and Physiology 120A:745-752.

Locke RM, Rial E, Nicholls DG. 1982. The acute regulation of mitochondrial proton conductance in cells and mitochondria from the brown fat of cold-adapted and warm-adapted guinea pigs. European Journal of Biochemistry 129:381-387.

Lund P, Wiggins D. 1990. Maintenance of energy-linked functions in rat liver mitochondria. Biochimica et Biophysica Acta 1018:98-102.

Mao WG, Yu XX, Zhong A, Li WL, Brush J, Sherwood SW, Adams SH, Pan GH. 1999. UCP4, a novel brain-specific mitochondrial protein that reduces membrane potential in mammalian cells. FEBS Letters 443:326-330.

Marsh CB, Wewers MD. 1996. The pathogenesis of sepsis. Factors that modulate the response to gram-negative bacterial infection. Clinics in Chest Medicine 17:183-97.

Martin SL, Maniero GD, Carey S, Hand SC. 1999. Reversible depression of oxygen consumption in isolated liver mitochondria during hibernation. Physiological and Biochemical Zoology 72:255-264.

Martins R, Atgie C, Gineste L, Nibbelink M, Ambid L, Ricquier D. 1991. Increased GDP binding and thermogenic activity in brown adipose tissue mitochondria during arousal of the hibernating garden dormouse (*Eliomys quercinus*). Comparative Biochemistry and Physiology 98A:311-316.

Millet L, Vidal H, Andreelli F, Larrouy D, Riou JP, Ricquier D, Laville M, Langin D. 1997. Increased uncoupling protein-2 and -3 mRNA expression during fasting in obese and lean humans. Journal of Clinical Investigation 100:2665-2670.

Millet L, Vidal H, Larrouy D, Andreelli F, Laville M, Langin D. 1998. mRNA expression of the long and short forms of uncoupling protein-3 in obese and lean humans. Diabetologia 41:829-832.

Milner RE, Wang LC, Trayhurn P. 1989. Brown fat thermogenesis during hibernation and arousal in Richardson's ground squirrel. American Journal of Physiology 256:R42-R48.

Monemdjou S, Kozak LP, Harper ME. 1999. Mitochondrial proton leak in brown adipose tissue mitochondria of Ucp1-deficient mice is GDP insensitive. American Journal of Physiology 279:E1073-E1082.

Mrosovsky N. 1971a. The conditions for torpor. Hibernation and the hypothalamus. New York: Appleton-Century-Crofts. p 168-207.

Mrosovsky N. 1971b. Control systems for annual cycles. Hibernation and the hypothalamus. New York: Appleton-Century-Crofts. p 103-146.

Mrosovsky N. 1976. Lipid programmes and life history strategies. American Zoologist 16:685-697.

Muralidhara DV, Desautels M. 1994. Changes in brown adipose tissue composition during fasting and refeeding of diet-induced obese mice. American Journal of Physiology 266:R1907-R1915.

Nibbelink M, Moulin K, Arnaud E, Duval C, Penicaud L, Casteilla L. 2001. Brown fat UCP1 is specifically expressed in uterine longitudinal smooth muscle cells. Journal of Biological Chemistry 276:47291-47295.

Nicholls DG, Locke RM. 1984. Thermogenic mechanisms in brown fat. Physiological Reviews 64:1-64.

Nicholls DG, Rial E. 1999. A history of the first uncoupling protein, UCP1. Journal of Bioenergetics and Biomembranes 31:399-406.

Nizielski SE, Billington CJ, Levine AS. 1995. Cold-induced alterations in uncoupling protein and its mRNA are seasonally dependent in ground squirrels. American Journal of Physiology 269:R357-R364.

Nunes S, Ha Cd T, Garrett PJ, Mueke E, Smale L, Holekamp KE. 1998. Body fat and time of year interact to mediate dispersal behaviour in ground squirrels. Animal Behavior 55:605-614.

Ormseth OA, Nicolson M, Pelleymounter MA, Boyer BB. 1996. Leptin inhibits prehibernation hyperphagia and reduces body weight in arctic ground squirrels. American Journal of Physiology 271:R1775-R1779.

Panov A, Scarpa A. 1996. Mg^{2+} control of respiration in isolated rat liver mitochondria. Biochemistry 35:12849-12856.

Pehowich DJ, Wang LCH. 1984. Seasonal changes in mitochondrial succinate dehydrogenase activity in a hibernator, *Spermophilus richardsonii*. Journal of Comparative Physiology B 154:495-501.

Pelleymounter MA, Cullen MJ, Baker MB, Hecht R, Winters D, Boone T, Collins F. 1995. Effects of the obese gene product on body weight regulation in *ob/ob* mice. Science 269:540-543.

Porter RK, Andrews JF. 1998. Effects of leptin on mitochondrial 'proton leak' and uncoupling proteins: implications for mammalian energy metabolism. Proceedings of the Nutrition Society 57:455-460.

Porter RK, Joyce OJP, Farmer MK, Heneghan R, Tipton KF, Andrews JF, McBennett SM, Lund MD, Jensen CH, Melia HP. 1999. Indirect measurement of mitochondrial proton leak and its application. International Journal of Obesity 23:S12-S18.

Prashker D, Wardlaw AC. 1971. Temperature responses of mice to *Escherichia coli* endotoxin. British Journal of Experimental Pathology 52:36-46.

Puigserver P, Herron D, Gianotti M, Palou A, Cannon B, Nedergaard J. 1992. Induction and degradation of the uncoupling protein thermogenin in brown adipocytes in

vitro and in vivo. Evidence for a rapidly degradable pool. Biochemical Journal 284:393-398.

Puigserver P, Wu Z, Park CW, Graves R, Wright M, Spiegelman BM. 1998. A cold-inducible coactivator of nuclear receptors linked to adaptive thermogenesis. Cell 92:829-839.

Reddy AB, Cronin AS, Ford H, Ebling FJP. 1999. Seasonal regulation of food intake and body weight in the male Siberian hamster: studies of hypothalamic orexin (Hypocretin), neuropeptide Y (NPY) and pro-opiomelanocortin (POMC). European Journal of Neuroscience 11:3255-3264.

Reynafarje B, Costa LE, Lehninger AL. 1985. O_2 solubility in aqueous media determined by a kinetic method. Analytical Biochemistry 145:406-18.

Richter C, Schweizer M, Ghafourifar P. 1999. Mitochondria, nitric oxide, and peroxynitrite. Methods in Enzymol 301:381-393.

Ricquier D, Kader JC. 1976. Mitochondrial protein alteration in active brown fat: a soidum dodecyl sulfate-polyacrylamide gel electrophoretic study. Biochemical and Biophysical Research Communications 73:577-583.

Roberts JC, Chaffee RRJ. 1972. Suppression of mitochondrial respiration in hibernation and its reversal in arousal. In: Smith RE, Shields JL, Hannon JP, Horwitz BA, editors. Proceedings of the International Symposia on Environmental Physiology: Bioenergetics and Temperature Regulation. Bethesda, MD: FASEB. p 101-107.

Rolfe DFS, Brand MD. 1996a. Contribution of mitochondrial proton leak to skeletal muscle respiration and to standard metabolic rate. American Journal of Physiology 271:C1380-C1389.

Rolfe DFS, Brand MD. 1996b. Proton leak and control of oxidative phosphorylation in perfused, resting rat skeletal muscle. Biochimica et Biophysica Acta 1276:45-50.

Rolfe DFS, Brown GC. 1997. Cellular energy utilization and molecular origin of standard metabolic rate in mammals. Physiologicak Reviews 77:731-758.

Rolfe DFS, Hulbert AJ, Brand MD. 1994. Characteristics of mitochondrial proton leak and control of oxidative phosphorylation in the major oxygen-consuming tissues of the rat. Biochimica et Biophysica Acta 1188:405-416.

Rolfe DFS, Newman JMB, Buckingham JA, Clark MG, Brand MD. 1999. Contribution of mitochondrial proton leak to respiration rate in working skeletal muscle and liver and to SMR. American Journal of Physiology 276:C692-C699.

Rose RW, West AK, Ye JM, McCormack GH, Colquhoun EQ. 1999. Nonshivering thermogenesis in a marsupial (The Tasmanian bettong *Bettongia gaimardi*) is not attributable to brown adipose tissue. Physiological and Biochemical Zoology 72:699-704.

Samec S, Seydoux J, Dulloo AG. 1998. Role of UCP homologues in skeletal muscles and brown adipose tissue: mediators of thermogenesis or regulators of lipids as fuel substrate? FASEB Journal 12:715-724.

Samec S, Seydoux J, Dulloo AG. 1999. Post-starvation gene expression of skeletal muscle uncoupling protein 2 and uncoupling protein 3 in response to dietary fat

levels and fatty acid composition - A link with insulin resistance. Diabetes 48:436-441.

Sanchis D, Fleury C, Chomiki N, Goubern M, Huang Q, Neverova M, Gregoire F, Easlick J, Raimbault S, Levi-Meyrueis C, Miroux B, Collins S, Seldin M, Richard D, Warden C, Bouillaud F, Ricquier D. 1998. BMCP1, a novel mitochondrial carrier with high expression in the central nervous system of humans and rodents, and respiration uncoupling activity in recombinant yeast. Journal of Biological Chemistry 273:34611-34615.

Scarpace PJ, Matheny M, Pollock BH, Tumer N. 1997. Leptin increases uncoupling protein expression and energy expenditure. American Journal of Physiology 273:E226-E230.

Scholander PF, Hock RJ, Walters V, Johnson F, Irving L. 1950. Heat regulation in some arctic and tropical mammals and birds. Biological Bulletin 99:237-258.

Schrauwen P, Saris WHM, Hesselink MKC. 2001. An alternative function for human uncoupling protein 3: protection of mitochondria against accumulation of nonesterified fatty acids inside the mitochondrial matrix. FASEB Journal 15:2497-2502.

Schrauwen P, Westerterp-Plantenga MS, Kornips E, Schaart G, van Marken Lichtenbelt WD. 2002. The effect of mild cold exposure on UCP3 mRNA expression and UCP3 protein content in humans. International Journal of Obesity 26:450-457.

Shiomi M, Wakabayashi Y, Sano T, Shinoda Y, Nimura Y, Ishimura Y, Suematsu M. 1998. Nitric oxide suppression reversibly attenuates mitochondrial dysfunction and cholestasis in endotoxemic rat liver. Hepatology 27:108-15.

Simonyan RA, Jimenez M, Ceddia RB, Giacobino JP, Muzzin P, Skulachev VP. 2001. Cold-induced changes in the energy coupling and the UCP3 level in rodent skeletal muscles. Biochimica et Biophysica Acta 1505:271-279.

Sivitz WI, Fink BD, Donohoue PA. 1999. Fasting and leptin modulate adipose and muscle uncoupling protein: divergent effects between messenger ribonucleic Acid and protein expression. Endocrinology 140:1511-1519.

Skulachev VP. 1998. Uncoupling: new approaches to an old problem of bioenergetics. Biochimica et Biophysica Acta 1363:100-124.

Smith RE, Horwitz BA. 1969. Brown fat and thermogenesis. Physiological Reviews 49:330-425.

Snapp BD, Heller HC. 1981. Suppression of metabolism during hibernation in ground squirrels (*Citellus lateralis*). Physiological Zoology 54:297-307.

South FE, House WA. 1967. Energy metabolism in hibernation. In: Fisher KC, Dawe AP, Lyman CP, Schonbaum E, South FE, editors. Mammalian Hibernation III. New York: Elsevier. p 305-324.

St-Pierre J, Brand MD, Boutilier RG. 2000. The effect of metabolic depression on proton leak rate in mitochondria from hibernating frogs. Journal of Experimental Biology 203:1469-1476.

Strausberg RL, Austin MJF. 1999. Functional genomics: technological challenges and opportunities. Physiological Genomics 1:25-32.

Strobel A, Issad T, Camoin L, Ozata M, Strosberg AD. 1998. A leptin missense mutation associated with hypogonadism and morbid obesity. Nature Genetics 18:213-215.

Stuart JA, Harper JA, Brindle KM, Jekabsons MB, Brand MD. 2001a. A mitochondrial uncoupling artifact can be caused by expression of uncoupling protein 1 in yeast. Biochemical Journal 356:779-89.

Stuart JA, Harper JA, Brindle KM, Jekabsons MB, Brand MD. 2001b. Physiological levels of mammalian uncoupling protein 2 do not uncouple yeast mitochondria. Journal of Biological Chemistry 276:18633-9.

Sultan A, Sokolove PM. 2001. Free fatty acid effects on mitochondrial permeability: An overview. Archives of Biochemistry and Biophysics 386:52-61.

Sundin U, Moore G, Nedergaard J, Cannon B. 1987. Thermogenin amount and activity in hamster brown fat mitochondria: effect of cold acclimation. American Journal of Physiology 252:R822-R832.

Tanizawa Y, Okuya S, Ishihara H, Asano T, Yada T, Oka Y. 1997. Direct stimulation of basal insulin secretion by physiological concentrations of leptin in pancreatic beta cells. Endocrinology 138:4513-4516.

Teruel T, Smith SA, Peterson J, Clapham JC. 2000. Synergistic activation of UCP-3 expression in cultured fetal rat brown adipocytes by PPAR α and PPAR γ ligands. Biochemical and Biophysical Research Communications 273:560-564.

Thomas SA, Palmiter RD. 1997. Thermoregulatory and metabolic phenotypes of mice lacking noradrenaline and adrenaline. Nature 387:94-97.

Toien O, Drew KL, Chao ML, Rice ME. 2001. Ascorbate dynamics and oxygen consumption during arousal from hibernation in Arctic ground squirrels. American Journal of Physiology 281:R572-R583.

Trayhurn P, Jennings G. 1988. Nonshivering thermogenesis and the thermogenic capacity of brown fat in fasted and/or refed mice. American Journal of Physiology 254:R11-R16.

Unger RH. 2000. Leptin physiology: a second look. Regulatory Peptides 92:87-95.

Van der Lee K, Willemsen PHM, Samec S, Seydoux J, Dulloo AG, Pelsers M, Glatz JFC, Van der Vusse GJ, Van Bilsen M. 2001. Fasting-induced changes in the expression of genes controlling substrate metabolism in the rat heart. Journal of Lipid Research 42:1752-1758.

Van der Lee KAJM, Willemsen PHM, Van der Vusse GJ, Van Bilsen M. 2000. Effects of fatty acids on uncoupling protein-2 expression in the rat heart. FASEB Journal 14:495-502.

Vidal-Puig A, Solanes G, Grujic D, Flier JS, Lowell BB. 1997. UCP3: an uncoupling protein homologue expressed preferentially and abundantly in skeletal muscle and brown adipose tissue. Biochemical and Biophysical Research Communications 235:79-82.

Vidal-Puig AJ, Grujic D, Zhang CY, Hagen T, Boss O, Ido Y, Szczepanik A, Wade J, Mootha V, Cortright R, Muoio DM, Lowell BB. 2000. Energy metabolism in

uncoupling protein 3 gene knockout mice. Journal of Biological Chemistry 275:16258-16266.

von Praun C, Burkert M, Gessner M, Klingenspor M. 2001. Tissue-specific expression and cold-induced mRNA levels of uncoupling proteins in the Djungarian hamster. Physiological and Biochemical Zoology 74:203-211.

Wang H, Bloom O, Zhang M, Vishnubhakat JM, Ombrellino M, Che J, Frazier A, Yang H, Ivanova S, Borovikova L, Manogue KR, Faist E, Abraham E, Andersson J, Andersson U, Molina PE, Abumrad NN, Sama A, Tracey KJ. 1999. HMG-1 as a late mediator of endotoxin lethality in mice. Science 285:248-251.

Wang Z, Zhou YT, Kakuma T, Lee Y, Kalra SP, Kalra PS, Pan W, Unger RH. 2000. Leptin resistance of adipocytes in obesity: role of suppressors of cytokine signaling. Biochemical and Biophysical Research Communications 277:20-26.

Weigle DS. 1994. Appetite and the regulation of body composition. FASEB Journal 8:302-310.

Weigle DS, Selfridge LE, Schwartz MW, Seeley RJ, Cummings DE, Havel PJ, Kuijper JL, BeltrandelRio H. 1998. Elevated free fatty acids induce uncoupling protein 3 expression in muscle: A potential explanation for the effect of fasting. Diabetes 47:298-302.

Wu ZD, Puigserver P, Andersson U, Zhang CY, Adelmant G, Mootha V, Troy A, Cinti S, Lowell B, Scarpulla RC, Spiegelman, BM. 1999. Mechanisms controlling mitochondrial biogenesis and respiration through the thermogenic coactivator PGC-1. Cell 98:115-124.

Yu XX, Mao WG, Zhong A, Schow P, Brush J, Sherwood SW, Adams SH, Pan GH. 2000. Characterization of novel UCP5/BMCP1 isoforms and differential regulation of UCP4 and UCP5 expression through dietary or temperature manipulation. FASEB Journal 14:1611-1618.

Zanetti G, Heumann D, Gerain J, Kohler J, Abbet P, Barras C, Lucas R, Glauser MP, Baumgartner JD. 1992. Cytokine production after intravenous or peritoneal gram-negative bacterial challenge in mice. Comparative protective efficacy of antibodies to tumor necrosis factor-α and to lipopolysaccharide. Journal of Immunology 148:1890-1897.

Zhang CY, Hagen T, Mootha VK, Slieker LJ, Lowell BB. 1999. Assessment of uncoupling activity of uncoupling protein 3 using a yeast heterologous expression system. FEBS Letters 449:129-134.

Zhang Y, Hufnagel C, Eiden S, Guo K, Diaz P, Leibel RL, Schmidt I. 2001. Mechanisms for LEPR-mediated regulation of leptin expression in brown and white adipocytes in rat pups. Physiol. Genomics 4:189-199.

Zhang Y, Olbort M, Schwarzer K, Nuesslein-Hildesheim B, Nicolson M, Murphy E, Kowalski TJ, Schmidt I, Leibel RL. 1997. The leptin receptor mediates apparent autocrine regulation of leptin gene expression. Biochemical and Biophysical Research Communications 240:492-495.

Zhang Y, Proenca R, Maffei M, Barone M, Leopold L, Friedman JM. 1994. Positional cloning of the mouse obese gene and its human homologue. Nature 372:425-432.

Zhou YT, Shimabukuro M, Koyama K, Lee Y, Wang MY, Trieu F, Newgard CB, Unger RH. 1997. Induction by leptin of uncoupling protein-2 and enzymes of fatty acid oxidation. Proceedings of the National Academy of Sciences of the United States of America 94:6386-6390.